18th International Conference on Structural Mechanics in Reactor Technology (SMiRT 18)
Beijing, China, August 7-12, 2005
SMiRT18-K10-7

SURVEY OF PAST BASE ISOLATION APPLICATIONS IN NUCLEAR POWER PLANTS AND CHALLENGES TO INDUSTRY/REGULATORY ACCEPTANCE

Sanjeev R. Malushte
Bechtel Power Corporation
5275 Westview Drive
Frederick, MD 21703, USA
Phone: 1-301-228-7697
Fax: 1-240-379-2811
E-mail: smalusht@bechtel.com

Andrew S. Whittaker
University at Buffalo
230 Ketter Hall
Buffalo, NY,14260, USA
Phone: 1-716-645-2114 x 2418
Fax: 1-716-645-3733
E-mail: awhittak@acsu.buffalo.edu

ABSTRACT

Seismic base isolation provides many benefits that can facilitate the standardization of future nuclear power plant structures and equipment while reducing the initial/life-cycle cost and construction schedule. This paper presents a survey of past seismic base isolation applications and studies related to nuclear applications and provides a discussion of the challenges that need to be overcome to gain industry and regulatory acceptance for deployment in future US nuclear power plants. Issues related to design, codes/standards/regulations, procurement, and construction, have been identified.

Keywords: Seismic Base Isolation, Nuclear Regulation, Codes and Standards, Seismic Gap, Isolator Testing, Quality Assurance

1. INTRODUCTION

Seismic isolation is a mature technology that has already been applied to many infrastructure and mission-critical facilities. There are many potential advantages of deploying seismic base isolation for future nuclear power plants. The most important advantage is that the overall reliability and safety of nuclear plants can be improved. This is because the design of the major plant equipment and structures can be standardized irrespective of the design ground motion; i.e., variation in the design seismic acceleration levels can be accommodated by making adjustments to the isolation system. Such standardization of equipment and superstructure in base isolated plants will cut costs and design/construction schedule for new nuclear power plants. Further, base isolation will enable decoupling of design development for equipment, piping, and components due to the use of generic in-structure response spectra associated with the standardized plant. Also, due to its superior seismic performance capability against the design basis earthquake as well as a beyond-design-basis seismic event, the plant safety margin will be improved (compared to a conventionally designed plant).

Application of base isolation will also help overcome the following emerging seismic issues:

- US Nuclear Regulatory Commission Regulatory Guide 1.165 (NRC, 1997) requires that the seismic design of nuclear plants be based on a probabilistic seismic hazard assessment (PSHA) for a 100,000-year return period. For many existing nuclear plant sites, especially in the central and eastern US (which are the likely candidates for next-generation units), the associated design ground motion is quite high (Carrato and Litehiser, 2005) such that construction of a new nuclear power plant could become exorbitantly expensive.
- For the prospective sites located within the central and eastern US, recent seismic hazard studies have confirmed increased high-frequency content in the design spectrum (and some collateral increase in the medium range frequency content). While the increase in high frequency content has a relatively small significance for the design of structures, the full extent of this problem has not yet been conclusively studied. Consideration of wave incoherency effects results in some benefit (Ostadan, et al, 2005); however, regardless of the structure size, base isolation will further reduce the shaking intensity transmitted to the superstructure.

The potential advantages of seismic base isolation notwithstanding, the US nuclear industry and regulatory agencies must proceed with caution by studying its past experiences with base isolation and ascertain how the currently available (and improved) isolator technologies can be justified for such a mission-critical application. In particular, the unique requirements for service in the nuclear industry must be properly carefully addressed prior to deployment. To this end, the authors of this paper have been canvassing various isolation experts, regulators, utility companies, equipment suppliers, and isolator vendors to develop a consensus and a strategy for eventual application of base isolation to nuclear power plants.

2. PAST STUDIES/APPLICATIONS OF BASE ISOLATION TO NUCLEAR FACILITIES

In the nuclear industry, there have been many past instances of either full deployment of base isolation or development of appropriate specifications to enable such deployment. This paper will discuss the lessons/perspectives gained from such applications and studies.

There are currently six seismically isolated Pressurized Water Reactor (PWR) units: four in France and two in South Africa. At the Cruas plant in France, each of the four units has been constructed on 1,800 neoprene pads measuring 500 by 500 by 65 mm. The seismicity at this site is moderate, with a safe shutdown earthquake (SSE) design acceleration of 0.20g. In Koeberg, South Africa, two units are isolated on a total of 2000 neoprene pads measuring 700 by 700 by 100 mm. In this case the SSE design acceleration is 0.30g. The pads are outfitted with flat sliders on the top surface, consisting of a lead-bronze alloy lower plate and a polished stainless steel upper plate. The sliding feature was implemented so that the lateral force transmitted to the reactor vessel is limited to the frictional resistance of the sliding interface (nowadays the Friction Pendulum System (FPS) method is widely preferred over flat sliders as it has a built-in re-centering ability without requiring the use of any special springs, as in case of flat sliders).

The long-term behavior of the isolators used in France and South Africa has been one of the issues that makes them unsuitable for an application to a US nuclear facility. Neither type of bearing used in France or South Africa are utilized nowadays for a seismic isolation project in the United States. Specifically, the synthetic rubber Neoprene used in the French isolators has been known to age-stiffen (changing the properties of the isolation system) and the bimetallic interface used in the South African isolators is now banned from use in seismic bearings because the mechanical properties of such interfaces can change substantially with time. Currently, there are significantly better types of isolation systems available (with re-centering capabilities) and the associated design/testing rules have been increasingly well codified and streamlined (e.g., ASCE, 2002). The past base isolation applications (in France and South Africa) are considered outdated in terms of the current state-of-the-art.

The Japanese government has sponsored various initiatives over the last 15-years to evaluate the viability of base isolation technology for nuclear facilities. In 1997, the Central Research Institute of Electric Power Industry (CRIEPI) issued appropriate guidelines for application to Fast Breeder Plants and Light Water Reactors. Although there are currently no seismically isolated nuclear reactors in Japan, these guidelines make them a possibility. Work has also been underway in Japan for applying seismic isolation to the International Thermonuclear Experimental Reactor (Fujita, 1997).

In 1998-1999, AECL, a Canadian NSSS supplier, actively explored and advocated the use of base isolation during its bid for the (now abandoned) Akkuyu nuclear power project in Turkey. Incidentally, data available from an AECL study (AECL, 1996) indicated that Teflon, used in sliding-type isolators, can withstand radiation dose levels as large as one Mrad without much performance deterioration. More recently, AECL's participation in the analytical research being conducted by the researchers at the University at Buffalo (Whittaker, et al, 2005) is helping quantify the benefits provided by base isolation.

Westinghouse also conducted a study of horizontal base isolation for its AP600 plant during the nineties (Westinghouse, 2004). This study was directed primarily to determine if the AP600 standard design could be applied to sites in Japan where the design ground motion exceeds the 0.30 g design basis for the AP600. It was felt that the AP600 and AP1000 plants needed more commercial success before applications (with or without seismic isolation) to sites with higher design ground motion were considered.

In the US, the Department of Energy (DOE) had sought to use the base isolation technology for the nuclear island facilities of its Advanced Liquid Metal Reactor (ALMR) project in order to improve safety and to allow the development of a standard design for varying regions of seismicity. The prototype ALMR design incorporates 66 high damping rubber bearings. Prototypes of these bearings have been tested extensively (Tajirian, 1990 and Clark, et al, 1995). The DOE has also been developing a Sodium Advanced Fast Reactor (SAFR), which incorporates seismic isolation. The prototype design is supported on 100 elastomeric isolators. Reduced scale isolators have been tested to verify their performance (Aiken, 1989).

Recently, INEEL and Bechtel studied the application of base isolation to a US nuclear power plant. Discussions with the utilities and NRC staff (NRC, 2004) indicated that any move to implement seismic base isolation on a nuclear power plant will require an extensive scrutiny of issues such as long-term behavior of isolators, in-service/pre-service inspection and testing of isolators, and the basis for choosing an adequate isolation gap (based on some beyond-design-basis consideration).

Most US suppliers of advanced light water reactors (and others wishing to enter the US market) have based the design of their plants on a peak ground acceleration of 0.30 g, with some ad hoc modification to the response spectrum shape specified in Regulatory Guide 1.60 (NRC, 1973) to reflect increased high frequency content encountered in the central/eastern US regions. They are hoping that the PSHA-based site-specific spectra for prospective sites can be enveloped by these presumptive design spectra. Recent early site permit studies however indicate that such hope may be misplaced because of the exceedances in both medium and high frequency ranges. The authors have generally found that while there is a desire to cautiously approach the base isolation solution, the biggest hurdle so far appears to be a collective inertia and/or lack of sufficient knowledge about the state-of-the-art practice, which prompts utilities and NSSS suppliers to keep choosing conventional design options.

3. DESIGN CONSIDERATIONS FOR BASE ISOLATED NUCLEAR POWER PLANTS

Several design considerations need to be factored in when designing seismic isolation systems for a nuclear power plant.

Selection of Isolation Criteria: While the seismic response consideration generally does not control the designs of nuclear power plant structures in low to moderately seismic areas (radiation shielding, accident loading, etc., often govern the design), the same is not necessarily true for many of the major equipment, piping, and other safety-related commodities. It is envisioned that the nuclear steam supply system (NSSS) equipment suppliers could specify the required response spectra (RRS) for their equipment based on known equipment fragility characteristics and/or economic design considerations. Unfortunately, NSSS suppliers generally tend to have a “linear" design process in that the discipline(s) responsible for design of equipment and its supports simply utilize the floor response spectra provided by the civil/structural discipline. The potential benefits of seismic isolation are not understood/realized in such a scheme unless the RRS is too high for the equipment designers to deal with. For base isolation to become an accepted practice, the NSSS suppliers and other major equipment vendors will need to play a critical role in helping develop sensible isolation criteria.

Isolation Diaphragm: To minimize the number of flexible couplings for systems that traverse between isolated and non-isolated facilities, it is preferable to isolate the entire nuclear island (i.e., all structures other than the balance of plant facilities) using a common diaphragm to support the associated structures above the isolators. Use of a common diaphragm will avoid large relative displacements between the superstructures of the various nuclear island facilities. Use of a common mat with large footprint will also result in increased benefit from wave incoherency effects. Having a large common mat may be undesirable because of the uneven mass/stiffness distribution and the differing base slab thickness requirements for the various nuclear island structures (including their internals). These factors pose difficulties from the standpoints of ease of construction and/or achieving a relatively uniform distribution of seismic demand on individual isolators. On the other hand, using separate diaphragms for each nuclear island structure will increase cost as well as schedule complexity, factors that will need to be weighed against the alternative of using a common diaphragm. For a large common mat with irregular mass and stiffness distribution, the use of prestressed isolators and appropriate isolator placement strategies will help overcome isolator uplift/overturning problems.

Longevity and Service Conditions: The next generation of power plants will likely be licensed for 60-year operation or more. Accordingly, the isolation system will need to have the requisite long-term reliability in a potential radiation environment and elevated temperatures (after a loss of coolant accident [LOCA] or main steam break event). If aging is shown to result in a diminished ability to provide seismic isolation, then it would be necessary to carry out an "end-of-the-life" analysis, considering appropriately conservative values for isolator properties. Also, appropriate in-service surveillance and maintenance for each type of isolation system will need to be performed to assure continued reliability. Among the common types of isolators available commercially, the friction pendulum (FP) isolators is expected to demonstrate relatively inert and durable characteristics. In any case, appropriate "end-of-life" isolator properties will need to be used to design for long-term performance.

Isolation/Expansion Joints: Balance of plant (BOP) systems, including major systems such as main steam and feedwater, that traverse from non-isolated facilities will need to be fitted with special flexible expansion joints that can accommodate the relative movements between the facilities. These relative movements are expected to be in the neighborhood of 1 to 2 feet (especially in high seismic areas), a significant challenge for the design of isolation joints. The procurement/design of these specialty items will need to be planned in advance with close dialog and coordination between the parties involved. In some ways, the viability of seismic base isolation and the choice of a particular type/layout of isolaton system itself will depend on the industry's ability to procure appropriate expansion joints for isolating the BOP systems. Therefore, an active effort will be needed to ensure that appropriate isolation joints are available (or can at least be manufactured economically) for high pressure/temperature pipes with large diameters.

Effects of Vertical Excitation: Response to vertical excitation is an important design consideration in a conventionally designed plant. For base isolated nuclear plants, the effects of simultaneous horizontal and vertical shaking needs to be studied to adequately capture the influence of vertical acceleration. Design of packaged isolators that can provide isolation from both horizontal and vertical seismic accelerations is also of interest. The isolation industry has been pursuing this challenge for a long time; however, the advent of a commonly accepted packaged isolation system has so far been elusive.

Specification of Beyond-Design-Basis Criteria: The NRC may stipulate some "beyond-design-basis" criteria in terms of increased hazard (i.e., higher ground motion) or some safety performance goal (i.e., limiting the deformation of plant SSCs). In the absence of any NRC-mandated criteria, the A/E and Owner will need to select suitable criteria. Whether the beyond-design-basis earthquake criteria are established by the Owner or dictated by an NRC regulation, the isolation system will need to be appropriately designed to meet the associated requirements. This will also have an impact on the capability of the isolation joints in the isolation system and the required seismic gap. As a remote possibility, springs/dampers may need to be provided to cushion the impact forces transferred when the limit of sliding travel is exhausted.

4. QUALITY ASSURANCE/QUALITY CONTROL AND CODE/STANDARD CONSIDERATIONS

Several QA, testing, and code/standard considerations need to be factored in when procuring materials and services for seismic isolation systems to be used in a nuclear power plant.

Procurement Issues: The U.S. Nuclear Regulatory Commission (NRC) will first need to approve (either generically or on a case-by-case basis) and subsequently regulate the use of isolation systems in U.S. nuclear power plants. For safety-related applications, the isolators will need to be procured in accordance with the QA/QC requirements of 10 CFR 50, Appendix B. Adapting to these requirements will be a major issue for isolator producers, as they are not accustomed to the kind of procedural rigor common in the nuclear industry (i.e., the QA/QC requirements associated with the design, testing, manufacturing, shipping/handling, and installation). Owing to the scale of each nuclear power plant project and the potential market size, the isolation industry will also need to gear up for adequate production capabilities in terms of isolator sizes, load-carrying capacity, and production rate.

It will be necessary to canvass suppliers to maintain open lines of communication and to help them prepare for the challenges that lay ahead. Notwithstanding the difficulties, it is noted that the isolation community has experienced increasing quality, testing, and peer review requirements imposed by code

bodies and customers (e.g., DOE projects for ALMR and SAFR projects and California Department of Transportation) that have used isolation systems for numerous mission-critical facilities over the past one and a half decade. As is customary in non-nuclear applications, it is expected that a third party review, conducted by independent experts, will also be required for nuclear applications in order to ensure quality design and procurement.

In the area of testing, the following issues will need to be addressed:

- *Types of Tests:* Some tests will be isolator-specific (e.g., characterization of friction behavior for sliding isolators, scragging for rubber-based isolators), while others will be generic (e.g., effect of long service, effects of temperature/radiation exposure)
- *Timing/Frequency of Tests:* During the design/production phase, a protocol will need to be developed for qualification testing and in-production testing. Prior to deployment and during service, a protocol will be needed for pre-service and in-service inspection, testing, and maintenance requirements.

Applicable Codes/Standards: Many US codes and standards include technical requirements pertaining to design and testing of base isolation systems (Whittaker, et al, 2005). Barring the ASCE 4-98 standard (ASCE, 1998), the rest of such documents are geared toward non-nuclear applications. This notwithstanding, many of the requirements from the various codes/standards can be adapted/modified to establish appropriate design criteria for a base isolated nuclear power plant. An industry-wide initiative (involving the NRC) will be needed to develop a suitable standard/design guide for this purpose. Following is a (partial) list of currently available codes/standards/specifications:

- *ASCE 4-98:* "Seismic Analysis of Safety-Related Nuclear Structures and Commentary." Section 3.5.6 of this document provides the analysis requirements for seismic-isolated structures; the NRC does not presently endorse this section. The authors are working through the ASCE 4 standard committee to significantly revise this section (including ground motion time history requirements). It is expected that the next version of ASCE 4 will serve as a platform for wider acceptance of seismic base isolation.
- *ASCE 7-02:* "Minimum Design Loads for Buildings and Other Structures." Section 9.13 of this standard contains provisions for seismically isolated structures based on the NEHRP 2000 document (FEMA, 2001). These provisions are not intended for nuclear power facilities (although a lot of relevant guidance can still be derived).
- *National Earthquake Hazard Reduction Program (FEMA, 2004):* Chapter 13 of this document provides the most current requirements for design of base isolated structures. The latest NEHRP provisions have been adapted in the upcoming revision of ASCE 7. Note that the provisions of this document are also not intended for nuclear power facilities.
- *NIST Report NISTIR 5800 and New ASCE Standard for Testing Seismic Isolation Systems:* In 1996 a committee was formed by the American Society of Civil Engineers (ASCE) to develop code provisions for testing seismic isolation systems. The committee used as a resource document an earlier guideline on testing developed at the National Institute of Standards and Technology (NIST Report NISTIR 5800). The standard will include procedures for basic property testing, prototype testing, and quality control testing of both elastomeric and sliding isolation systems.

The above-mentioned documents address both design and testing issues for isolation systems. With active industry involvement, the material from these documents can eventually lead to appropriate topical reports and/or regulatory guides (which may also include additional guidance/provisions for testing protocol, QA/QC requirements, and isolation joints for BOP systems). Such a progression toward regulatory acceptance is key to successful deployment and will require a collective effort on the part of the nuclear industry, the isolation industry, and the regulatory community.

5. CONSTRUCTION CONSIDERATIONS

Application of base isolation to nuclear power plant structure(s) will involve several challenges with regard to planning, scheduling, and execution. On the whole, base isolation is expected to reduce the overall schedule because the design of the superstructure, major equipment, and piping can be significantly standardized. Some of the construction challenges are discussed below:

Isolation Diaphragm: A common isolation diaphragm for containment plus auxiliary building will present a construction challenge because of its size and expected thickness variations. Thickness changes in the diaphragm can be minimized, albeit at some increase in concrete/rebar quantities. A cost-benefit analysis will need to be performed to evaluate the increased quantities versus the ease of construction (and the expected schedule expediency). Close and early coordination between the design and construction teams will be needed to reach the right decision in this regard. The option to employ separate diaphragms/foundations for the nuclear island structures is deemed preferable from the construction standpoint; however, it likely will entail some adverse schedule and cost implications (i.e., the additional cost to procure an increased number of BOP isolation joints).

Adequate headroom between the diaphragm and the foundation will be needed to permit easy access to isolators for inspection, maintenance, surveillance, and potential removal for in-service testing. Another issue to be addressed is the design concept for the tendon gallery of the prestressed concrete containments. It is likely that the tendon gallery would become a part of the isolation diaphragm, thus requiring local thickening of the diaphragm.

Moat/Seismic Gap: To accommodate lateral movements of an isolated building, a clearance space, or "seismic gap," must be provided around the perimeter of the base. For partially buried structures such as the containment and auxiliary buildings, the isolation system will be located below grade and the seismic gap will take the form of a moat. The width of the moat will need to exceed the maximum calculated lateral displacement under some appropriate "beyond-design-basis" seismic design criterion.

Special architectural features are associated with the seismic gap. For nuclear power plants, the seismic gap will take the form of a moat because the reactor building and auxiliary building are normally embedded several meters below grade. Construction of a moat will require retaining walls to hold the soil in place. For deeper embedment of containment/auxiliary buildings, the design and construction of the moat will need to be carefully planned. The embedment itself can be reduced to a minimum because of the reduced seismic demands provided by the base isolation system.

Another architectural consideration is the configuration of elevator pits and sumps. Typically, the elevator pits in isolated buildings are suspended below the first floor of the structure, within the space provided for the seismic isolators. Sufficient clearance will need to be provided around the elevator pits and sumps to avoid interference when the isolation system undergoes the maximum possible lateral displacement.

6. SUMMARY AND CONCLUSIONS

There are many industry/regulatory issues that need to be studied and evaluated when making the case for base isolation of US nuclear power plants. This paper addressed the following issues:

- Quality Assurance/Quality Control capabilities of isolator vendors
- Production capabilities of isolator vendors (in terms of isolator size, capacity, and production rate)
- Development of appropriate testing protocol for isolators, including testing for demonstration of long service life in a potential radiation environment with somewhat elevated service temperatures
- Development of appropriate qualification/in-production testing requirements for isolators
- The need/extent for isolator surveillance, maintenance, and in-service testing during service life
- Development of specific codes, standards, and regulatory documents for addressing design and construction of isolated nuclear facilities
- Development of suitable performance criteria, especially with inputs from equipment vendors
- Determination of the division of responsibility between the owner, engineer/constructor, and NSSS supplier, with emphasis on increased participation by NSSS suppliers
- Ability to provide suitable isolation joints for systems connected across isolated and non-isolated facilities (especially for large diameter, high-energy pipes)
- Constructability issues associated with isolation diaphragm, clearance/moat, and access space for surveillance/inspection of isolators
- Need for further isolation research, industry education and regulatory participation/acceptance

The authors believe that it is the right time to address these issues to pave the way for first deployment.

REFERENCES

1. US Nuclear Regulatory Commission Regulatory Guide 1.165 (1997), “Identification and Characterization of Seismic Sources and Determination of Safe Shutdown Earthquake Ground Motion”
2. Carrato, P. J. and Litehiser, J. J. (2005), “Characterization Of Design Ground Motion For Central And Eastern United States”, Transactions of the 18th International Conference on Structural Mechanics in Reactor Technology (SMiRT 18), K02-4
3. Ostadan, F. (2005), “Soil-Structure Interaction Analysis Including Ground Motion Incoherency Effects”, Transactions of the 18th International Conference on Structural Mechanics in Reactor Technology (SMiRT 18), K04-7
4. ASCE Standard 7 (2002), “Minimum Design Loads for Buildings and Other Structures”, published by the American Society of Civil Engineers
5. Fujita, T. (1997), “Progress of applications, R&D and design guidelines for seismic isolation of civil buildings and industrial facilities in Japan”, International Post-SMiRT Conference Seminar on Seismic Isolation, Passive Energy Dissipation and Active Control of Seismic Vibrations of Structures, Taormina, Italy
6. AECL Report MED-99853-96-001 (1996), “Phase 1 Radiation and Temperature Testing of ARGO Style 5000”
7. Huang, Yin-Nan, Whittaker, A. S., Constantinou, M. C., and Malushte, S. R. (2005), “Protection of Secondary Systems in Nuclear Power Plant Facilities”, Transactions of the 18th International Conference on Structural Mechanics in Reactor Technology (SMiRT 18), K11-7
8. Private communications between Bechtel and Westinghouse (2004)
9. Tajirian, F. F. (1990), Seismic isolation study final report, Technical Report, Bechtel Corporation
10. Clark, P. W., Aiken, I. D., Kelly, J. M., Tajirian, F. F., and Gluekler, E. L. (1995), “Tests of Reduced-Scale Seismic Isolation Bearings for the Advanced Liquid Metal Reactor (ALMR) Program”, ASME Pressure Vessel and Piping Conference, Honolulu, Hawaii, USA
11. Aiken, I. D., Kelly, J. M., and Tajirian, F. F. (1989), “Mechanics of Low Shape Factor Elastomeric Seismic Isolation Bearings”, Report No. UCB/EERC-89/13, University of California at Berkeley
12. NRC Public Meeting (2004), “Use of Seismic Base Isolation for Nuclear Structures”, with participants from Bechtel, INEEL, and University at Buffalo, Rockville, MD, USA
13. US Nuclear Regulatory Commission Regulatory Guide 1.60, Revision 1 (1973), “Design Response Spectra for Seismic Design of Nuclear Power Plants”
14. Whittaker, A. S., Constantinou, M. C., and Malushte, S. R. (2005), “Building Structures with Damping Systems: From Research to Design Practice”, ASCE Structures Congress, New York City, NY, USA
15. ASCE Standard 4 (1998), “Seismic Analysis of Safety-Related Nuclear Structures and Commentary”, published by the American Society of Civil Engineers
16. FEMA 368 and 369 (2001), “NEHRP 2000 Recommended Provisions and Commentary for Seismic Regulations for New Buildings and Other Structures”, published by the US Federal Emergency Management Agency (now part of the Department of Homeland Securities)
17. FEMA 450 and 451 (2004), “NEHRP 2003 Recommended Provisions and Commentary for Seismic Regulations for New Buildings and Other Structures”, published by the US Federal Emergency Management Agency (now part of the Department of Homeland Securities)
18. Shenton, H. W. (1996), “Guidelines for Pre-Qualification, Prototype and Quality Control Testing of Seismic Isolation Systems,” Report NISTIR 5800, Structures Division, Building and fire Research Laboratory, National Institute of Standards and Technology, Gaithersburg, MD, USA

18th International Conference on Structural Mechanics in Reactor Technology (SMiRT 18)
Beijing, China, August 7-12, 2005
SMiRT18-K10-2

A DEVELOPMENT OF THREE-DIMENSIONAL SEISMIC ISOLATION FOR ADVANCED REACTOR SYSTEMS IN JAPAN - PART 2

Kenji Takahashi*
The Japan Atomic Power Company（JAPC）, Ibaraki, Japan
Phone: +81-29-267-4141
takahashi.kenji@jnc.go.jp

Kazuhiko Inoue
JAPC, Ibaraki, Japan
inoue.kazuhiko@jnc.go.jp

Asao Kato
JAPC,Tokyo,Japan
asao-kato@japc.co.jp

Masaki Morishita
O-arai Engineering Center, Japan Nuclear Cycle Development Institute, Ibaraki, Japan
morisita@oec.jnc.go.jp

Takafumi Fujita
Institute of Industrial Science, The University of Tokyo, Tokyo, Japan
tfujita@iis.u-tokyo.ac.jp

ABSTRACT

Two types of three-dimensional seismic isolation systems were developed for the fast breeder reactor (FBR). One is the three-dimensional entire building base isolation system It was developed by collecting concepts Japanese companies from which a combination system with air springs and hydraulic rocking suppression devices was selected. The other is the vertically isolated system for main components with horizontally entire building base isolation, which was developed by adopting coned disk spring devices.

In the study, seismic condition was assumed based on a strict reference ground motion. Design data of the building and components are referred to FBR being developed as the “Commercialized Fast Reactor Cycle System”. Analysis based on these assumed conditions showed suitable combinations of natural frequencies and damping ratios for isolation. Devices were developed to satisfy the combinations.

In five years research and development, several verification tests were performed including shake table tests with scaled models. Finally it is found that the two types of seismic isolation systems are available for FBR. The result is reflected in the preliminary design guideline for the three-dimensional isolation system.

KEY WORDS: fast breeder reactor, seismic isolation system, air spring, hydraulic rocking suppression system

1. INTRODUCTION

The FBR design feature, compared with Light Water Reactor (LWR), is that the components are operated at high temperature and low pressure. High temperature generates large thermal strains in the components. Applying thinner component could reduce the stress intensity. Components with thin plate, however, do not resist intensive seismic loads. This is the reason the seismic isolation technology is suitable to FBR design. Seismic isolation technology enables not only mitigating the seismic design condition and realizing the thin plate components but also enhancing the structural integrity of the reactor building. The design guideline for the horizontal seismic isolation system was already published in Japan [1]. The next challenge is to mitigate the seismic load in the vertical direction. A project named ‘Three-Dimensional Seismic Isolation for Advanced Reactor System’ [3] was conducted from April 2000 to March 2005. This paper summarizes the whole project; mainly design condition, test results and practicability of the isolation systems.

2. SYSTEM CONCEPT

Two types of three-dimensional seismic isolation systems for FBR were selected in this R&D project through the viewpoints of realization and economic competency. One is the three-dimensional entire building seismic isolation system (3DeSIS), the other is the vertical isolation of main components with horizontal base isolation system (Vertical+2D SIS), which are schematically shown in Figure 1. In 3DeSIS, 3D seismic isolation devices support the entire reactor building. In the Vertical+2D SIS, horizontal seismic isolation devices support the building and the vertical seismic isolation devices support the 'common deck' that holds main components such as reactor vessel (RV), intermediate heat exchanger(IHX) and pumps.

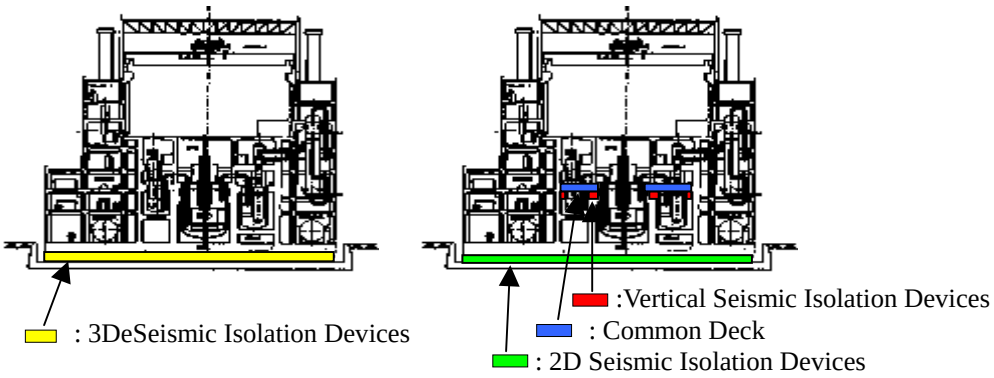

(a) 3D entire building Seismic Isolation System (b) Vertical+2D Seismic Isolation

Figure 1 Three-Dimensional Seismic Isolation Systems

3. REQUIREMENTS

3.1 Seismic Condition

The seismic condition for the research was defined sufficiently large so not as to be required as a condition in the future. A horizontal ground motion spectrum once defined in a past study (Kato M. et al., 1995 [2]) is adopted (Figure 2). This spectrum envelopes all the S_2 design ground motions for the Japanese LWR in the short period acceleration range and the spectral velocity was extended up to 2.0 m/s in the period ranging from 0.62 s to 10.0 s since the long period range is important for the seismic isolation systems. The vertical ground motion spectrum is defined applying a spectral ratio of 0.6 through the entire period, resulting in the maximum spectral velocity of 1.2 m/s (also shown in Figure 2). A set of ground motion time histories was generated to be compatible to these spectra. Their maximum accelerations in the horizontal and vertical time histories are 8.31 m/s^2 and 5.56 m/s^{2}respectively.

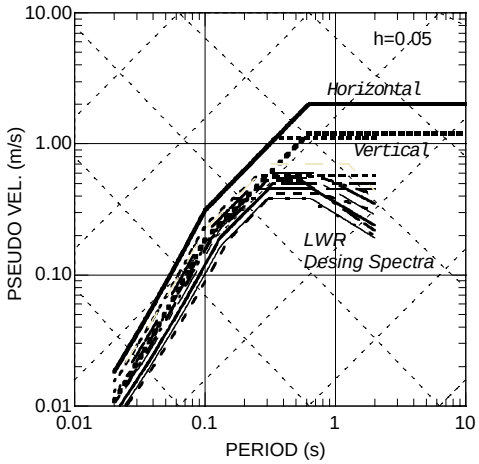

Figure 2 Design ground motion

3.2 Plant Condition

To obtain the requirements from the reactor building, middle-scaled sodium cooling type FBR plant was

adopted for reference, which is one of the promising plants in the ongoing R&D project for commercialized FBR. Figure 3 shows the layout of the reactor building. Table 2 shows the major specifications of the plant [4].

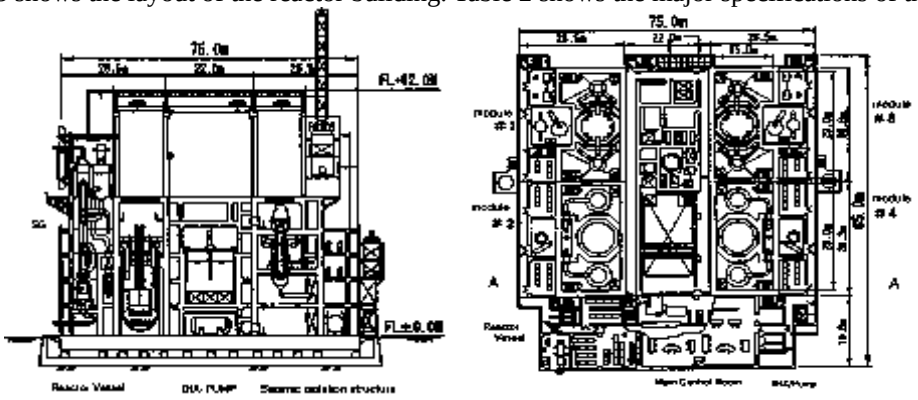

(a) Cross-section of the plant (b) Floor layout plan of the plant

Figure 3 Layout of the reactor building

Table 2 Major specifications of the plant

Items	Specifications
Reactor type	Sodium-cooled loop type reactor
Electricity output	750MWe×4
Building size	82m×75m×62m
Weight of the reactor building	About 2650MN

3.3 Required Performance

In the beginning of the project, to define the appropriate range of isolation period, performances required of the seismic isolation devices were investigated from the response analysis of the components and the building structures.

(1) Component design aspect

-To sufficiently reduce vertical acceleration → Acceleration at the reactor support <14m/s^2 (at 3Hz), <9m/s^2 (at 1Hz) and so on

-To avoid fuel assembly uplift → displacement of the reactor support plate< 6.5mm

-To avoid reactor vessel buckling. → Keep the theoretical formula with safety ratio 1.35

-To suppress relative displacement of piping → Displacement <0.7m for 3DeSIS, <0.12m for Vertical SIS

(2) Building structure design aspect

-To suppress amplification of vertical acceleration → Acceleration of the building <9.8m/ s^2

-To avoid uplift of isolation devices → Acceleration of the device<9.8m/ s^2

-To reduce horizontal acceleration (not to generate rocking motion)

→Acceleration of the building with rocking motion <19.6m/ s^2

Suitable combinations of appropriate frequency and damping ratio both for 3DeSIS and Vertical SIS were mapped by analysis with simulation models (Table 3). The target combination s for the devices shown in Table 4 are included in the suitable region s.

Table 3 Target frequency and damping

(a) For 3D SIS

Frequency (Hz)	Damping (%)			
	2	10	20	40
20				
3.0				
1.5				
1.0				
0.67				
0.5				

(b) For Vertical+2D SIS

Frequency (Hz)	Damping (%)			
	2	10	20	40
20				
3.0				
1.5				
1.0				
0.67				
0.5				

Table 4 Targets for the seismic Isolation devices

Seismic isolation system type	Vertical Frequency (Hz)	Vertical Damping Ratio (%)
3DeSIS	Less than or equal to1.0	20～40
Vertical +2D SIS	Around 1.0	20～40

4. THREE-DIMENSIONAL ENTIRE BUILDING SEISIMIC ISOLATION SYSTEM

4.1 System Concept

At the beginning of this R&D, several conceptual ideas for a 3DeSIS were proposed. These ideas were evaluated with tests using some reduced scale models. Finally the 'rolling seal (U-shape rubber) type air spring' [7] was selected for further development. Criteria for the selection were isolation performance, system reliability, applicability to the real plant, maintainability and economic competency. The idea of the 'hydraulic type of rocking-suppression cylinder system' [6] was also selected to suppress the excessive rocking motion of the building, which occurs on the three-dimensionally isolated structure. Figure 4 shows the selected combined concept of 3DeSIS. At the bottom of the reactor building, 160 air springs are delivered at the inner area and 112 hydraulic supports function with rocking suppression systems at the outer area. The rocking suppression cylinder system is shown in Figure 5. Hydraulic pressure of the load support cylinder is connected to the rocking suppression cylinder and further to the accumulator unit which mitigates the shock of the vertical load by gas inside. All piston rods of the rocking suppression cylinder are connected to each other so that pistons at both ends of the building compensate the vertical counter force and suppress the rocking motion.

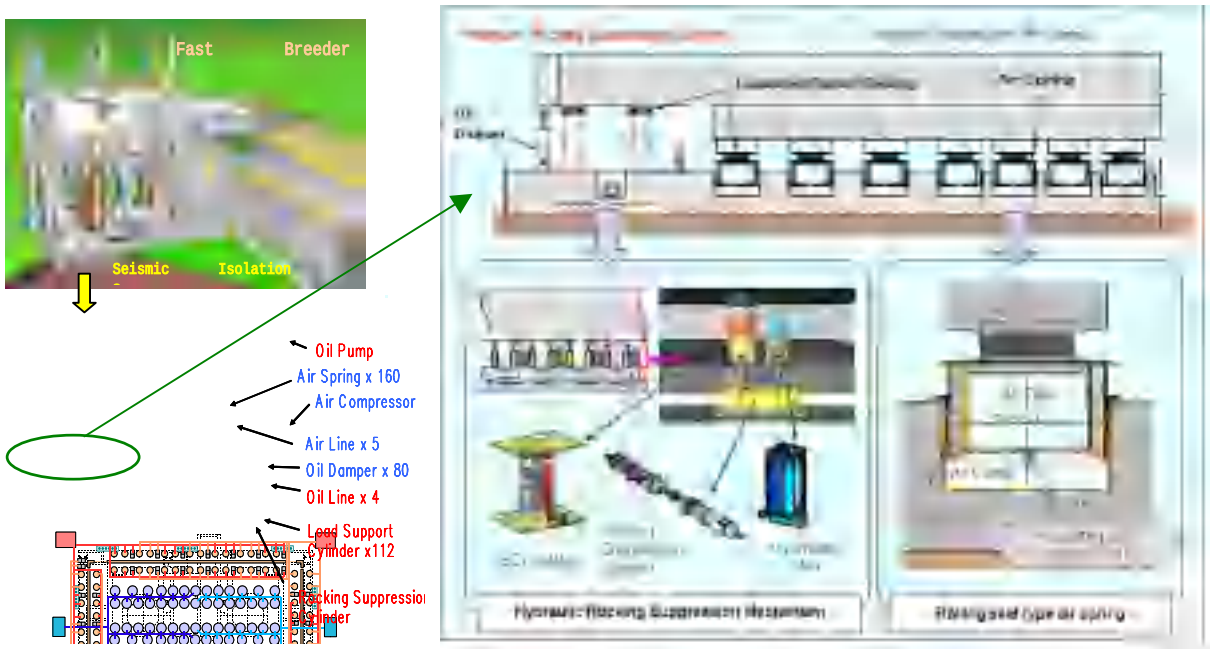

Figure 4 Concept of three-dimensional entire building seismic isolation system

Table 5 Main specifications of the candidates

	Hydraulic rocking suppression sys.	Rolling seal type air spring
Load Capacity	9.8 MN	9.8 MN
Inner Pressure	25 MPa	1.6 MPa
Vertical Period	2sec	
Horizontal Period	2.8sec	

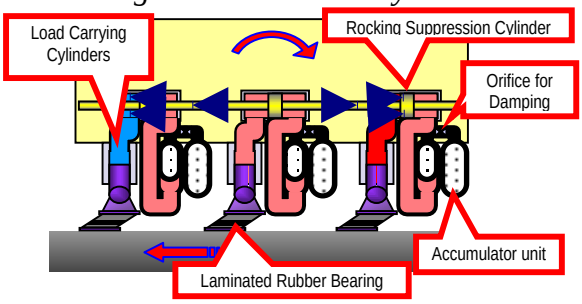

Figure 5 Rocking suppression system function

4.3 Verification Tests

(1) Air spring test

The Rolling seal type air spring was tested on the shake table with a 1/7 scaled model. The model consists of four air springs and four oil dampers. From the test result, natural frequency and damping ratio of the air spring and the oil damper were measured. The data were used for the combined system test on the shake table.

(2) Hydraulic function test

To investigate the performance of each element of the hydraulic rocking suppression system, cyclic load test was conducted with a 1/7 scaled model which consists of load support cylinder, rocking suppression cylinder, accumulator and corner cylinder. Natural frequency of the hydraulic rocking suppression system in the vertical direction and damping force were measured. Obtained data were used for the shake table test of the combined system.

(3) Combined system test

To investigate movement of the combined system of air spring and hydraulic rocking suppression system, shake table tests with a 1/7 scaled combined system were conducted (Figure 6). The scaled model consists of a building model, four air springs and four hydraulic support cylinders which are connected to four accumulators via four rocking suppression cylinders. The rods of the rocking suppression cylinders are connected to the corner cylinders installed at the corner of the shake table.

Figure 6 Picture of Combined System

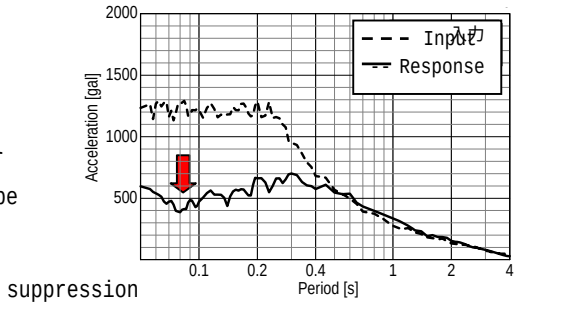

Figure 7 Floor Response Spectra (Vertical direction, model scale)

(4) Test results

- Support and isolation ability (Figure 7) were confirmed. Vertically, natural period and damping ratio (respectively 2.0sec, 40% in transformed real scale) satisfy the requirement.
- Devices move soundly. Especially, vertical movement of the sliding devices functions as expected.
- Damping by orifice shows good approximation to the analyzed value. Friction force accounts for a large part of the damping ratio. Applied to the real plant, friction is expected to become smaller.
- Damping ratio in the horizontal direction depends on the laminated rubber bearing with lead damper. This device functions as expected.
- Rocking motion was suppressed well by the rocking suppression device (inclination: less than 1/ 1000).
- Interference of vertical force and horizontal force are negligible. Analysis can be performed individually.

4.4 Applicability to the Plant

Based on the result of the verification test, applicability of the system was considered.

(1) Applicability of the Isolation Device

The test results show good approximation to the analyzed value in the simulation model. Designing factors were confirmed in the simulation. To design the real plant, a simplified practical model is applied to the simulation. The upper building elements are added to the practical model. Figure 8 shows the practical model. Vertical direction and horizontal direction are analyzed separately. The analyzed result with the practical model shows approximate value to the test result (Figure 9). The practical model is found to be applicable to the real plant.

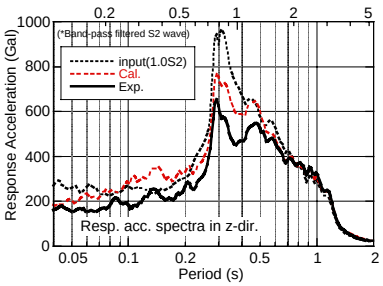

Figure 8
Floor Response Spectra
(Vertical direction)
-Comparison of experimental value and analysis of practical model without upper elements -

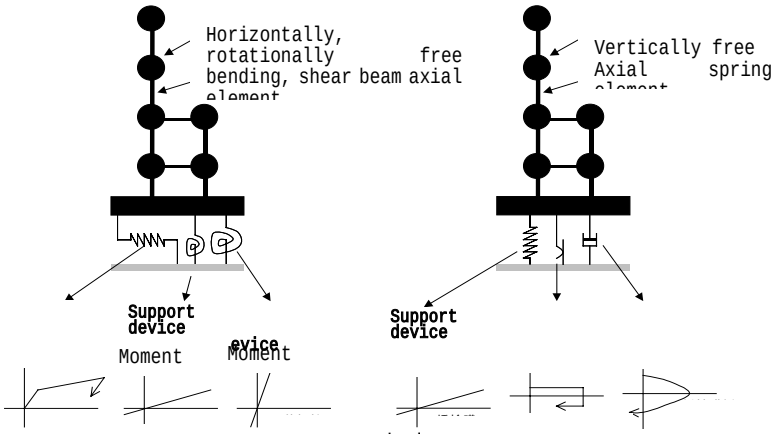

Figure 9 Practical model analysis -With upper elements-

(2) Practicability evaluation

Practicability of 3DeSIS for the FBR is evaluated by confirming the specifications. Requirements and provided specifications are shown in Table 6. Values in Table 6 are shown on the real plant scale.

Table 6 Practicability Evaluation

Required Items		Air spring	Hydraulic rocking suppression sys.
Performance	Variable range of natural period	1.0s～3.0s	1.7s～2.8s
		Whole system: 1.7s～2.8s	
	Damping ratio	Air spring : 10% Oil damper : 10%	25%
		Total :more than 20%	
	Stroke margin	less than 1/2 of physical limitation	less than 1/2 of physical limitation
System reliability	Numbers of support device	160(5 lines)	112(4 lines)
	Protection from environmental condition	With protection cover (Applicable range -35C～55C)	Dust seal
	Thermal condition	Air Conditioned	
	Exchange time of devices	Air spring : 0～1time/60 years Oil damper :0 time/60 years	Oil seal: less than 1 time /20 years Bladder: less than 1 time/10 years Oil: less than 1 time/10 years
Applicability	Work space for maintenance	Space around the spring : 0.5m Width of the corridor : 3.5m Height of corridor : 2.2m (without adaptation of building)	Width of the corridor : 2.5m (without adaptation of building)
	Installation (With trial schedule)	Not causing bottleneck (Total 4.5 months)	Not causing bottleneck (Total 7.5 months)
	Allowable damaged device number*	27	8 (59)**
Maintainability	Required man-days for inspection	Patrol 1day by 2men ISI 4days by 6men	Patrol 4.5days by 4men ISI 18 days by 7men
	(Remarkable note)	- Sliding device is inspected intensively. - Sampling test device for durability affirmation is delivered.	

* In the condition of 1.0 S2 seismic force
** In the case that the damaged devices are not located at one side.

5. VERTICAL SEISMIC ISOLATION SYSTEM

5.1 System Layout

Figure 10 shows the layout of vertical SIS based on the design of FBR. The common deck which supports main components (RV, IHX, Pump, piping) is vertically isolated from the reactor building by 20 seismic isolation device units. One unit consists of 70 coned disk springs. In the unit, five springs are stacked in the same direction and the next five springs are in the opposite direction. Washers are inserted between every 5 spring sets. Damping force is obtained from the three dampers attached at the top of the isolation unit. The damper is a type of cantilever made of steel.

Horizontally, the common deck is held by four key functions at every side and four sliding guides around the reactor. These functions keep the horizontal rigidity of the common deck. The temperature of the common deck is controlled and thermal expansion in the operation does not affect the support function.

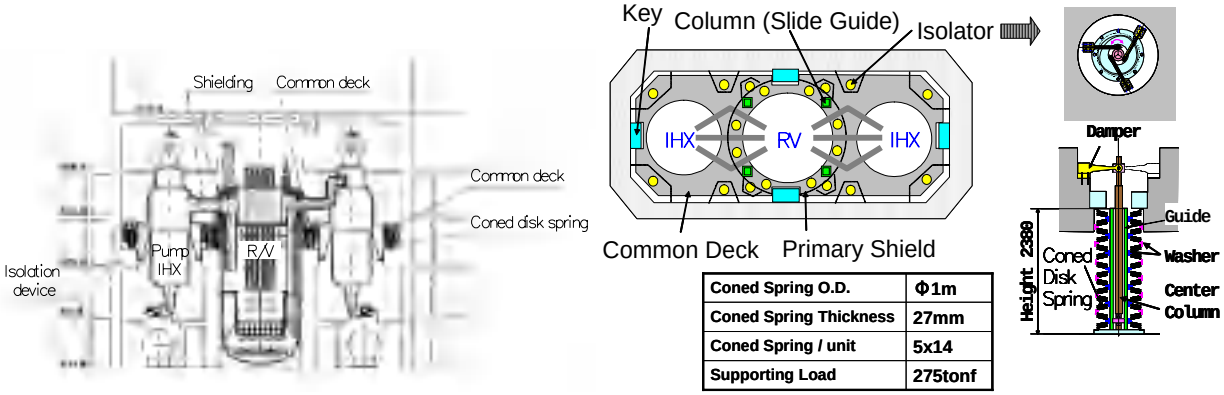

Coned Spring O.D.	Φ1m
Coned Spring Thickness	27mm
Coned Spring / unit	5x14
Supporting Load	275tonf

Figure 10 Layout of vertical seismic isolation system

5.2 Verification Test

(1) Coned disk spring test

Test of the coned disk spring was conducted with several scale test pieces [5]. Properties were investigated with real size test piece because the size is huge and beyond the Japanese industrial standards.

(2) Damper test

Damper's characteristics were investigated with real size test pieces. This damper was designed to obtain 150kN damping force. In order to confirm the stability of dynamic characteristics and fatigue strength of the damper, cyclic loading tests with constant displacement with the estimated response wave were conducted.

(3) System test

To confirm the feature of the system, shake table tests were conducted with a 1/8 scale model of the common deck. Figure 11 shows the model, which has four coned disk spring units, four key functions and slide guides. In the basic test, system characteristics (response, natural period, damping ratio) were measured. Obtained data are applied to the design of a real plant. To raise the credibility of the system, a mass balance test was performed. Rocking motion with imbalanced masses delivered on the common deck was measured.

(4) Horizontal force test

Affection of the horizontal force and displacement to the vertical movement was investigated. The test was performed with a 1/8 scale model (5stack x 14) and 1/2 scale model （5stack x 4）.

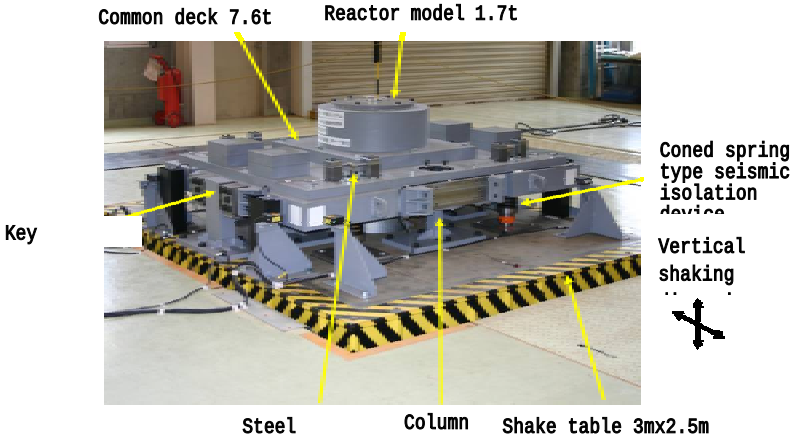

Figure 11 Picture of the vertical isolation system test

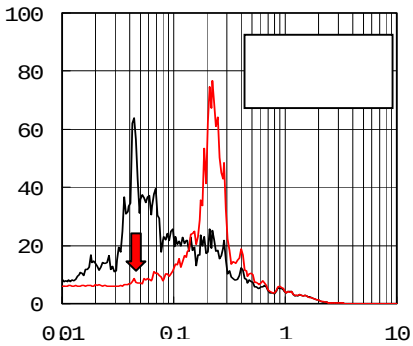

Figure 12 Floor response spectra (Vertical direction arranged to real plant scale)

(5) Test results
- The system moved soundly and performed the expected isolation ability (Figure 12).
- The large dimensional coned disk performed according to the theoretical rule.
- Friction coefficient between the coned disk springs (and washers) was about 0.1.
-The steel damper satisfied required damping ratio and durability.
- Rocking motion is negligible in the condition that the gravity center of the isolated staffs (components, piping and so on) is located inside the structure of the common deck.
- Affection of horizontal displacement is negligible for the vertical movement of the isolation device.
- Displacement of the isolation unit is not observed when washers with high rims are applied.

5.3 Applicability to the Plant

(1) Applicability of the isolation device

The test results show the system has the isolation ability in the real scale. Real size data of the coned disk spring were obtained. Analysis can be performed with the vertical and horizontal models. The gap between the common deck and supporting key is not generated in the normal operating temperature.

(2) Practicability evaluation

Practicability of the vertical SIS for FBR is evaluated by confirming the specification. Requirements and specifications are shown in Table 7. Values in Table 7 are shown on the real scale.

Table 7 Practicability evaluation

Items	Required Item	System
Performances	Variable range of natural period	0.6 ～ 0.8 s
	Damping ratio	20～40%
	Vertical stroke margin	±100mm (less than 1/ 2 of physical limitation)
System Reliability	Numbers of support device	20 coned disk spring isolation units /common deck
	Protection from environmental condition	Air conditioned (Temperature:20C～40C)
	Exchange time of devices	No exchange in life time (maintenance free)
Applicability	Work space for maintenance	Operation floor
	Install term (With trial schedule)	Not causing bottleneck 65days /common deck
	Allowable damaged device number	20 units (trifle damage)* The unit functions in the condition of slight damages
Maintainability	Required man days for inspection	Patrol: 16 man days In service inspection: 19 man days

* In the condition of 1.0 S2 seismic force

6. CONSIDERATION

6.1 Applicability

Noticeable points to adopt the isolation system are as follows.

(1) 3D entire building seismic isolation system

(a) Layout concept in the plant building is almost the same as the conventional plant. Isolation system is applied to the plant with little modification.

(b) The area where the isolation system is installed is not affected by radiation. In-service inspection can be done easily. Maintenance can be conducted any time when a failure is found in the daily patrol.

(c) Numbers of support device are 272. Function failure of 10% of total system devices does not lose isolation function. Device is able to be exchanged in the operation term.

(d) Oil, oil seal, bladder in hydraulic system and rubber in air spring are exchanged once in 10～30years. It can be detected in advance by investigating the sampling test device for durability affirmation.

(e) In order to keep the building floor level horizontal, pressure in the device and surrounding air temperature need to be controlled.

(2) Vertical + 2D seismic isolation system

(a) The coned dish spring is reliable and essentially maintenance free in its whole life.

(b) The common deck is installed at the area where components and piping are concentrated. A minimum number of isolation devices are installed.

(c) The common deck makes the reactor building a little larger.

(d) The system is installed at the area affected by radiation. Material and lubricant of the isolation equipment need to be radiation-proof. Access time needed for inspectors is limited and inspection is usually done with remote monitors.

(e) To exploit the function of horizontal isolation system under the reactor building, the common deck needs to be supported firmly in the horizontal direction. Temperature of the common deck needs to be controlled.

6.2 Further Research

To make the system more reliable, economical and practical, further research should be performed.

(1) Enhancement of reliability

(a) Verification test with real size model (3DeSIS)
- -To obtain better designing properties
- -To confirm behavior of the devices at near their performance limit

(b) Test with real building
- -To obtain data in the real condition

(2) Cost reduction

(a) High pressurized air spring (3DeSIS)
- -To make the air spring smaller and flexibly delivered
- -To make the manufacturing cost lower

(b) Improvement of hydraulic seal (3DeSIS)
- -To make the hydraulic seals stronger and durable

(c) Improvement of the layout (Vertical SIS)
- -To avoid interference of equipment, i.e. horizontal support structure, cooling pipe
- -To reduce the factors which make the reactor building large.

(3) Preparation of design guideline
- -To stipulate combination way of force, margin, criteria, etc.
- -To accumulate real and concrete data about the plant, i.e. inclination, temperature, water proof etc.

7. CONCLUSIONS

Three-dimensional seismic isolation systems for the nuclear plant were developed. From tests of the system element and analysis, both the '3D entire building seismic isolation system' and the 'Vertical+2D seismic isolation system' were found to be applicable and their practicability should be developed further. Following are the basic items obtained in the study.

(1) Two types of isolation systems, a 3D entire building and a vertical +2D seismic isolation system were developed.

(2) For the 3DeSIS system, the 'rolling seal type air spring with hydraulic rocking suppression system' was finally selected from several kinds of concepts.
(3) For the vertical +2D system, the coned disk spring technology is applicable.
(4) Seismic condition for the analysis adopted a conventional ground motion used for the previous R&D. The ratio of the vertical to horizontal directions is settled to be 0.6.
(5) As the vertical frequency target, less than or equal to 1.0Hz in the case of 3DeSIS, around 1.0Hz in the case of vertical +2D SIS were settled. As the vertical damping ratio, 20 to 40% for both systems was settled.
(6) Verification tests of 3DeSIS were conducted. Isolation and rocking suppression were confirmed by shake table test with their combined 1/7 scale model furnishing four air springs and four hydraulic rocking suppression systems. Test results and analysis prove that the system is applicable to the real plant.
- Supporting load and isolation values (spring ratio, damping ratio) were reasonable and similar to the expected values.
- Rocking motion is suppressed by the hydraulic rocking suppression system.
- The practical simulation model for analysis is available to real plant design. Design data is prepared by adjusting the test result by scale factor.

(7) Verification test of vertical SIS was conducted and basic properties of the coned disk spring were measured.
- Each element of the isolation unit, coned disk spring, steel damper, and rimmed washer performed to the expected ability.
- Isolation systems including the common deck performed to vertical isolation ability.
- Horizontal force and displacement in the normal operation does not disturb vertical movement of the isolation devices.

(8) Practicability of the systems was evaluated with isolation performance, system reliability, applicability to the plant and maintainability.

AKNOWLEDGEMENTS

This study was made as a part of the Ministry of Economy, Trade and Industry of the Japanese government sponsored R&D project on 3D seismic isolation. At the same time, a part of the data was quoted from the study results of the electric power utilities on 3D seismic isolation. The authors give special thanks to the members of the committee of the 3D seismic isolation system.

REFERENCES

[1] JEAG 4614-2000,"Design Guideline of seismic Isolation Systems for Nuclear Power Plants", Japan Electric Association, (2000)
[2] Kato M. et al. "Design study of the seismic-isolated reactor building of demonstration FBR plant in Japan", Trans. of the 13th SMiRT, Vol.3, Div. K, pp579-584, Brazil, August, (1995)
[3] Kato A. et al., "A Development Program of Three-Dimensional Seismic Isolation for Advanced Reactor Systems in Japan." 17th SMiRT (2003)
[4] Hishida M. et al. "An Innovative Concept of Sodium-Cooled Middle-Scale Modular Reactor Pursuing High Economic Competitiveness", GENES4/ANP (2003)
[5] Kitamura S, Morishita M, Moro S. "Study on Vertical Component Seismic Isolation System with Coned Disk Spring", ASME PVP (2004)
[6] Shimada T, Fujiwaka T, Moro S, "Study on Three-dimensional Seismic Isolation System for Next Generation Nuclear Power Plant: Hydraulic Three-dimensional Base Isolation System", ASME PVP (2004)
[7] Hagiwara T, Suhara J, Moro S, "Three-dimensional Seismic Isolation Device with Rolling Seal Type Air Spring", ASME PVP (2004)

18th International Conference on Structural Mechanics in Reactor Technology (SMiRT 18)
Beijing, China, August 7-12, 2005
SMiRT18-K11-4

EXPERIMENTAL STUDY ON VERTICAL COMPONENT ISOLATION SYSTEM

Shigeki Okamura
Japan Nuclear Cycle Development Institute, Ibaraki, Japan
Phone: +81-29-267-4141,Fax: +81-29-267-5279
E-mail: okamura.shigeki@jnc.go.jp

Seiji Kitamura
Japan Nuclear Cycle Development Institute, Ibaraki, Japan
Phone: +81-29-267-4141,Fax: +81-29-267-5279
E-mail: kita@oec.jnc.go.jp

Kenji Takahashi
Japan Atomic Power Company, Tokyo, Japan
E-mail: takahashi.kenji@jnc.go.jp

Takahiro Somaki
O-BAYASHI Company, Tokyo, Japan
Phone: +81-3-5769-2723,Fax: +81-3-5769-1943
E-mail: somaki.takahiro@obayashi.co.jp

ABSTRACT

In Japan, several kinds of three-dimensional seismic isolation system for next-generation nuclear power plant such as fast reactors have been studied in recent years. We proposed a structural concept of a vertical component isolation system, assuming a building adopting a horizontal base isolation system. In this concept, a reactor vessel and major primary components are suspended from a large common deck supported by vertical isolation devices consisting of large coned disk springs. In order to verify the isolation performance of the vertical component isolation system, shaking table tests using a 1/8 scaled model were conducted. The test model was composed of 4 vertical isolation devices, common deck and horizontal load support structure. For the design earthquake, the system smoothly operated, and sufficient isolation characteristics were shown. The simulation analysis results matched well the test results, so the applicability of the design technique was verified. As the result, the prospect that the vertical isolation system applied to the FBR plant could technically realize was obtained.

Keywords: Three-dimensional Seismic Isolation device, Vertical isolation system, Coned disk spring, Common deck, Shaking Table Test

1. INTRODUCTION

Although the horizontal force of an earthquake ground motion is sufficiently reduced by a base isolation system with laminated rubber bearings, the vertical force is transmitted directly. If a three-dimensional isolation were achieved by adding a vertical isolation system, it would substantially enhance plant economy and safety. In order to realize a three-dimensional isolation system, two types of systems can be considered. One is a three-dimensional base isolation system, and the other is a combination of base horizontal isolation and vertical component isolation. In FBR plants, structural problems in which the consideration for vertical motion is required are uplift of fuel assemblies, reactivity change and buckling of reactor vessel. Since vertical isolation coverage can be limited to the area in which a reactor vessel and primary coolant system are installed, we have constructed a structural concept of a vertical component isolation system called “common deck vertical isolation system” [1].

When the vertical isolation system is adopted in individual component separately, the relative displacement will be dynamically taken in the primary coolant system piping, because each response characteristic is different. In order to avoid this problem, a reactor vessel and major primary components are suspended from a large slab

structure called “common deck”, and vertical isolation devices are installed between the deck and substructures. Coned disk springs were chosen for spring element of the vertical isolation device. The disk spring can be stacked in various configurations. By stacking the coned disk springs of the same shape in parallel, it is possible to increase support load per one device. By stacking this set more and more in several series, large stroke can be achieved.

We designed the vertical isolation device with coned disk springs and steel beam dampers for FBR plants, which could be achieved vertical isolation frequency of 1Hz and damping ratio of 20%. Full scale coned disk spring and damper performance tests were carried out, and the validity of design method was confirmed [2].

In this paper, a series of shaking table test using a 1/8 scale model of the common deck vertical isolation system is described.

2. OUTLINE OF VERTICAL ISOLATION SYSTEM

2.1 Isolation Device

A coned disk spring for seismic isolation device has following features. 1) The restoring force characteristics show nonlinearity. 2) The effect of the ground end cannot be disregarded. 3) The effect of the friction becomes remarkable, because large number of coned disk is stacked. Considering these features, a single coned disk (Fig.1) is designed using the following equation by Curti and Orland [3].

$$P = \frac{E\delta}{a^2}\left\{(h0-\delta)(h0-\delta/2)Ct + Dt^3\right\} \tag{1}$$

where,

$$C = \frac{2\pi}{1-\nu}\frac{\alpha^2}{(\alpha-1)^3}\left(\frac{1+\alpha}{2} + \frac{\nu}{1+\nu}\frac{\alpha^{\nu+1}-1}{1-\alpha^{\nu}}\right)$$

$$D = \frac{\pi}{6}\frac{a}{d}\frac{\alpha}{\alpha-1}$$

$$d = \frac{\nu}{1-\nu}a\frac{\alpha^{\nu-1}-1}{1-\alpha^{\nu}}$$

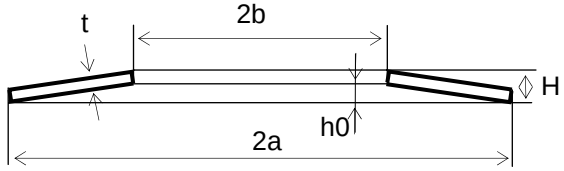

Fig.1 Coned disk spring

P : Spring load of single disk
δ : Deflection of single disk
E : Modulus of elasticity
b : Inside radius of spring
$h0$: Initial cone height of spring
υ : Poisson’s ratio
a : Outside radius of spring
α : Ration of outside to inside diameter = b/a
t : Thickness of single disk

And, the equation of Niepage [4] which can appropriately consider the effect of the friction is also used in the design of the isolation device.

$$P_1 = \frac{P}{\left\{1 \pm \mu M (n-1)\frac{\alpha}{\alpha-1}\frac{1}{a/t}\right\}} \times \frac{1}{\left[1 \pm \frac{\alpha}{\alpha-1}\frac{1}{a/t}\left\{\frac{h0}{t}\left(1-\frac{\delta}{h0}\right)+1\right\}\mu R\right]} \tag{2}$$

$$P_f = n \times P_1$$

$$\delta_f = m \times \delta$$

where,

P_f : Spring load of stack
n : Number of single disk stacked in parallel
μM : Factor to account for inter-surface friction
δ_f : Deflection of stack
m : Number of disks stacked in series
μR : Factor to account for edge friction

A schematic drawing of the isolation device is shown in Fig.2. The coned disk spring is made of the ordinary high tensile spring steels, Japanese Industrial Standard (JIS) SUP10, which is almost the same as SAE 6150 in USA. Outside diameter of the coned disk was set to be 1m and thickness was set to be 27mm, considering current productivity from the viewpoint of machining and heat treatment. By stacking 5 disks in parallel and 14 sets in series, the isolation device is made up 70 disks in total. The middle washers are inserted

between coned disk springs of the serial stack in order to prevent side slip. And, the center guide is installed inside of disks. The unloaded height of a stack becomes about 2.5m. Steel beam dampers with the hysteretic behavior are installed at the upper part of the device. In order to increase the low cycle fatigue strength, a tapering beam damper was designed. It is possible to produce the necessary damping force, when the device was combined with 3 dampers per one device.

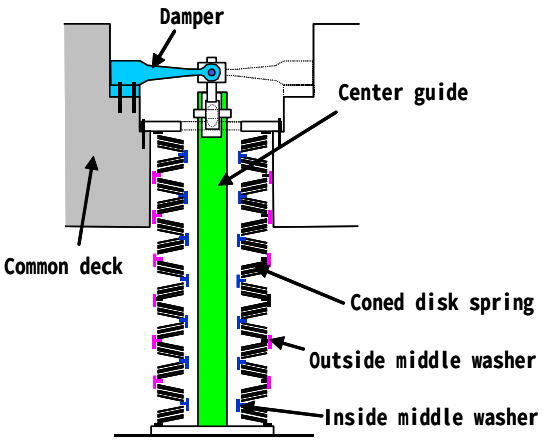

Fig. 2 Schematic drawing of isolation device

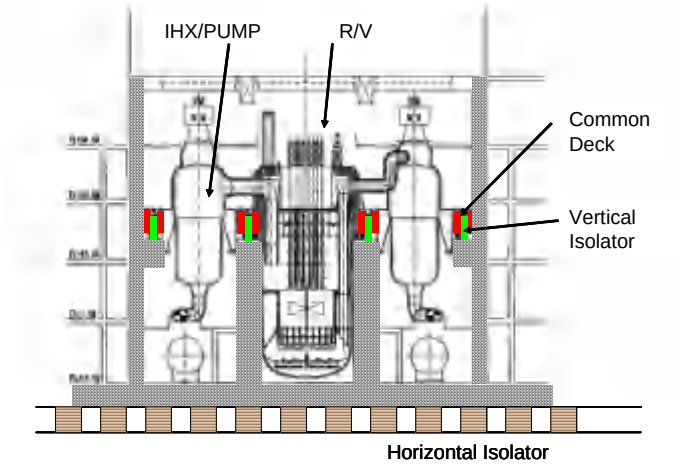

Fig.3 Plant layout

2.2 Plant layout

Application of the common deck isolation system to a 750MWe sodium cooled loop type FBR plant [5] is shown in Fig.3. In this plant, the common deck supports reactor vessel and two integrated components which combined the intermediate heat exchanger with the pump. The deck becomes a rectangle of 32m×12m size. The thickness of the deck is made to be about 2m in order to ensure the necessary rigidity. Total installation weight is about 57MN, and it is supported by 20 isolation devices. Considering weight distribution and rigidity allocation, the isolation device was mainly placed at circumference of reactor vessel and peripheral part of the deck. Horizontal load acting on the common deck is the horizontal seismic load and thermal expansion load as a result of temperature change by operating state. Horizontal load support structure is established so that it may not exert the horizontal load on the vertical isolation element. It shows the design concept of horizontal support structure in the following.

1) The horizontal load is not exerted on the isolation element.

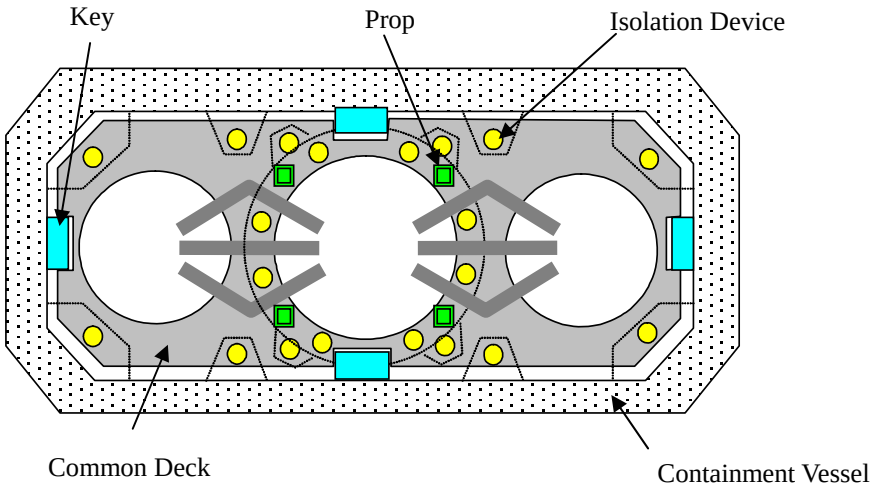

Fig.4 Design of common deck and horizontal load support structure (Application example to 750MWe sodium cooled loop type FBR plant.)

2) It smoothly operates in the vertical direction.
3) The thermal expansion is not restricted.

As a design example of horizontal load support structure, key and prop are installed. The key is horizontally supported through the cylindrical rollers in the horizontal and vertical directions. It is installed on the symmetric line of the common deck, and the thermal expansion of the symmetric axis direction is not restricted. The prop is installed in the circumference of the reactor vessel, and the thermal expansion displacement is absorbed in the elastic deformation of the prop.

3. TEST MODEL

3.1 Common deck

Objectives of the shaking table test are to confirm the isolation performance of the proposed isolation system during the earthquake.

The test model was composed of 4 vertical isolation devices, which were reduced at the ratio of the length in 1/8, common deck and horizontal load suspension system. The law of similarity is shown in Table 1, and the dimension of the test model is shown in Tables 2.

The test model is shown in Fig.5 and Photo 1. The dimension of the common deck model is 1.7m×2.2m with thickness of 0.2m. The cylindrical mass, which is modeled a reactor vessel, is set up in the center of the common deck. The sum total weight of the common deck model and the cylindrical mass is 76.2kN.

Table.1 Law of similarity

Physical Quantity	Dimension	Test model / Actual system
Length	L	1/n
Time	T	$1/n^{1/2}$
Mass	M	$1/n^{2}$
Velocity	L/T	$1/n^{1/2}$
Acceleration	L/T^2	1
Stress	$M(L/T^2)/L^2$	1

Table.2 Specification of test model

Physical Quantity	Actual System	Scale Model
Outside diameter	ϕ1000	ϕ130
Period	1.1 Hz	2.8 Hz
Support load	2.8MN (5 in parallel)	18.6kN (2 in parallel)

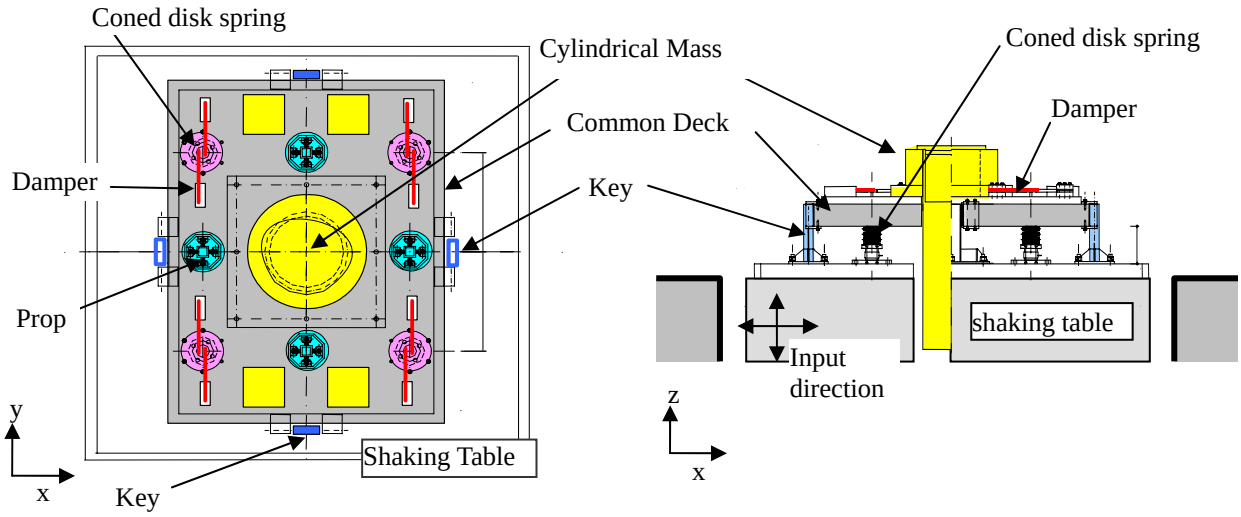

Fig. 5 Testing arrangement

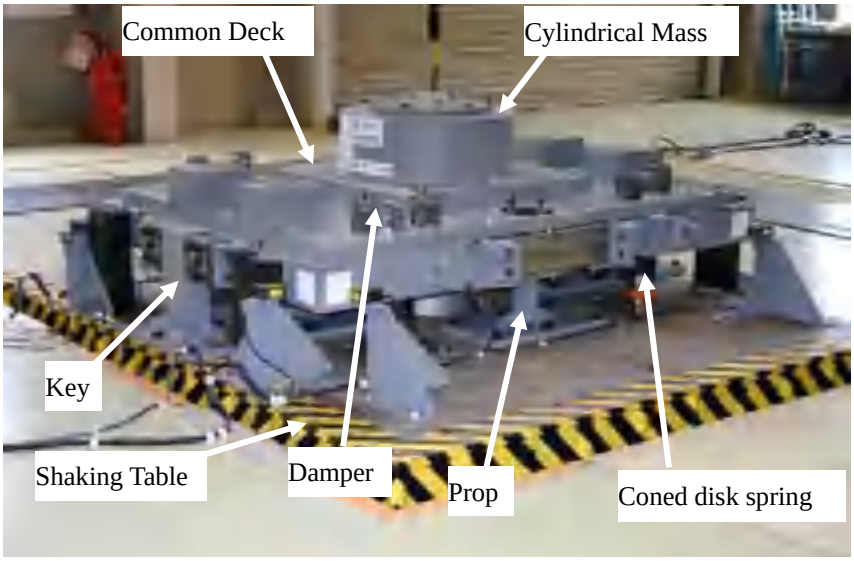

Photo 1 Test specimen on shaking table

3.2 Isolation Device

The geometry of single coned disk spring specimen is shown in Fig.6. The coned spring is standard product by press forming. The combination of coned disk springs for the vertical isolation device model is designed to be 2 in parallel and 14 in series, and then one device model consists of 28 disk springs in total. A preassembled disk spring stack is shown in Photo 2. The characteristic of a vertical isolation device is shown in Fig.7.

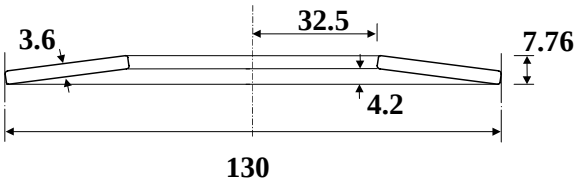

Fig.6 Geometry of coned disk spring in mm

Photo 2 Coned disk spring

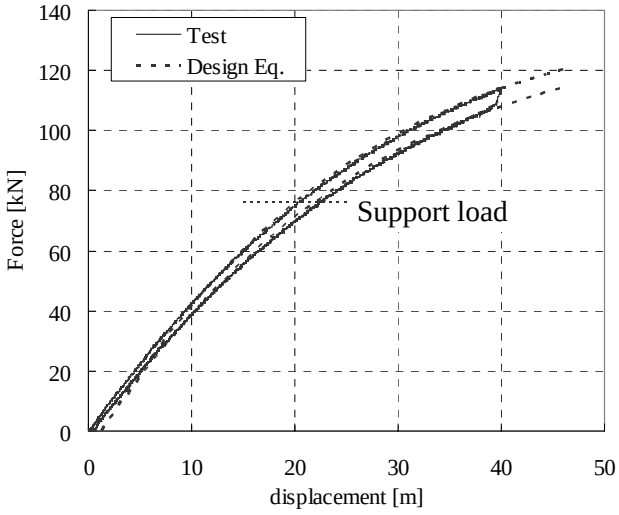

Fig. 7 Restoring force of vertical isolation device

3.3 Damper

The geometry of the damper model is shown in Fig.8. The damper is made of general steel, and it has taper so that stress distribution may become uniform. Photo 3 shows the installation view of the damper. Two dampers are installed in one device. One end of the damper is fixed on the common deck, and the other end is connected to the center guide using a spherical bearing. Two spherical bearings are attached to both end of the guide. As shown in Photo 3, three spherical releases the rotation that results from the reducing axial length when the damper deforms.

The damping force was designed considering the law of similarity and parallel number of coned disk spring. The restoring force characteristics of two dampers are shown in Fig.9. From the results of a design analysis, the vertical frequency of the test model increased to 4.5Hz by the initial stiffness of the damper.

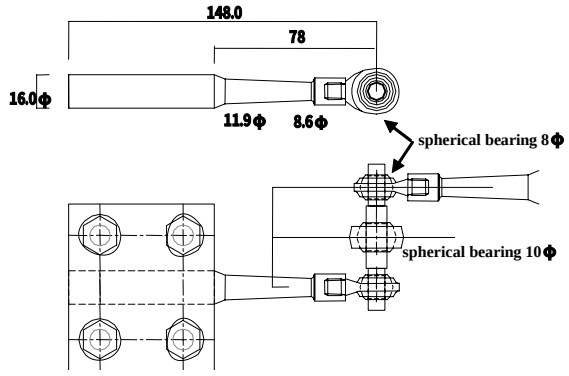

Fig. 8 Geometry of damper

Photo 3 Steel beam damper

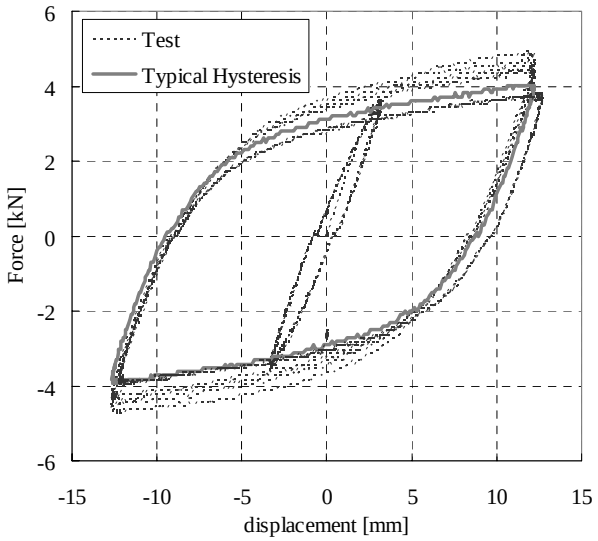

Fig. 9 Restoring force of damper

4. SHAKING TABLE TEST

4.1 Test Cases

The frequency response characteristics in horizontal and vertical directions of the test model were measured by sine sweep tests. In order to confirm the isolation performance of the isolation system during the earthquake, a series of seismic wave tests was carried out. Test cases are shown in Table 3.

Table.3 Test Case

Test Case	direction	Input wave		
Sine Sweep Test	horizontal	Sine	2-60[Hz]	0.45 [m/s^2]
	vertical		2-20[Hz]	0.60 [m/s^2]
				1.20 [m/s^2]
				2.40 [m/s^2]
Seismic Wave Test	horizontal and vertical	0.67 times seismic wave		
		seismic wave		
		1.5 times seismic wave		
Horizontal Load Support Structure Test		seismic wave		

The input seismic wave was set in the following procedures.

1) The design earthquake, named "Case Study S2", was set for the isolation device development by "The three-dimensional isolation development project in Japan" [6].
2) Response acceleration at the isolation device installation level was evaluated by seismic response analysis of a typical FBR building (Fig.10) for the design earthquake.
3) Time axis of the response acceleration was reduced to 1/2.8 ($=1/\sqrt{N}: N=7.7$) according to the law of similarity. Floor response spectrums are compared in Fig.11.

In addition, in order to investigate the effect on the response by preload and clearance of the roller of the horizontal load support structure, Horizontal Load Support Structure Test was carried out.

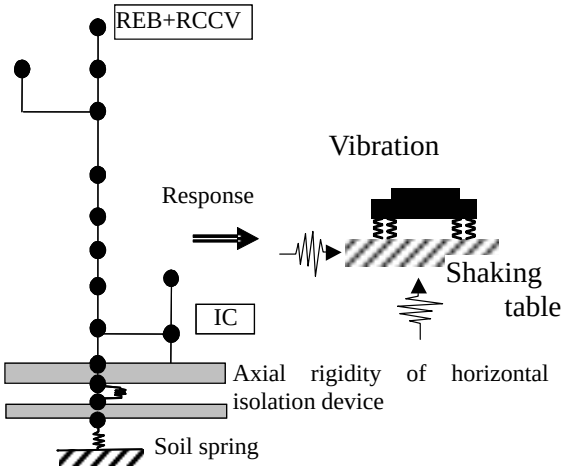

Fig.10 Analysis model of FBR building

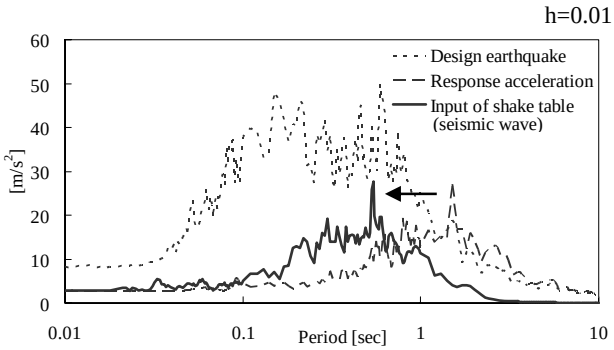

(a) Horizontal direction

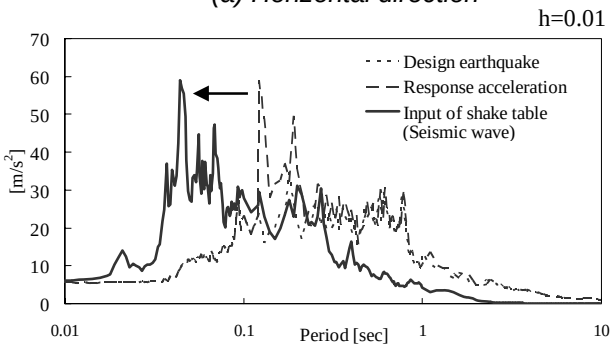

(b) Vertical direction

Fig.11 Floor response spectrum of input wave

4.2 Frequency Response Performance

The transfer functions obtained by the sine sweep tests are shown in Fig.12. The horizontal dominant frequency of the test model is about 25Hz, which is determined by the total stiffness of the horizontal load support structures. The vertical resonance frequency is about 3.5Hz, 4.5Hz, 5.0Hz for input level 0.60m/s^2,

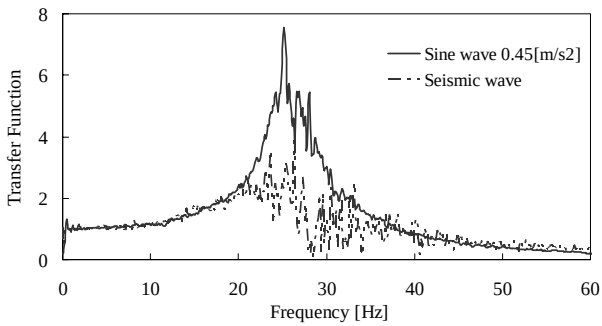

(a) Horizontal direction

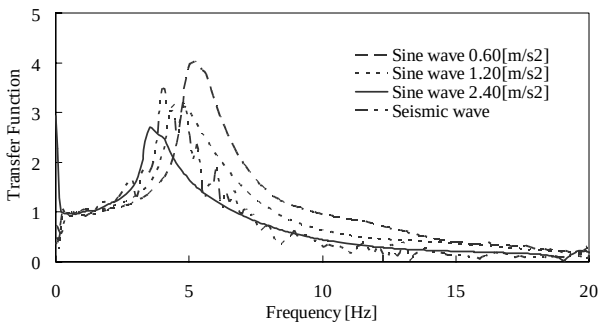

(b) Vertical direction

Fig.12 Transfer function obtain by Sweep Test

1.20m/s^2, 2.40m/s^2 respectively. As the input level increases, the vertical frequency increases, because the characteristic of the isolation device which consists coned disk springs and steel dampers have the softening property. In Fig.12, frequency response performance curve obtained by the seismic wave test is also plotted. In this case, vertical resonance frequency becomes about 4.8Hz, and almost the same as the design value 4.5Hz. Damping ratio obtained by the curve fitting method using the transfer function of the seismic wave test is about 20%, which is well consistent with the design value. Therefore, it can be judged that the design method of the vertical isolation device was appropriate.

4.3Seismic Wave Test

Seismic wave tests were carried out using the seismic wave in several times, it was confirmed that the system smoothly responded. The typical results of the seismic wave test are shown in Fig.13. In the figure, the acceleration at the center of common deck, the displacements of common deck in horizontal and vertical directions are shown.

In horizontal direction, there is no difference between the input and the response acceleration. Relative displacement between the common deck and the shaking table is very small. Therefore, it was confirmed that the horizontal load supporting systems sufficiently supported the horizontal seismic load.

In vertical direction, we can see the high frequency component has faded away from the waveform of the response acceleration. Maximum value of the response acceleration is almost the same as that of the input. Maximum value of the response displacement is about 9mm.

Fig. 14 shows the Floor Response Spectra (FRS) at the center of common deck for each input level, comparing with the seismic wave. The parts of the arrow in these figures are natural period band, reduced by the law of similarity, of the main equipment and piping. Though the FRS in horizontal direction is amplified a little near 0.04sec of the natural period of horizontal support systems, the FRS of the seismic wave test is less than the acceleration value of equipment design criteria of 9.8m/s^2.

The vertical isolation performance was confirmed, because the FRS around natural period band of the main equipment and piping was sufficiently reduced.

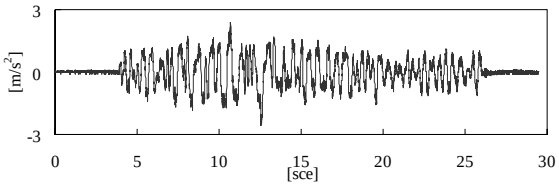

(a) Horizontal input acceleration

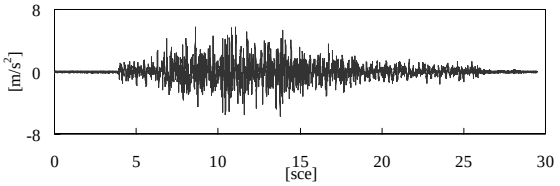

(d) Vertical input acceleration

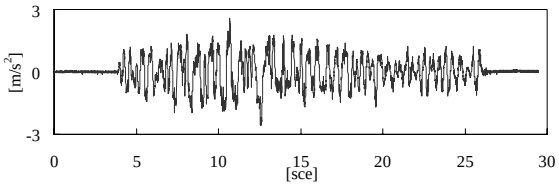

(b) Acceleration on the deck in horizontal direction

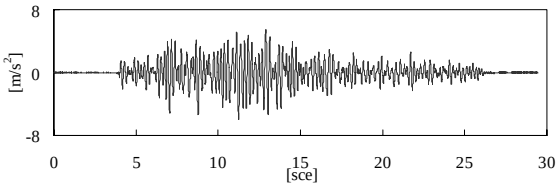

(e) Acceleration on the deck in vertical direction

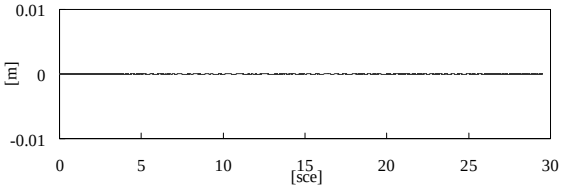

(c) Relative displacement of the deck in horizontal direction

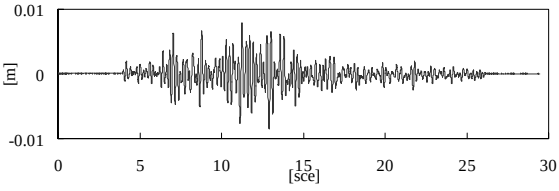

(f) Relative displacement of the deck in vertical direction

Fig. 13 Time histories of seismic wave test

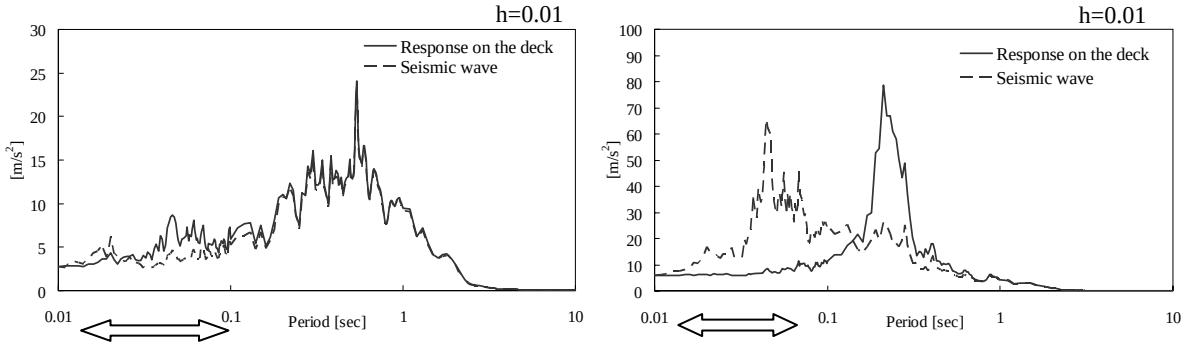

(a) Horizontal direction *(b) Vertical direction*

Fig.14 Floor response spectra of seismic wave test

4.4 Horizontal Load Support Structure Test

The horizontal load support structure test was carried out in order to examine the effect of the preload of the roller on the response. The standard setting of the preload of the roller was made to be 0.1 times of horizontal seismic load calculated by static analysis. The horizontal support structure test was carried out under following conditions.

Case-1: The preload of key-1 is set at 10 times of the standard setting.
Case-2: All rollers are made to be the contact condition.
Case-3: Clearance of 1mm is set at the roller of key-1 and key-2.
Case-4: Clearance of 1mm is set at all rollers.

Table.4 Condition of Horizontal Load Support Structure Test

Condition	Condition of Horizontal Load Support Structure		
	Key-1	Key-2	Prop and Key
Case-0	Standard setting		
Case-1	10 times	standard setting	
Case-2	contact		
Case-3	Clearance 1mm		contact
Case-4	Clearance 1mm		

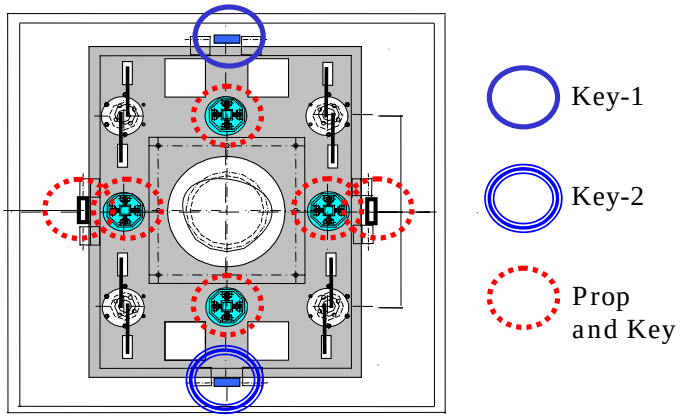

Fig.15 Position of horizontal load support structure

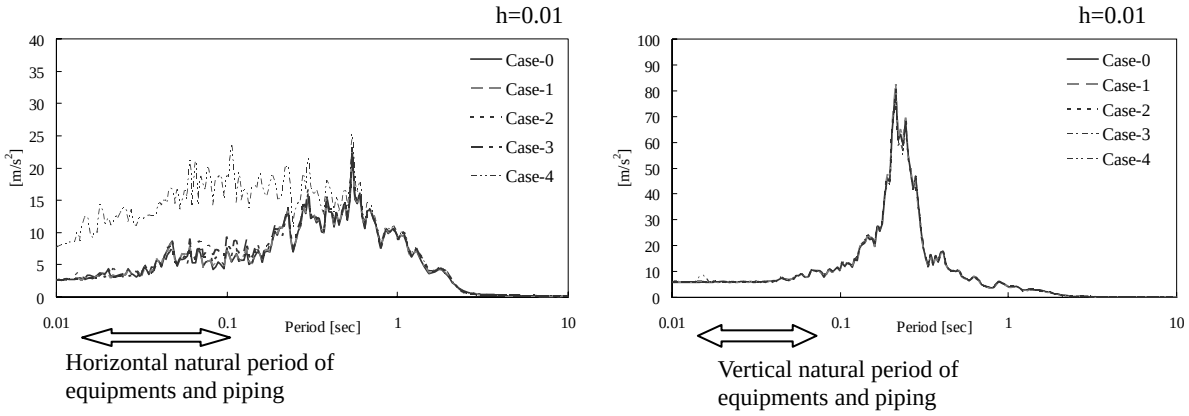

(a) Horizontal direction *(b) Vertical direction*

Fig.16 Floor response spectra of seismic wave test

Fig.16 shows the floor response spectra (FRS) at the center of the common deck model. In vertical FRS, the effect of the preload is not recognized. The effect of the preload of the horizontal support structure can be seen in the low-period region of horizontal FRS. Especially, the horizontal response is greatly increased in the case-4. Therefore, it is necessary that the clearance would not occur in the real machine design.

The clearance does not occur in the roller of the prop, because the thermal expansion displacement is absorbed in the elastic deformation of the prop. By ensuring the rigidity of the prop so that it may not affect the floor response, there is no amplification of the horizontal response, as the result of case-3 shows. By the effect of the gamma exothermic effect, the temperature of the common deck rises. The cooling unit is founded in the inside of the deck so that the temperature of the common deck may not rise. As a result of the thermal expansion analysis, it has been proven that the temperature around the key with much proportion of the steel product tends to rise higher than the temperature of the common deck. Therefore, the clearance does not occur in the roller of the key.

5. SIMULATION ANALYSIS

5.1 Analysis Model

Simulation analysis of the test model was conducted. The analysis model is shown the Fig.17. In horizontal direction, analysis model is two-degrees-of-freedom with two-mass model which consists of the common deck and the cylindrical mass. Two nodes are connected by the beam element which has equivalent bending stiffness of the cylindrical mass. The stiffness of the horizontal supporting system is considered. In vertical direction, analysis model is single-degree-of-freedom model. The restoring force characteristics of the coned disk spring and the damper were used the measured results of Fig.7 and Fig.9, respectively.

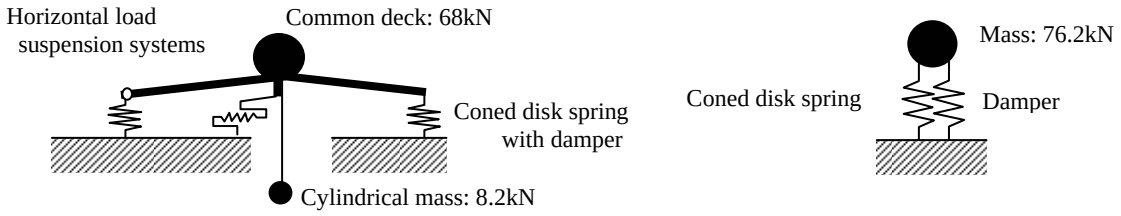

(a) Horizontal analytical model *(b) Vertical analytical model*

Fig.17 Analytical model

5.2 Result of Analysis

Fig.18 and Fig.19 show the comparison of FRS between analysis and tests results in horizontal and vertical directions, respectively. In horizontal direction, FRS increases at about 0.04sec (25Hz) which is a natural period of the horizontal load supporting system in comparison with the seismic wave. In FRS of cylindrical mass, FRS increases at about 0.014sec (71.4Hz) which is a natural period of the cylindrical mass. The analysis is similar to the test results in both directions. The response of the analysis is bigger than that of the shaking table test, and it is a safe side. Therefore, it was confirmed that this analysis method is applicable to the response estimation for the common deck isolation system.

The comparison of load-displacement relationships of the vertical isolation device for the seismic wave is shown in Fig.20. In this figure, the load is sum total of four isolation devices.

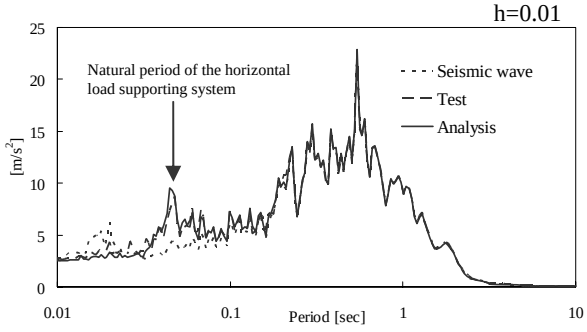

(a) Center of common deck

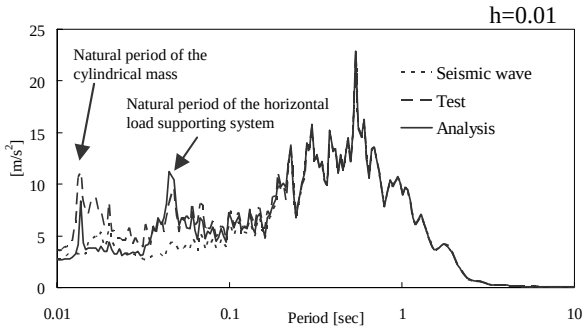

(b) Cylindrical mass

Fig.18 Comparison of Floor Response Spectra in horizontal direction

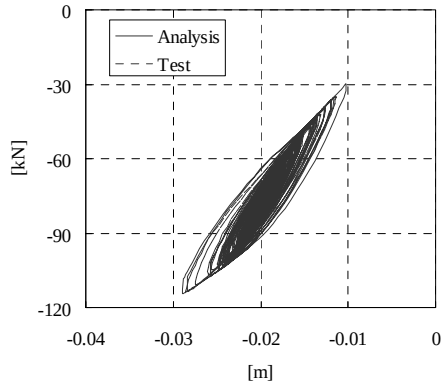

Fig.20 Comparison of Load-displacement relations

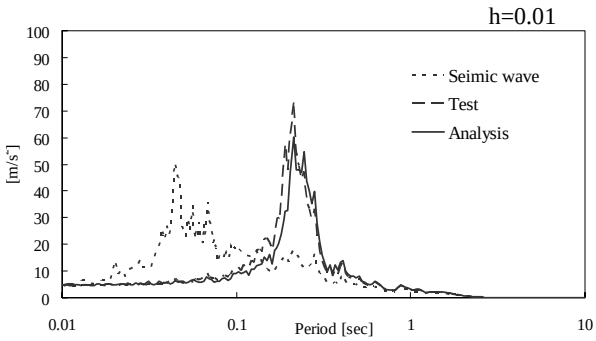

(a) 0.67 times seismic wave

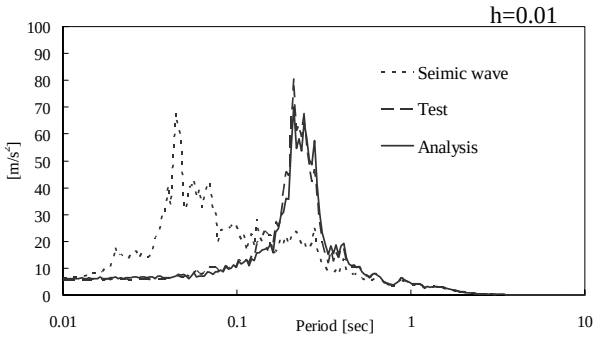

(b) Seismic wave

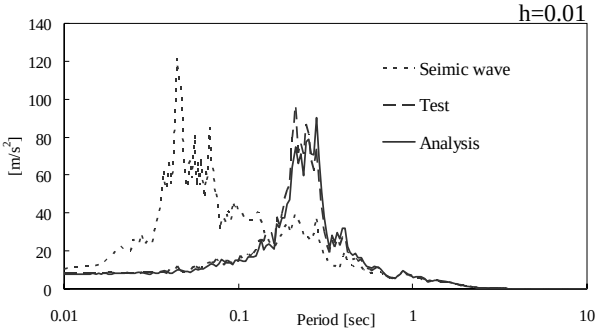

(c) 1.5 times seismic wave

Fig.19 Comparison of floor response spectra in vertical direction

6. CONCLUSIONS

The shaking table test using 1/8 scale model of the common deck isolation system was carried out. The characteristics in horizontal and vertical direction of the test model were grasped, and it was confirmed that isolation performance of the proposed isolation system during the earthquakes. As the result, the prospect that the vertical component isolation system applied to the FBR plant could technically realize was obtained.

ACKNOWLEDGMENTS

This study was made as a part of the Ministry of Economy, Trade and Industry of the Japanese government sponsored R&D project on three-dimensional seismic isolation. It has been advanced with Miyamoto of Obayashi Corporation and Kamishima, Moro, Yokoi of Advanced Reactor Technology Co. Ltd.

REFERENCES

1. M. Morishita, S. Kitamura, Y. Kamishima, T. Nakatogawa, A. Miyamoto, and T. Somaki, “Structure of 3-Dimensional Seismic Isolated FBR Plant with Vertical Component Isolation System”, SMiRT-17, K10-1, 2003
2. S. Kitamura, T. Nakatogawa, A. Miyamoto T. Somaki, “Experimental Study on Coned Disk Spring for Vertical Seismic Isolation System”, SMiRT-17, K10-2, 2003
3. Curti G. and Orland M., “Ein neues Berechnungsverfahren fur Tellerfedern”, DRAHT 30-1, pp.17-22, 1979
4. Niepage P., “Uber den Einfluß der Reidung und kreiskegelformiger Last einleitungselement auf die Kennlinie von Einzeltellerfedrn und Tellerfederpaketen”, Konstruktion, pp.379-384, 1984
5. M.Ichimiya, T. Mizuno and M Konomura “A Promising Sodium-Coold Fast Reactor Concept and its R&D Plan“, Global 2003, November 16-20, New Orleans, 2003.
6. A. Kato, S. Moro, M. Morishita, T. Fujita, S. Midorikawa “A Development Program of Three-Dimensional seismic isolation for Advanced Reactor System in Japan” , Proc. of SMiRT-17, K09-1, 2003

18th International Conference on Structural Mechanics in Reactor Technology (SMiRT 18)
Beijing, China, August 7-12, 2005
SMiRT18-K10-3

RESEARCH ON 3-D BASE ISOLATION SYSTEM APPLIED TO NEW POWER REACTOR
3-D SEISMIC ISOLATION DEVICE WITH ROLLING SEAL TYPE AIR SPRING: PART 2

Junji Suhara
Shimizu Corporation,No.2-3, Shibaura 1-chome, Minato-ku, Tokyo 105-8007, Japan
Phone:+81-3-5441-0859,Fax:+81-3-5441-0370
E-mail: junji-suhara@shimz.co.jp

Ryoichiro Matsumoto
Shimizu Corporation, Japan
Phone:+81-3-5441-0859,Fax:+81-3-5441-0370
E-mail: matsumotor@shimz.co.jp

Shinsuke Oguri
Shimizu Corporation, Japan
Phone:+81-3-5441-0859,Fax:+81-3-5441-0370
E-mail: guri@shimz.co.jp

Yasuo Okada
Shimizu Corporation, Japan
Phone:+81-3-5441-0859,Fax:+81-3-5441-0370
E-mail: okapi@shimz.co.jp

Kazuhiko Inoue
The Japan Atomic Power Company, Japan
Phone:+81-29-267-4141,Fax:+81-29-267-7173
E-mail: inoue.kazuhiko@jnc.go.jp

Kenji Takahashi
The Japan Atomic Power Company, Japan
Phone:+81-29-267-4141,Fax:+81-29-266-3675
E-mail: takahashi.kenji@jnc.go.jp

ABSTRACT

A three dimensional seismic base isolation device was developed for heavy structures and buildings such as nuclear power reactor buildings. The device realizes 3-D isolation by combining a LRB (laminated rubber bearing) for horizontal isolation with an air spring for vertical isolation in series. In this study, scale models of the 3-D base isolation device were made and were tested to examine the dynamic properties and ultimate strengths of the device.

The performance of the device under earthquake excitation was examined through shaking table tests of 1/7 scale models. As the results, it was confirmed that the device worked smoothly under the horizontal and vertical excitations, and that the theoretical formulae of the orifice damping could explain the test results.

The high-pressure air springs of trial production were forced to burst to find out which factor influenced ultimate strength. It was confirmed from results of the burst test that the strength of the air spring depended upon the diameter of rolling part of the bellows and the number of layers of the reinforcing fibers.

Judging from the results of the shaking table test and the burst test, the developed 3-D base isolation device was applicable to a nuclear power plant building.

Keywords: Shaking table test, Seismic base isolation, LRB, Air spring, 3-D

INTRODUCTION

A 3-D seismic isolation device was developed to use as a base isolation system for a heavy building like a nuclear power reactor building. The 3-D seismic isolation device consists of a laminated rubber bearing with a lead plug (LRB) and a rolling seal type air spring placed in series.

Both LRBs and air springs are reliable, as they are individually used for ordinary buildings and industrial structures widely. However, when these two components are combined, the following points should be checked.

1) Performance of the device, when vertical force and horizontal force acted simultaneously
2) Capability of supporting excessive weight
3) Damping performance to reduce vibration

The performance and the applicability of the 3-D base isolation device itself were already studied in feasibility tests (Suhara,2002, Suhara,2003, Hagiwara,2004). In this paper, results of the shaking table test, in which the base isolation system was demonstrated to function smoothly, and the burst test of high-pressure air springs are presented.

THREE-DIMENSIONAL (3-D) SEISMIC BASE ISOLATION DEVICE

The concept of the 3-D seismic isolation device is outlined in Fig.1. Dynamic properties and specifications of the device are summarized in Table 1. These dynamic properties are determined from the results of earthquake response analysis of an actual nuclear power plant (Kato,2002). The device realizes 3-D isolation by combining LRB for horizontal isolation with the air spring for vertical isolation.

The specifications of the LRB were determined from the results of the previous research (Kato, 1995). The air spring is set in the lower basemat. A rolling seal type air spring was adopted, because the stroke of the air spring should be long enough so that the device can be in operation even after experiencing large vertical deformation. The contact region shall be designed so that the horizontal force can be transmitted with small friction. Regular pressure of the air spring is 1.6MPa, which is relatively high compared with the pressure of an ordinary air spring (about 0.3-0.9 MPa). Therefore, the long-term reliability of the air spring using high pressure is important.

Horizontal damping performance is provided by the lead plug of the LRB. Vertical damping performance is provided by the orifice damping and viscous damping of the oil damper, which is set at the perimeter zone of the basemat.

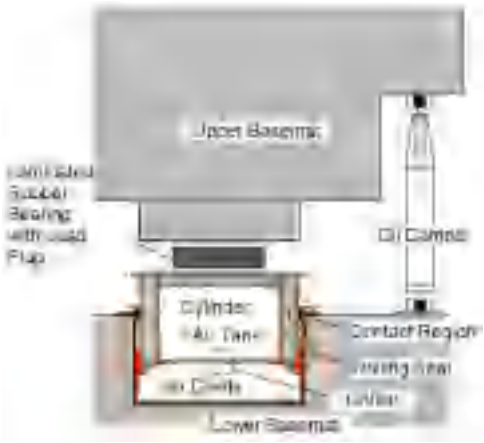

Fig. 1 Concept of 3-D Isolation Device

Table 1 Outline of 3-D Seismic Isolation Device

Dynamic Properties	Horizontal Initial Period	1.0 s
	Horizontal Isolation Period	2.8 s
	Horizontal Yield Coefficient	0.1
	Vertical Isolation Period	2.0 s
	Vertical Damping Factor	0.2
Specifications	Supporting Load	9800kN
	Diameter of Rubber Bearing	1.6 m
	Total rubber thickness	0.225m
	Diameter of Air Cavity	3.0m
	Pressure of Air Cavity	1.6MPa

SHAKING TABLE TEST

(1) SIMILARITY LAW

The similarity law used in this study is shown in Table 2. Both acceleration and density of the model are equal to those of the prototype in this similarity law. The scale ratio of the model to an actual prototype device is 1:7.

Table 2 Similarity Law

Parameter	Similitude	λ=7
Length	$1/\lambda$	1/7
Velocity	$1/\lambda^{1/2}$	1/2.7
Acceleration	1	1
Time	$1/\lambda^{1/2}$	1/2.7
Mass	$1/\lambda^{3}$	1/343
Stress	$1/\lambda$	1/7
Density	1	1

(2) DESIGN OF TEST MODEL

a. LRB for the Test Model

The sectional view and specification of the LRB with a lead plug used in the model are shown in Fig.2 and Table 3. Since the similarity law summarized in Table 2, in which the density of the model is equal to that of the prototype, is adopted, the shape of the LRB for the model is more slender than the LRB for prototype.

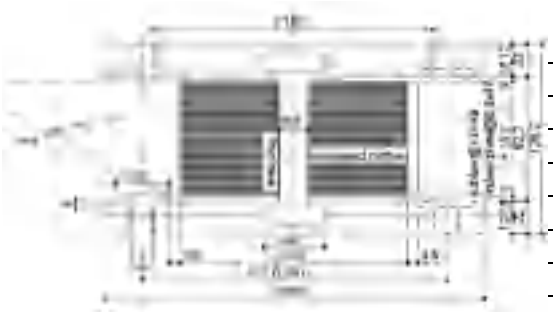

Fig.2 LRB used in Test Model

Table 3 Dimension of Laminated Rubber Bearing

Parameter	Prototype	Model
Support load (kN)	9800	28.9
Horizontal isolation period (s)	2.8	1.07
Diameter of LRB (m)	1.72	1.49
Total rubber thickness (m)	0.23	0.048
Diameter of lead plug (m)	0.35	0.019
Axial stress (MPa)	4.4	0.83

b. Test Model of Air spring

The sectional view and specification of the air spring model are shown in Fig.3 and Table 4.

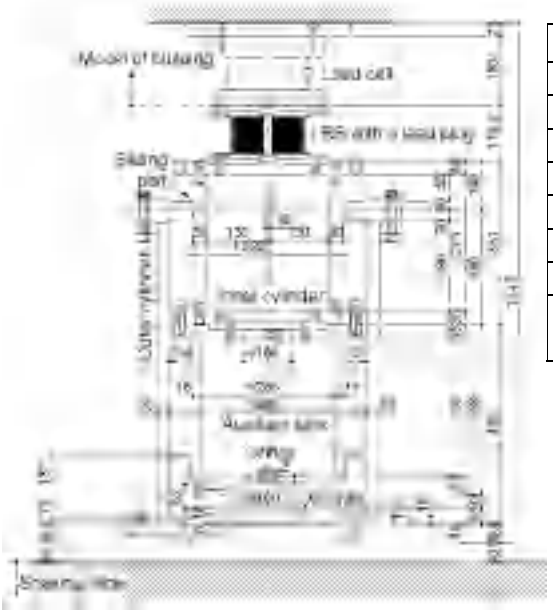

Fig.3 Test Model of Air Spring

Table 4 Dimension of Air Spring

Parameter	Prototype	Model
Support load (kN)	9800	28.6
Vertical isolation period (s)	2.0	0.76
Pressure of air cavity (MPa)	1.6	0.26
Effective diameter of air cavity (m)	2.82	0.37
Maximum stroke (mm)	600	50
Volume of air spring (m3)	9.4	0.03
Volumetric ratio of auxiliary tank to air cavity	1:1	1:1.65

c. Test Model of Oil Damper

The shape and specification of an oil damper are shown in Fig.4 and Table 5.

Fig.4 Test Model of Oil Damper

Table 5 Dimension of Oil Damper

Parameter	Prototype	Model
Damping factor (%)	20*	10*
Vertical natural period (s)	2.0	0.76
Damping coefficient (kN·s/m)	1260	4.9
Design stroke (mm)	900	129
Design velocity (m/s)	2.83	1.07
Design damping force (kN)	3500	5.2

* : Two models correspond to one prototype damper

d. Test Model of Building and Pantagraph type rocking suppression device

The weight which represents the building consists of steel plates and steel frame to support plates. Size of the weight is 2.35m in horizontal direction. Mass of the weight is 11.66t. Height of the center of the mass is 1/3.5 of horizontal length (=2.35m) measured from the center level of the LRBs. A pantagraph type rocking suppression device which is made of steel pipes and bearings is attached to the steel frame. Sectional view of the building model and a pantograph types rocking suppression device are shown in Fig.5.

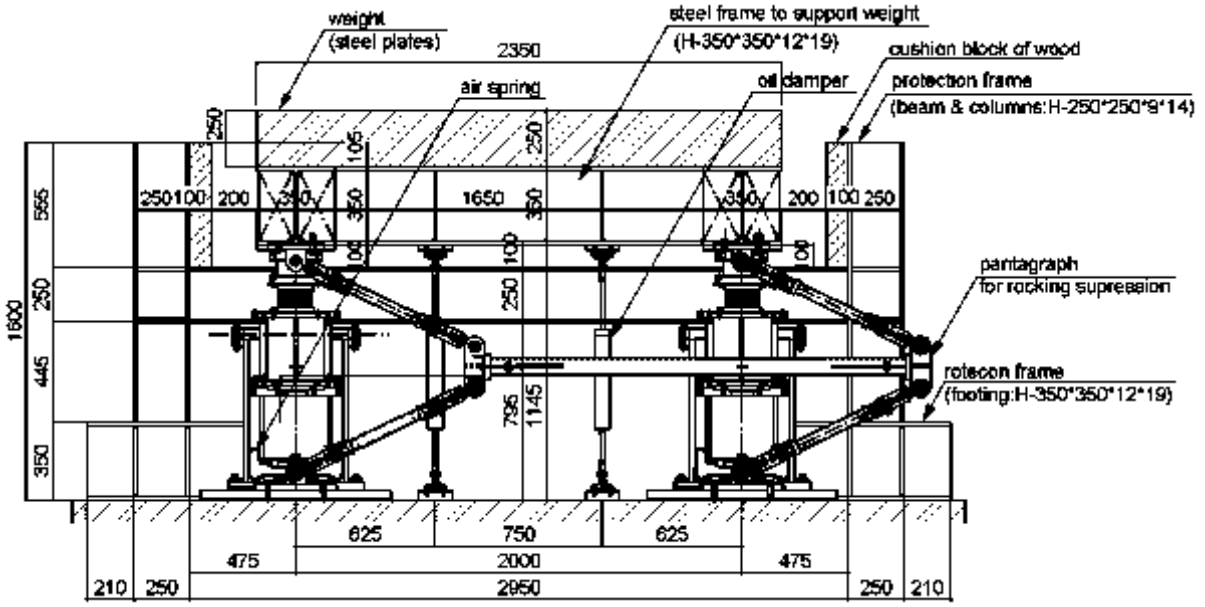

Fig.5 Setup of Test Model

e. Photographs of Shaking Table Test

The model used for the shaking table test consists of four air springs, four oil dampers, and a rigid body building model which weighs 114kN. The photographs of the test model are shown in Photo.1.

Photo.1 View of Shaking Table Test

(3) SINUSOIDAL EXCITATION TEST

Transfer functions and hysteresis loops of vertical response to sinusoidal excitation are shown in Fig.6 and 7. Figure 6 shows the case where the acceleration amplitude of the input sinusoidal wave is 20Gal, and Figure 7 is the case of 100Gal input.

Four lines for four air springs are plotted in each graph of transfer functions. In case of hysteresis loops, averaged data of four air springs are plotted. Amplitude of the transfer functions become largest at frequency of 1.4Hz. Phase angle of the transfer functions become -90deg. at the frequency a little bit higher than 1.4Hz. Curves of the hysteresis loops look smooth even in the case of 20Gal input. It is clear that orifice damping becomes large, as amplitude becomes large.

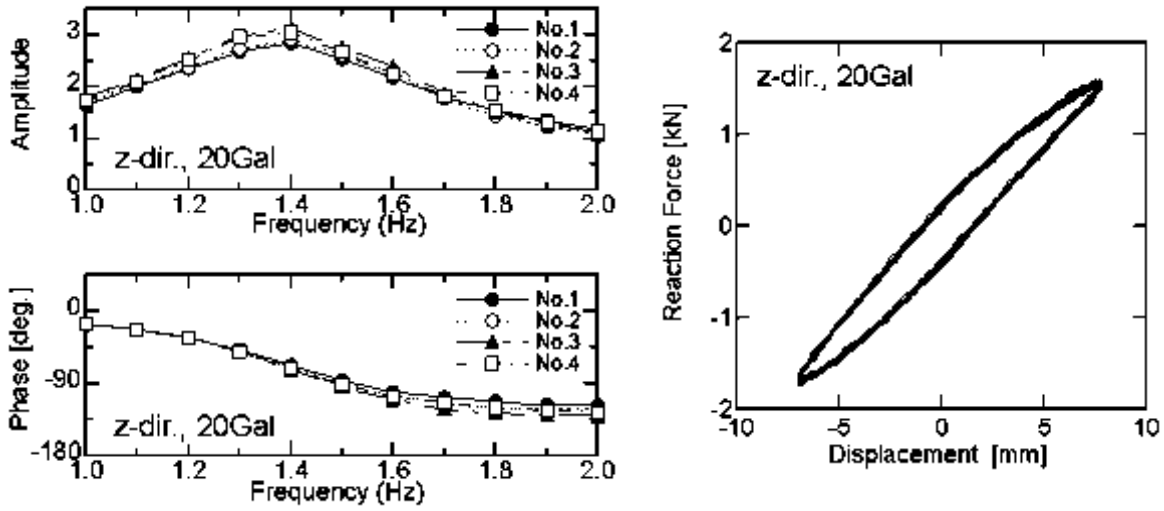

a. Transfer Function b. Vertical Hysteresis Loop

Fig.6 Response of Sine Wave Excitation (maximum input acceleration is 20Gal)

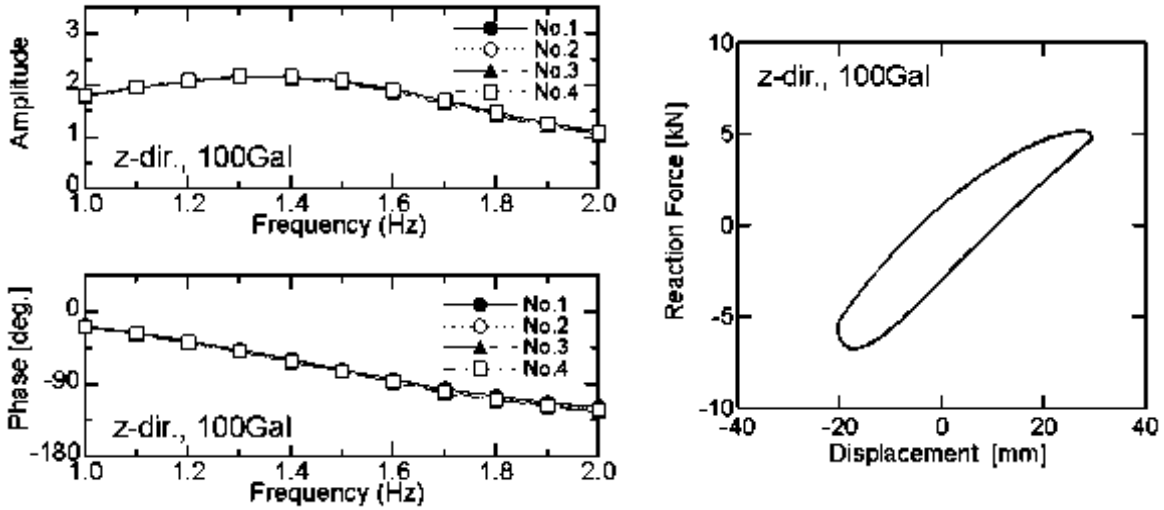

a. Transfer Function b. Vertical Hysteresis Loop

Fig.7 Response of Sine Wave Excitation (maximum input acceleration is 100Gal)

(4) INPUT EARTHQUAKE WAVES

An artificial earthquake wave S_2, velocity response spectra (h=5%) of which reaches 2m/s in horizontal direction and 1.2m/s in vertical direction, was made in the preceding study (Kato, 1995). In this study, the earthquake wave S_2 is adopted as the greatest seismic excitation. Because of restrictions of the shaking table capacities, band-pass filtered S_2 wave was used if horizontal wave and vertical wave were input simultaneously.

Pass band of the digital filter is set to be 0.794Hz-3.44Hz, so that frequency components dominant for seismic isolation devices were not reduced.

Time history waves and response spectra of the original S_2 waves, scaled S_2 waves, and band-pass filtered S_2 waves are shown in Fig.8 and Fig.9. Upper scale of x-axis in Fig.9 shows frequency in prototype.

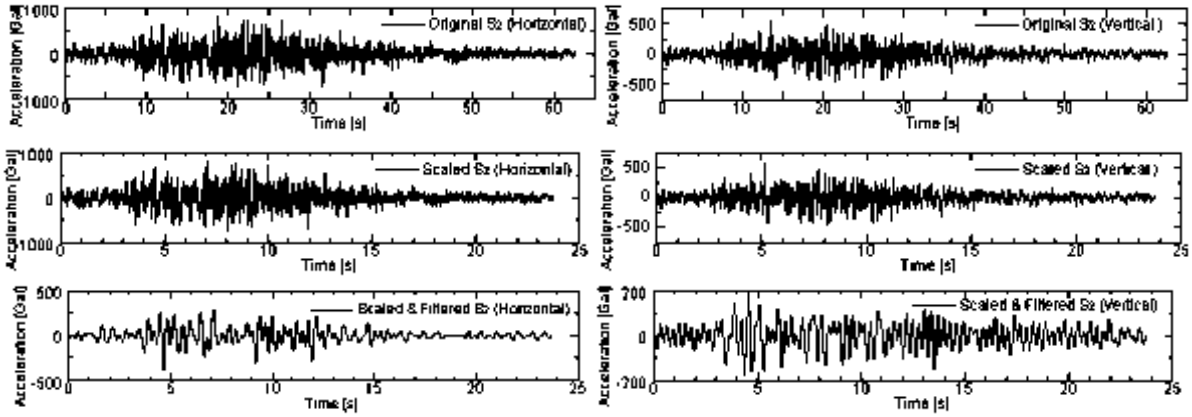

Fig.8 Acceleration Time History of Input Earthquake Waves

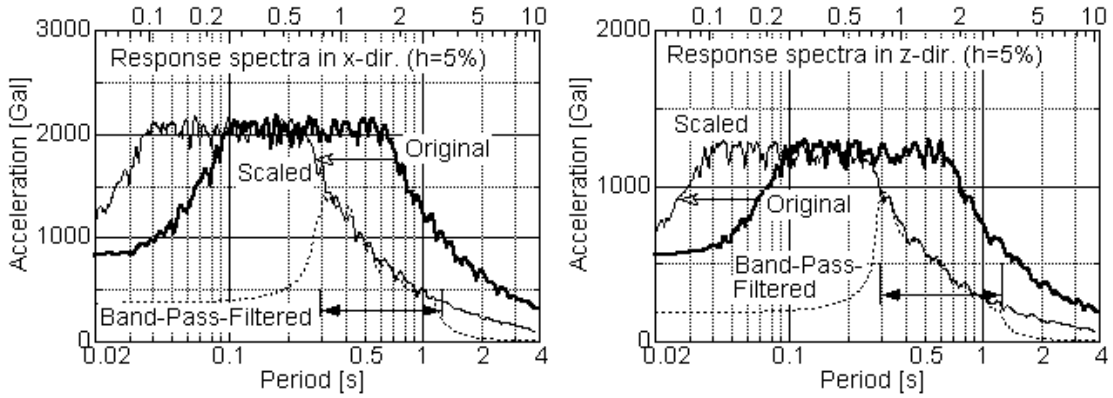

b. Acceleration Response Spectra

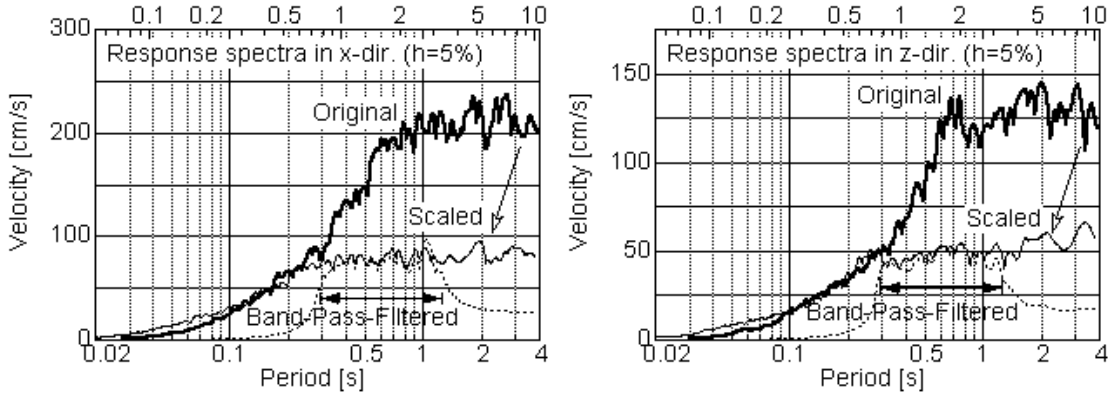

c. Velocity Response Spectra

Fig.9 Response Spectra of Input Earthquake Waves

(5) EARTHQUAKE WAVE EXCITATION TEST

Hysteresis loops of vertical response to earthquake excitation are shown in Fig.10 and Fig.11. The response to vertical input and the response to vertical and horizontal input are compared in these figures. Figure 10 shows the response to S_2(filtered) input and Fig.11 shows that of 1.5*S_2(filtered) input. Acceleration response spectra of the same cases are plotted in Fig.12. Upper scale of x-axis in these graphs shows frequency in prototype. It is obvious from these figures that horizontal response has little influence on vertical response in this test. Also plotted in Fig.13 are hysteresis loops and time history wave of response to non-filtered original input wave.

Response spectra are shown in Fig.12 and Fig.13. Though effect of base isolation is not so obvious in case of band-pass filtered S_2 wave as high frequency components of input wave were small, most of these high frequency components are cut by the isolation device, as is shown in Fig.13.

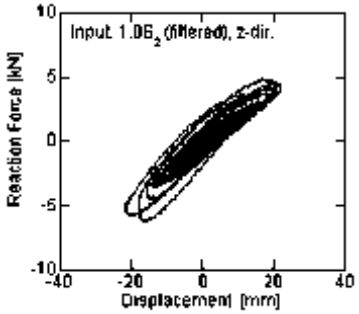

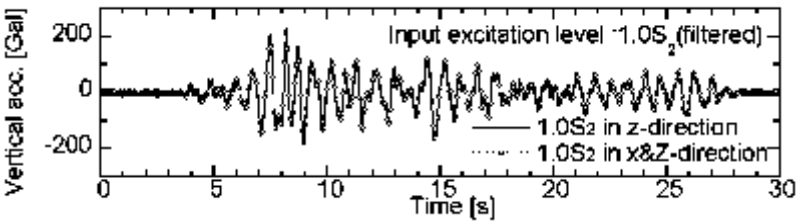

b. Time history of response acceleration

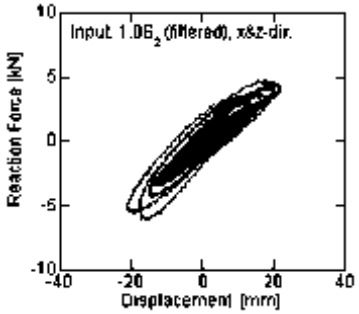

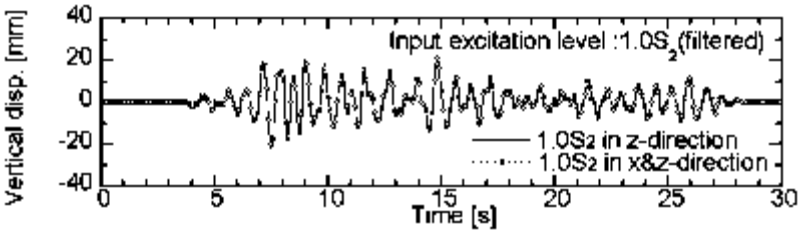

c. Time history of response displacement

a. Hysteresis loop

Fig.10 Vertical Response to Earthquake Excitation (Input: S2, Filtered Wave)

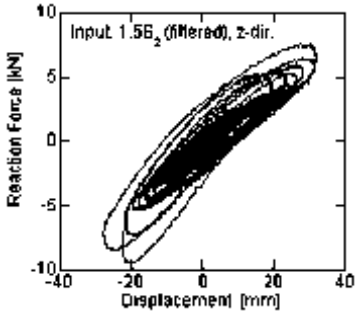

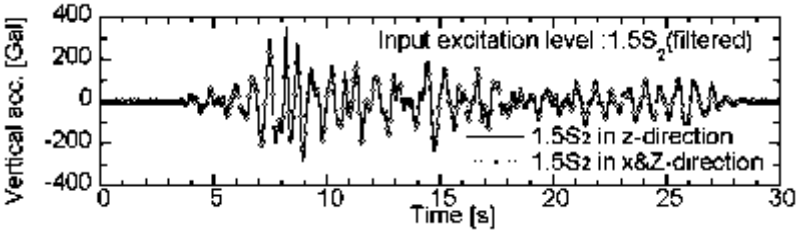

b. Time history of response acceleration

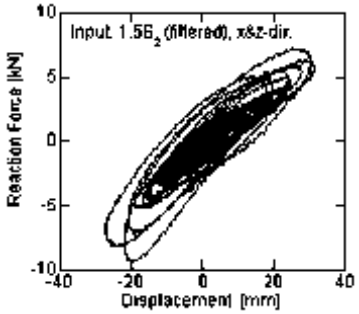

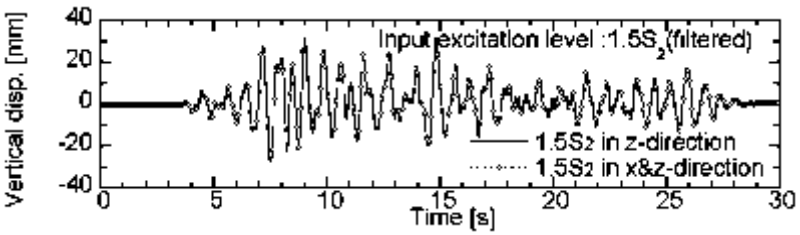

c. Time history of response displacement

a. Hysteresis loop

Fig.11 Vertical Response to Earthquake Excitation (Input:1.5S2, Filtered Wave)

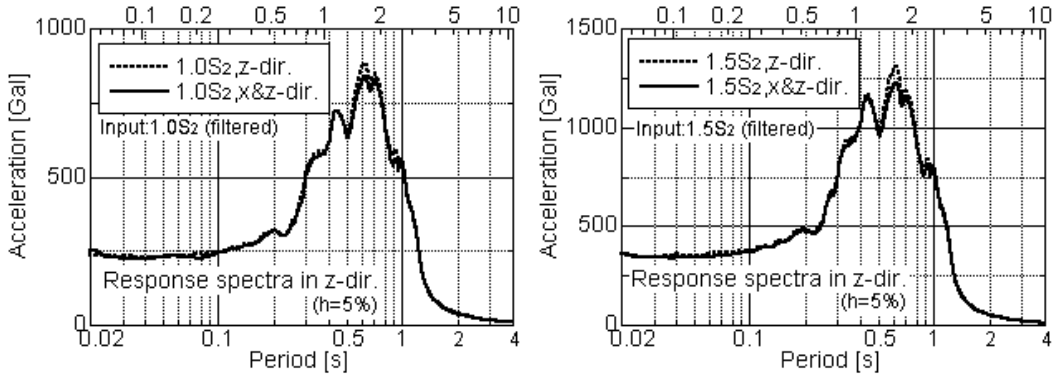

Fig.12 Influence of Horizontal Input on Vertical Response Spectra

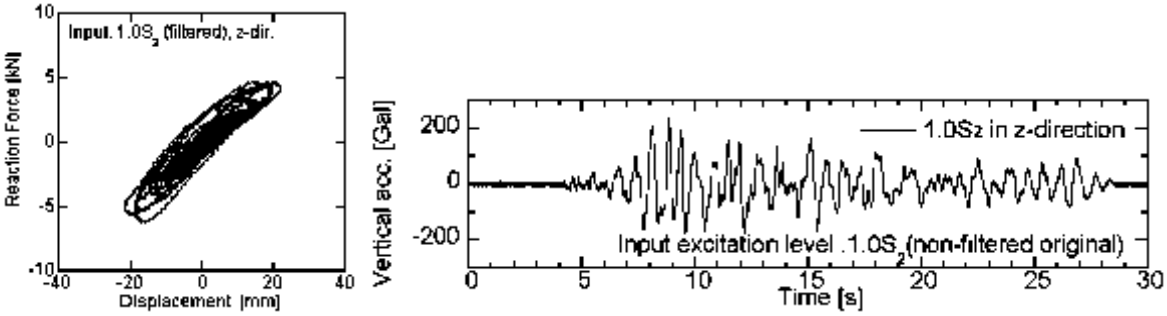

a. Hysteresis loop b. Time history of response acceleration

Fig.13 Vertical Response to Non-filtered Original Earthquake Excitation

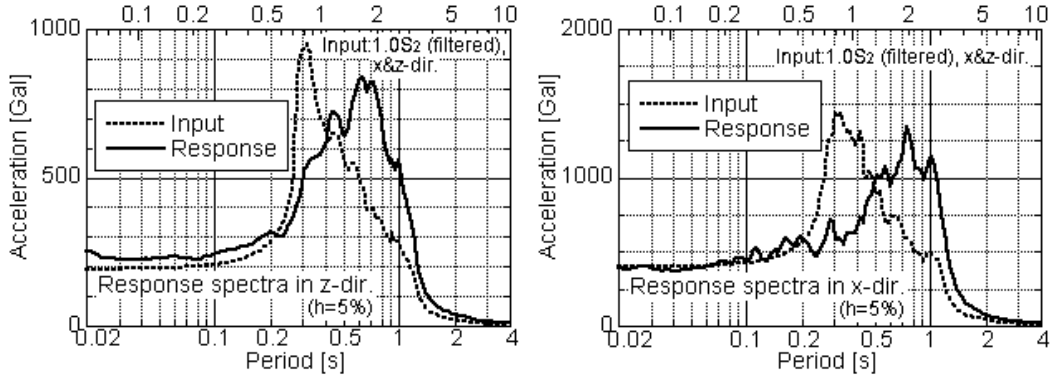

a. Vertical b. Horizontal

Fig.14 Response Spectra (Input:1.0S2, filtered wave)

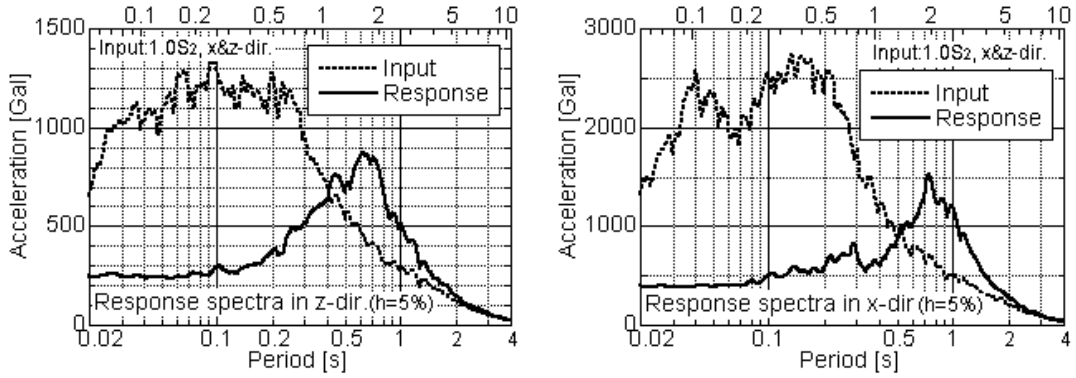

a. Vertical b. Horizontal

Fig.15 Response Spectra (Input:1.0S2, non-filtered original wave)

(6) SIMULATION ANALYSIS OF EARTHQUAKE EXCITATION TEST

The response of the test model was calculated by the analysis model shown in Fig.16. Results of calculation are shown in Fig.17 and Fig.18. Though the air spring shows weak non-linearity and the stiffness for downward displacement increment is higher than that for upward displacement increment, the analysis model used here is so simple to ignore this fact. Thus calculated results slightly differ from experimental results, it is possible to get reasonable estimation of the response of the base isolated building by this quite simple analysis.

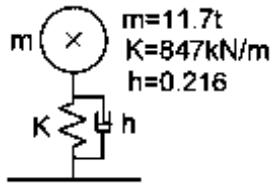

Fig.16 Analysis Model

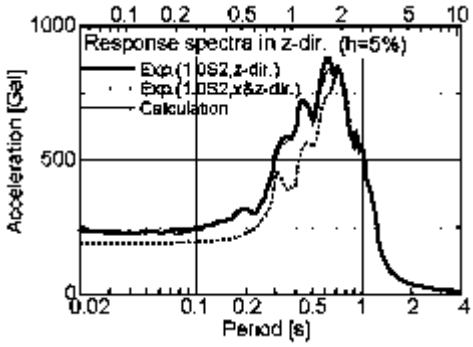

Fig.17 Response Spectra

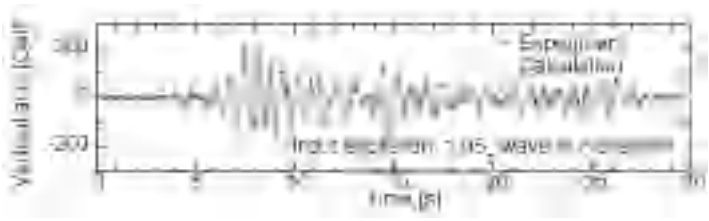

a. Vertical Acceleration

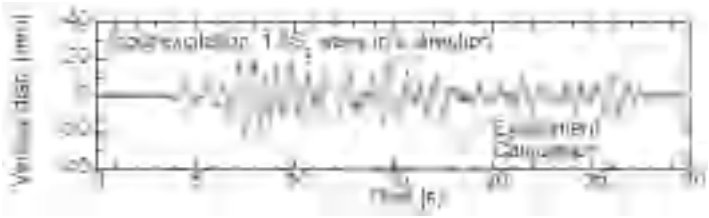

b. Vertical Displacement

Fig.18 Time History of Calculated Response Compared to Experiment

BURST TEST OF AIR SPRINGS

It is possible to cut down the size of the device, if high-pressure air springs are available. Adoption of the high-pressure air springs leads to easiness of fabrication and maintenance of the device and cost down. It is also possible to expect greater margin regarding ultimate strength.

To examine the ultimate pressure and failure mode of the rubber bellows of the air spring, burst test was done. Setup of the test is shown in Fig.19 and Photo.2. After pouring water into the air spring, vertical load was applied to bring the air spring to burst. The test results are summarized in Fig.20 and Table 6. The shape of the burst air spring is shown in Photo.3.

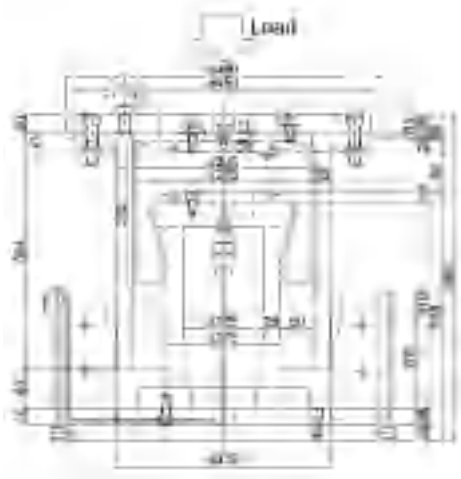

Fig.19 Setup of Burst Test

Photo.2 Test Machine

Photo.3 Air Spring Bellows After Burst

The strength of air spring becomes high, if the diameter of rolling part of the air spring is small, the initial gap is small, or rubber bellows of the air spring is reinforced enough.

From these test results, it is proved that the air spring, the maximum pressure of which exceeds 20MPa, can be made.

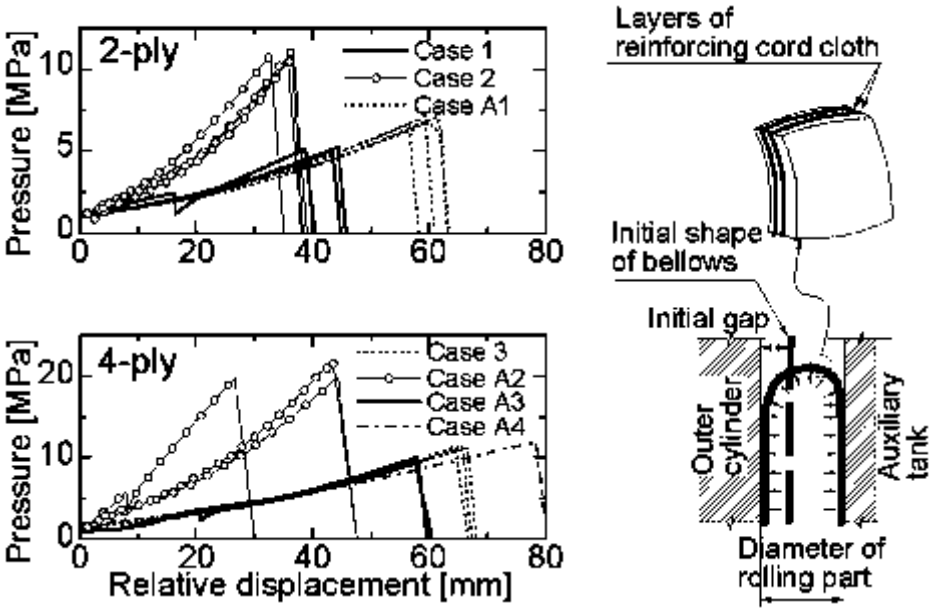

Fig.20 Displacement-Pressure Curves

Table 6 Burst Pressure of Air Springs

#	Diameter of rolling part (mm)	Ply of reinforcing cord cloth	Initial gap (mm)	Bead wire arrangement	Maximum pressure (MPa)	Failure mode
1	50	2	29	4x4 loops	5.15 5.28 5.11	bellows
2	30	2	16	4x4 loops	10.89 11.26 10.41	bellows
3	50	4	16	4x5 loops	11.38 11.19 11.37	bead
A1	50	2	16	4x4 loops	6.71 6.77 7.15 7.15	bead bellows
A2	30	4	16	4x5 loops	19.85 21.75 19.87	bellows
A3	50	4	29	4x5 loops	9.40 10.07 9.76	bellows
A4	50	4	16	4x6 loops	11.90	bead

CONCLUSIONS

Performance of the 3-D seismic isolation devices which used air springs was examined through shaking table tests. The specimen consisted of a weight, four air springs and four oil dampers. Pantographs made of steel pipes and bearings were also attached to the specimen to suppress rocking motion mechanically. Designed values of dynamic properties of the specimen such as natural frequency and damping factor were attained in the test, to prove the performance of the air springs. It was also confirmed that the maximum earthquake response values and floor response spectra in vertical direction were reasonably evaluated by linear response analysis using equivalent damping factor and spring constant.

The high-pressure air springs of trial production were brought to burst to examine strength. The target of the maximum pressure to actualize compact air spring devices was set to be 17.5MPa. Among several cases tested, the specimen of four layers of reinforcement fiber membranes achieved the maximum pressure of 20.5MPa, when the size of the rolling part was set to be 30mm.

As the result of these test, the developed 3-D base isolation system was judged to be applicable to an actual nuclear power plant.

ACKNOWLEDGMENT

This study is a part of project sponsored by the Japanese government (METI) and was conducted by the Japan Atomic Power Company in collaboration with Japan Nuclear Cycle Institute. The authors wish to express their profound appreciation to the project committee members.

REFERENCES

Kato, M., et al., (1995), Design study of the seismic-isolated reactor building of demonstration FBR plant in Japan, 13th SMIRT, pp579-584

Suhara, J., et al., (2002), Development of Three Dimensional Seismic Isolation Device with Laminated Rubber Bearing and Rolling Seal Air Spring, ASME PVP, Seismic Engineering

Kato, A., et al., (2002), A large Scale Ongoing R&D Project on Three-Dimensional Seismic Isolation for FBR in Japan, ASME PVP, Seismic Engineering

Suhara, J., et al., (2003), Research on 3-D Base Isolation System Applied to New Power Reactor 3-D, Seismic Isolation Device with Rolling Seal Type Air Spring : Part 1, 17th SMIRT, K10-2

Tetsuya Hagiwara, et al., (2004), Three-Dimensional Seismic Isolation Device with Rolling Seal Type Air Spring, ASME PVP, Seismic Engineering

18th International Conference on Structural Mechanics in Reactor Technology (SMiRT 18)
Beijing, China, August 7-12, 2005
SMiRT18-K10-4

STUDY ON 3-DIMENSIONAL BASE ISOLATION SYSTEM APPLYING TO NEW TYPE POWER PLANT REACTOR: PART 2 (HYDRAULIC 3-DIMENSIONAL BASE-ISOLATION SYSTEM)

Takahiro Shimada
1, Shin-Nakahara-cho, Isogo-ku, Yokohama, JAPAN
Phone: +81-45-759-2825, Fax: 2208
E-mail: takahiro_shimada@ihi.co.jp

Junji Suhara
2-3, Shibaura 1-chome, Minato-ku, Tokyo, JAPAN
Phone: +81-3-5441-0859, Fax: 0370
junji-suhara@shimz.co.jp

Kenji Takahashi
4002 Narita, O-arai-machi, Ibaragi
Phone: +81-29-267-4141, Fax: +81-29-266-3675
E-mail: takahashi.kenji@jnc.go.jp

ABSTRACT

Three dimensional (3D) seismic isolation devices have been developed to use for the base isolation system of the heavy building like a nuclear reactor building. The developed seismic isolation system is composed of rolling seal type air springs and the hydraulic type springs with rocking suppression system for vertical base isolation device. In horizontal direction, the same laminated rubber bearings are used as horizontal isolation device for these systems.

The performances and the applicability have already been evaluated by the technical feasibility tests and performance tests for each system. In this study, it was evaluated that the performance of the 3D base isolation system with rolling seal type air springs combined with hydraulic rocking suppression devices. In this paper, the results of performance tests for hydraulic rocking suppression system will be reported.

A 1/7 scaled model of the 3D base isolation devices were manufactured and some performance test were executed for each device. For the hydraulic rocking suppression system, forced dynamic loading test was carried out in order to measure the frictional and oil flow resistance force on each cylinder.

And the vibration table tests were carried out with supported weight of 228 MN in order to evaluate and to confirm the horizontal and vertical isolation performance, rocking suppression performance, and the applicability of the this seismic isolation system as the combined system. 4 rolling seal type air springs and 4 hydraulic load-carrying cylinders with rocking suppression devices supported the weight.

As a result, the proposed system was verified that it could be applied to the actual nuclear power plant building to be target.

Keywords: Three Dimensional Base Isolation, Seismic Isolation, Hydraulic, Rocking

1. INTRODUCTION

The 3D seismic isolation system is a means of isolating a structure from seismic movement in vertical as well as horizontal direction. In Japan, the relevant technology has been the subject of active research and development for its being considered an indispensable asset for letting nuclear installations combine the properties of earthquake resistance and economic viability. Other buildings and structures of more general nature also are considered to have potential need for this technology [1]. The current status of this technology, however, is that

three-dimensional seismic isolation has been realized for application to an each floor, but coverage of the entire building including the upper stories has been awaiting development. A structure or mechanism needed to be found that would, white carrying a load of several hundred tons, present a flexible property against vertical movement (e.g. possessing a natural frequency above 1 see). Another difficulty was suppression of rocking response to seismic movement.

As a means of overcoming the foregoing obstructions, the present authors have proposed two three-dimensional seismic isolation devices those are rolling seal type air springs and the rocking suppression devices incorporating hydraulic mechanism. So far, the forced dynamic loading tests on reduced-size rolling seal type air springs and shaking table tests on rocking suppression devices, together with modelized analysis [2, 3].

With the aim of approaching a step closer to practical application, the next step envisaged is to verify the performances of integrated three-dimensional seismic isolation system composed of air springs and hydraulic rocking suppression devices through further tests and analyses, and examination of design problems.

The present paper takes up the performance aspect of the system, with a description of experiments using models covering:

- The forced dynamic loading tests on hydraulic rocking suppression devices
- The shaking table tests on the integrated system

2. DESIGN OF TEST MODEL

2.1. Similarity Law

The scale ratio of the model to an actual prototype structure is 1/7 and both acceleration and density are equal to those of the prototype. The similarity law is shown in Table 1.

Table 1 Similarity Law

Parameter	Similitude	$\lambda=7$
Length	$1/\lambda$	1/7
Velocity	$1/\sqrt{\lambda}$	1/2.7
Acceleration	1	1
Time	$1/\sqrt{\lambda}$	1/2.7
Mass	$1/\lambda^3$	1/343
Stress	$1/\lambda$	1/7
density	1	1

2.2. Test Model of Laminated Rubber Bearing

The sectional view and specification of a model of the laminated rubber bearing with a lead plug are shown in Fig. 1 and Table 2. Since the similarity law, which suits the prototype by the model about density, is adopted, the shape of laminated rubber bearing model is more slender than the prototype.

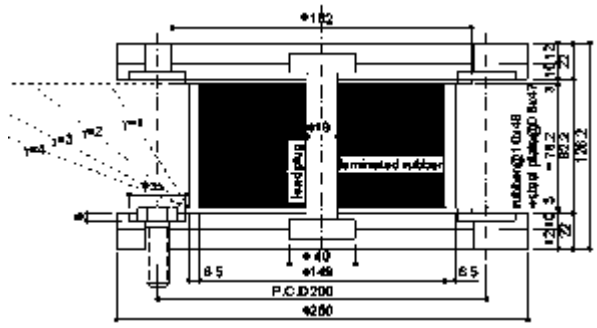

Fig. 1 Test Model of laminated rubber bearing

Table 2 Dimension of laminated rubber bearing

Parameter	Prototype	Model
Support Load (kN)	9800	28.9
Horizontal Isolation Period (s)	2.8	1.07
Diameter of RB (m)	1.72	1.49
Total rubber thickness of RB (m)	0.23	0.048
Diameter of Lead plug (m)	0.35	0.019
Axial Stress (MPa)	4.4	0.83

2.3. Test Model of Rocking Suppression Devices

Rocking suppression system is composed of the load carrying cylinders, the rocking suppression cylinders, and the angle linkage cylinders. Each cylinder is connected with the pipe of 25mm in the inside diameter. The laminated rubber bearing set up in the upper part of the load carrying cylinder is the same as that of the air spring.The sectional view and specification of hydraulic rocking suppression device models are shown in Fig.2 and Table 3.

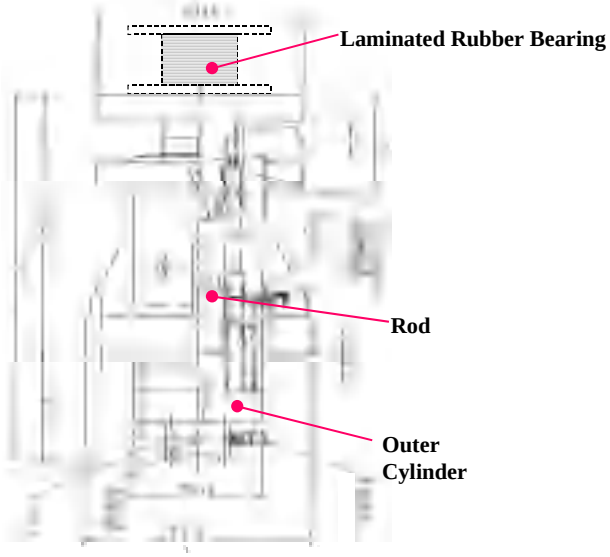

(a) Load Carrying Cylinder

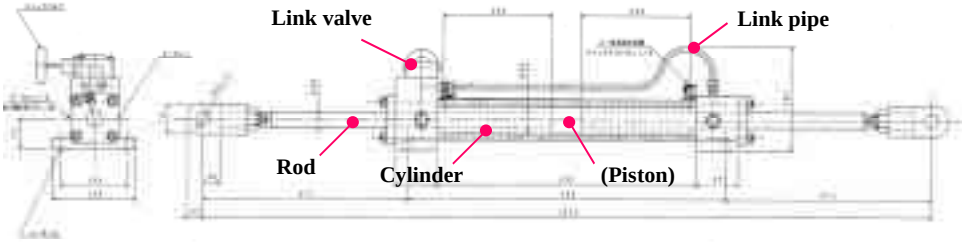

(b) Rocking Suppression Cylinder

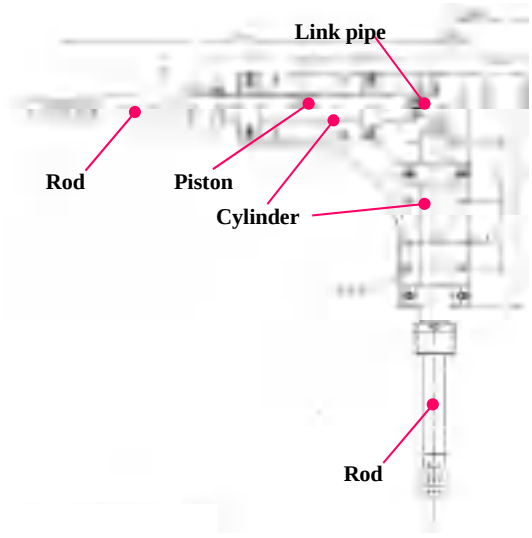

(c) Corner Linkage Cylinder

Fig.2 Test Model of Rocking Suppression Devices

Table 3 Dimension of Rocking Suppression Devices

Device	Parameter	Prototype	Model
Common	Support Load (kN)	9800	28.6
	Vertical Isolation Period (s)	2.0	0.76
	Pressure (MPa)	25	3.57
Load Carrying Cylinder	Diameter of Cylinder (mm)	720	100
	Movable Stroke (mm)	350	50
Accumulator unit	Volume of N_2 gas (Liter)	650	1.8
	Volume Ratio of main-Tank to assist-Tank	1 : 2	1 : 2
Rocking Suppression Cylinder	Diameter of Piston (mm)	800	60
	Diameter of Rod (mm)	500	36
	Movable Stroke (mm)	1400	250
Corner Cylinder	Diameter of Rod (mm)	800	60
	Movable Stroke (mm)	1400	250

3. TEST OF ROCKING SUPPRESSION DEVICES ALONE

3.1. Outline of Test

In this test, one unit of four unit used by the shaking table test were taken out and the test was executed. Each cylinder (load carrying cylinder, rocking suppression cylinder, and corner cylinder) was connected with the pipe of 25mm in the inside diameter. Forced vibration displacement in the vertical direction was given to the load-carrying cylinder. The frictional resistance force generated from each cylinder and the damping force generated by the differential pressure before and behind the gas throttle installed between the accumulator and the backup bottle was measured.

To confirm the influence that a horizontal load gives to the frictional force in the vertical direction, the forced vibration test in the vertical direction was also executed under acting a horizontal static load.

The test apparatus is shown in Photo 1.

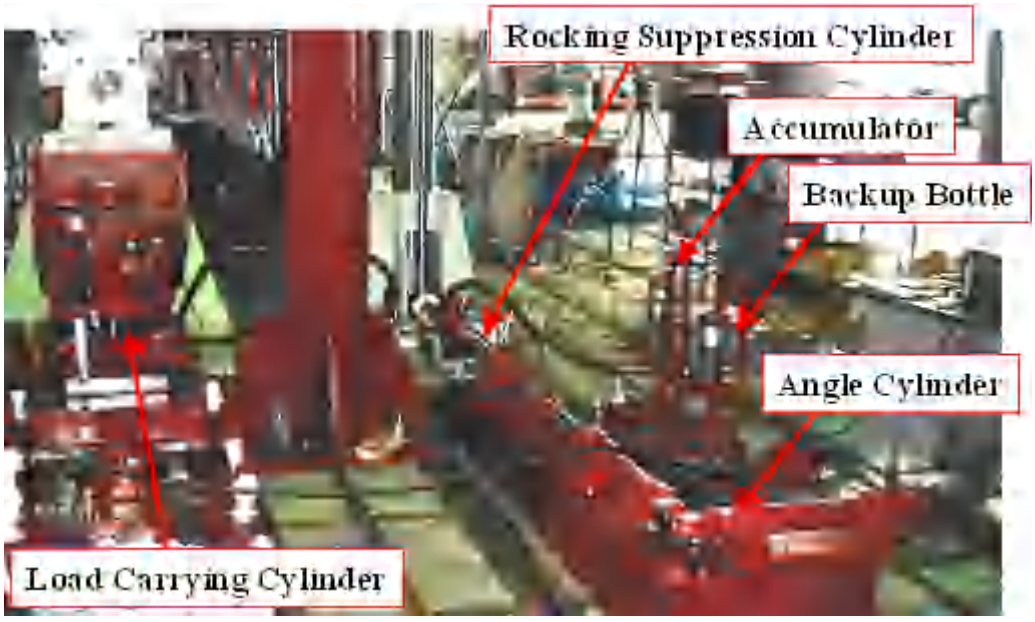

Photo 1 Test Apparatus of Rocking Suppression Devices

3.2. Frictional Force Measurement

Figure 3 shows the hysteresis loop in vertical direction. In this figure, LC is Load-carrying Cylinder, RC is Rocking-suppression Cylinder, and CC is Corner Cylinder. The behavior of frictional force is stable. The frictional force that occurs from each cylinder(LC, RC, and CC) can be separated according to the difference of the frictional force of three curves in this figure, and it is summarized in Table 4.

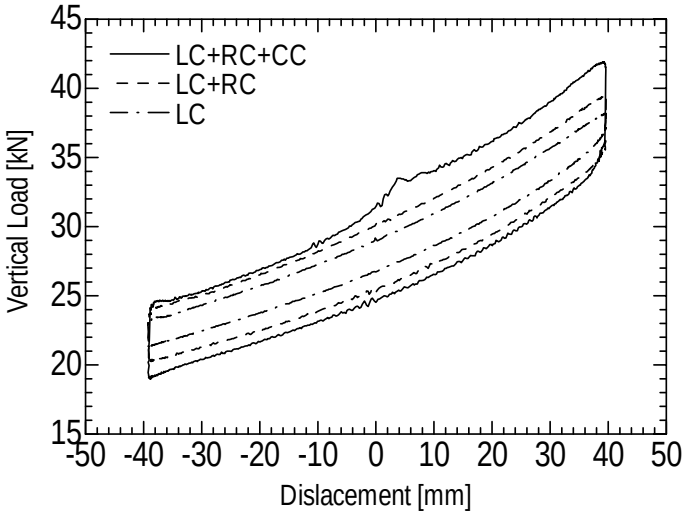

Fig. 3 Vertical Hysteresis Loop

Table 4 Frictional Force

Cylinder	Frictional Force (kN)
LC	1.10
RC	1.15
CC	1.25

Figure 4 shows the change in the frictional force in the vertical direction generated by the magnitude of the horizontal load. When the swivel works effectively, the vertical friction force became as a curve of the round symbols show in Fig.4. When the swivel is fixed, vertical friction force became as the curve shown as the square symbols.

It is confirmed that the increment of the frictional force becomes small by the effect of the swivel as a result. However, the effect of the swivel is not so higher than frictional force generated by RC and CC.

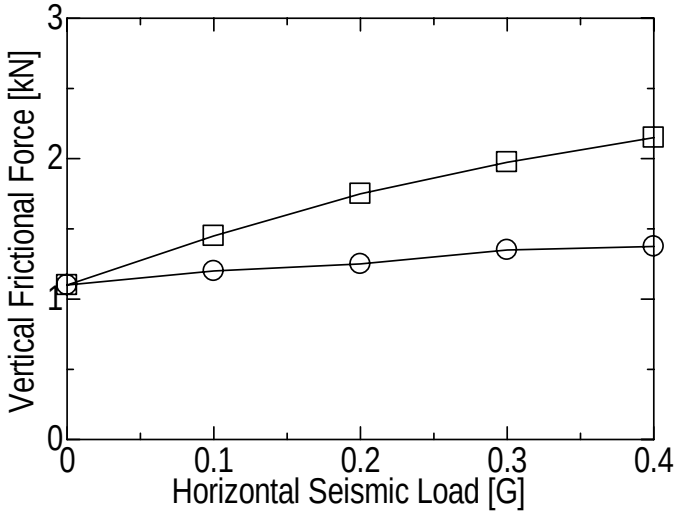

Fig. 4 Vertical Friction Force

3.3. Damping Force Measurement

The damping force generated by the pressure loss before and behind the gas throttle when the forced vibration displacement of the sine wave was given was measured. Figure 5 shows the hysteresis loop of pressure loss for each excitation frequency. Excitation amplitude of displacement (X0) is 10mm and 20mm.As shown in Fig.5, the area of hysteresis of pressure loss depends on both frequency and excitation amplitude of displacement.

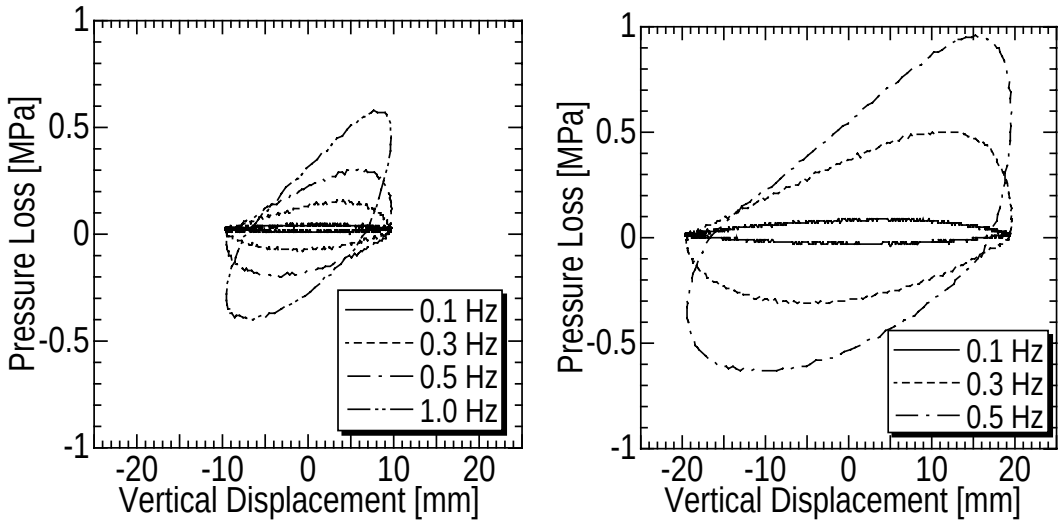

a. X_0=±10mm *b. X_0=±10mm*

Fig. 5 Hysteresis Loop of Pressure Loss at Gas Throttle

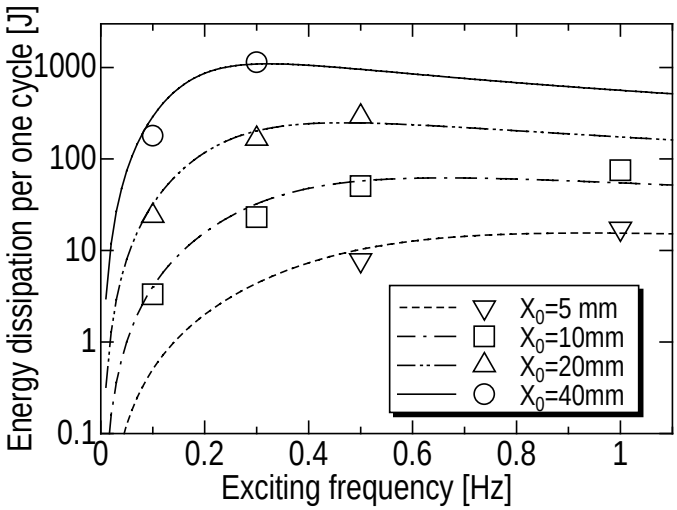

Fig. 6 Energy Dissipation of Gas Throttle

Figure 6 shows the relationship between the excitation frequency and dissipated energy per a cycle for each amplitude of excitation vibration displacement. The plots show the value obtained by the experiment in this figure, and the curves are a theoretical value obtained by three-element model [3].

The experimental values show the good agreement with the theoretical curves, thus the validity of the theory for obtaining the damping force generated by the throttle valve is confirmed.

4. SHAKING TABLE TEST OF COMPOSED DEVICES

4.1. Outline of Shaking Table Test

The model used for an shaking table test consists of four air springs and oil dampers, and four load carrying cylinders, rocking suppression cylinders, accumulator units and corner cylinders. Four air springs and four load carrying cylinders supported the building model of 248kN by eight points in total and 31kN was supported equally respectively.

The rigid body model was designed so that the ratio of base width and center-of-gravity height might become the same by the actual plant and the model, which is 3.5:1. Figure 7 shows the schematic drawing of arrangement of the devices for shaking table test, and the photograph of the model is shown in Photo 2.

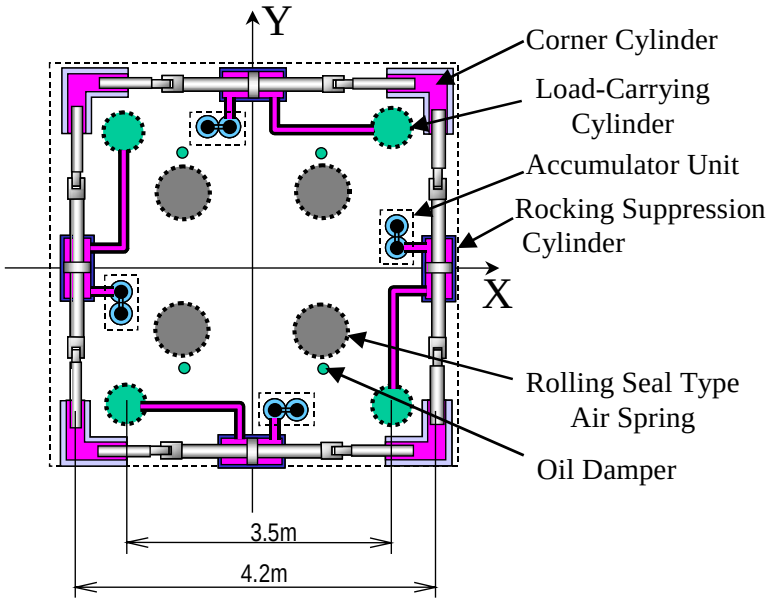

Fig.7 Schematic Drawing of Shaking Table Test Model (Top View)

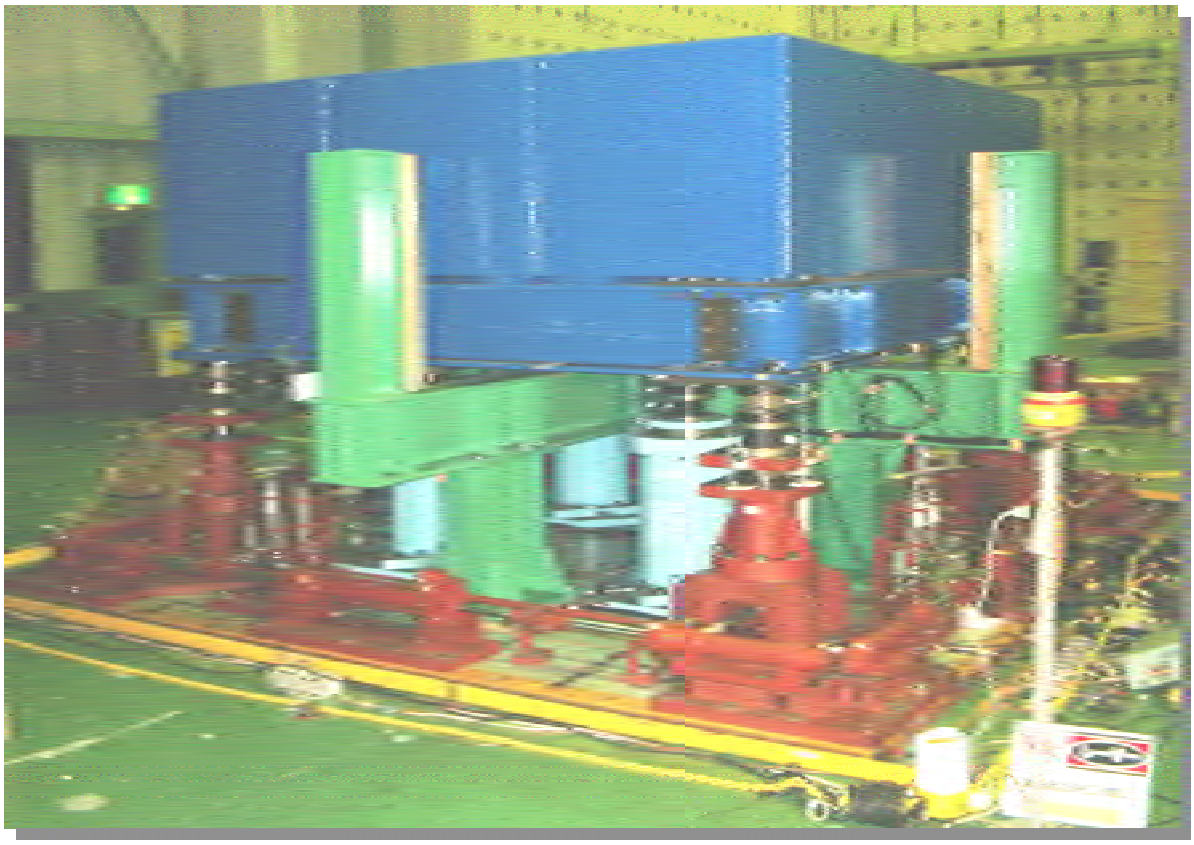

Photo 2 Shaking Table Test Model with Air Springs and Rocking Suppression System

4.2. Sine Wave Excitation Test

The sine wave excitation test was carried out in order to confirm the vertical damping characteristics of the air springs and of rocking suppression devices were suitable for the designed characteristics.

Figure 8 shows the hysteresis loop of reaction forces measured by the load-cells installed on the air springs and the load carrying cylinders of rocking suppression devices.

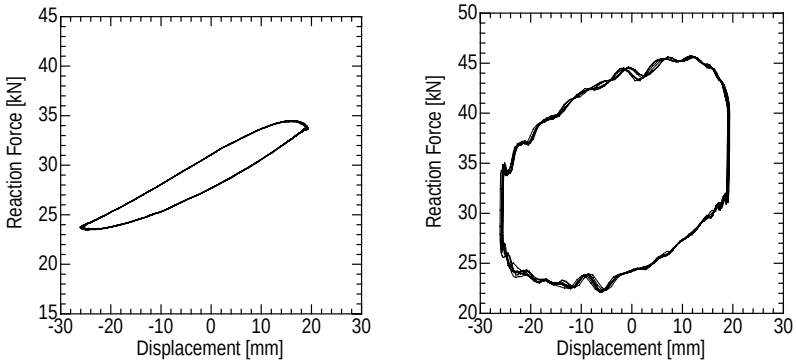

a. Air Spring *b. Load Carrying Cylinder*

Fig. 8 Hysteresis Loop of Reaction Force

The reaction force of air spring was similar to the test result of air springs only.The area of hysteresis loop of rocking suppression device is consists of the damping force generated by the gas throttle, the frictional force generated by cylinders, and the pressure loss of oil piping. These components can be calculated from reaction force and hydraulic pressures measured in the test as shown in Fig.9.

The equivalent damping factor calculated from the area of hysteresis is summarized in Table 5. For the air spring, the equivalent damping factor is suitable to designed value. For the rocking suppression device, the equivalent damping factor of gas throttle and piping is suitable to designed value, but that of frictional force is larger than designed value. But the influence of friction becomes 1/7 in a real size device, because the support pressure increases to seven times that of the model.

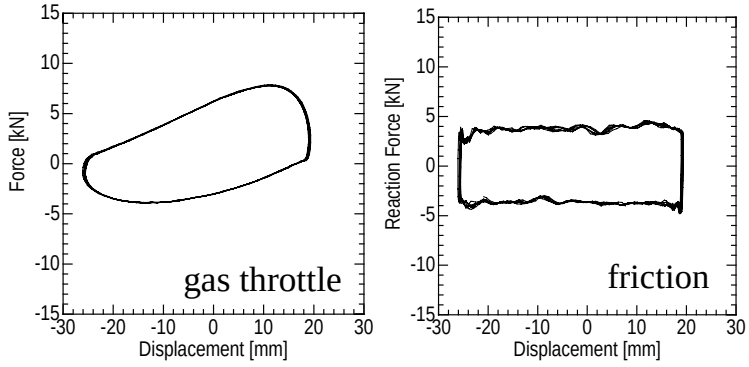

a. pressure loss of gas throttle *b. friction of cylinders*

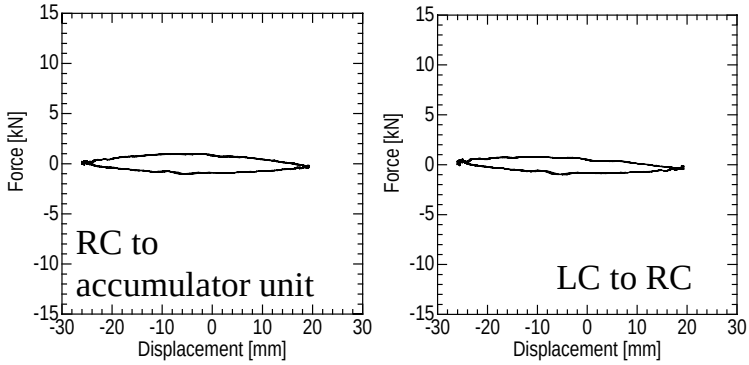

c. pressure loss of oil piping

Fig. 9 Hysteresis of Rocking Suppression Devices

Table 5 Equivalent Damping Factors

		Aarea of Hyst. [Nm]	h_{eq} [%] (Measured)	(Target)
Air Spring	Orifice	130.6	6.5	6.3
	Oil Damper	-	(4.7)	5.0
Rocking Suppression Device	Throttle	272.3	13.6	12.5
	Oil Piping 1	67.2	3.3	2.0
	Oil Piping 1	74.6	3.7	2.0
	Friction	427.5	21.3	(3.0)

4.3. Earthquake Wave Excitation Test

4.3.1. Input Motion

The input earthquake motion into a shaking table is taken as the greatest excitation S2 whose response spectrum of 5% of damping in a long period is 2 m/s. However, an input earthquake motion cuts a long period and a short period with a band path filter because of restrictions of the shaking table capability. (Refer to Fig. 10).

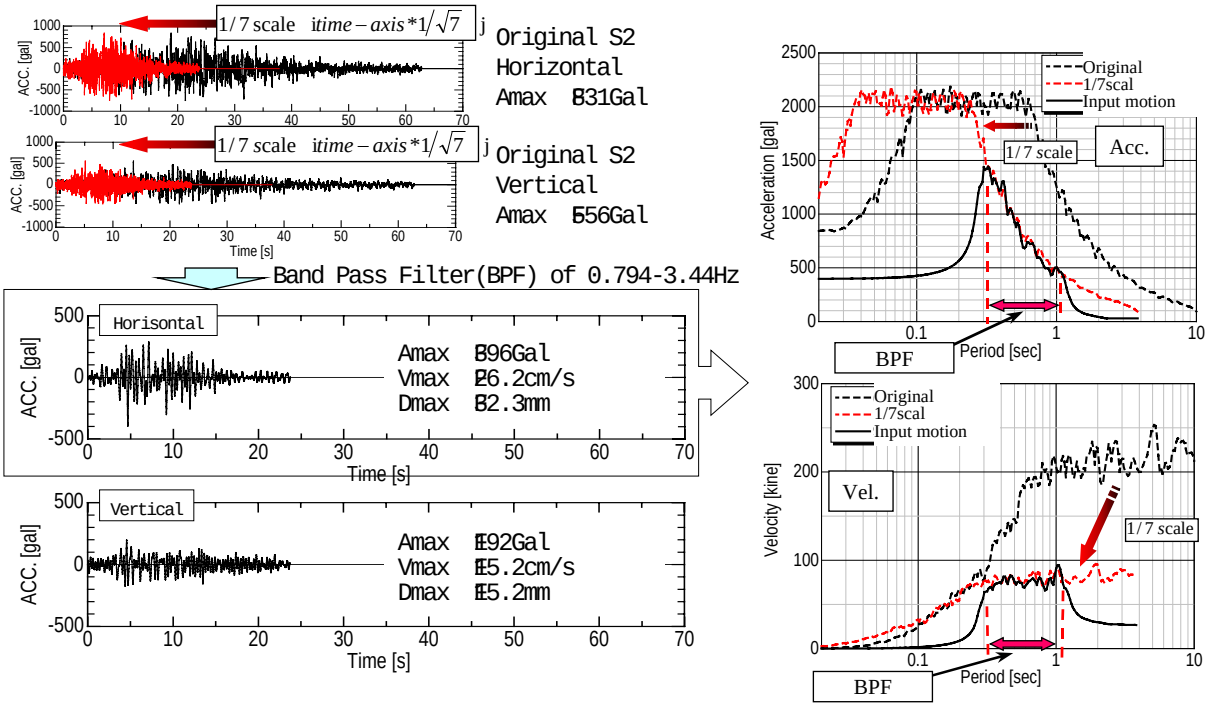

Fig. 10 Input motion

4.3.2. Test Cases

The cases of earthquake wave excitation test are summarized in Table 6. Though the wave that gave the band-pass filter processing was used in most cases, the tests that used the wave that gave the high-pass filter that left the high frequency element was executed in the case with the excitation only of the direction of Z. The band pass filter processing wave is the same as the test of the air springs alone .

Table. 6 Test Case of Earthquake Wave Excitation Test

Input Level	Exciting Direction*	Filter
S2 x 1.0	X, Y, Z, XY, XZ, XYZ	0.794-3.44 Hz BPF
S2 x 1.0	Z	0.3Hz HPF
S2 x 1.5	X, Y, Z, XZ	0.794-3.44 Hz BPF

* 'XY' means earthquake wave in X and Y direction input simultaneously.

4.3.3. Isolation Performance

Figure 11 shows the response spectrum of input acceleration and of response acceleration of the building model

in case of that 1.0*S2 wave in X (horizontal) direction and Z (vertical) direction input simultaneously. In horizontal direction, the response under the period of 0.5 sec is isolated obviously. Similarly, the response acceleration in vertical direction under the period of 0.5 sec has been isolated, but vertical isolation performance is not as clear as that of horizontal direction because of the lower cut off frequency of band-pass filter, which is about 0.3 sec is close to 0.5 sec.

Figure 12 shows the time history of the response acceleration of the building model. As shown in Fig.12, maximum acceleration of input 553 gal was reduced to 304 gal.

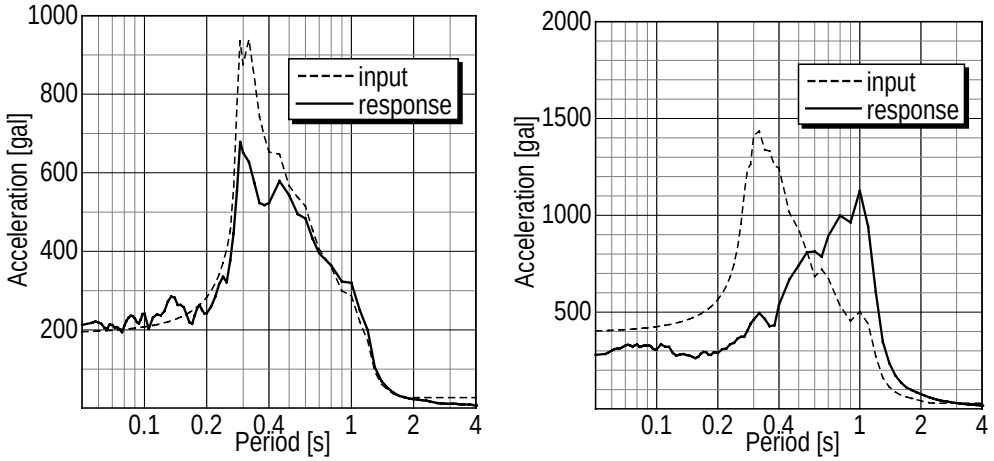

*Fig. 11 Response Spectrum in case of 1.0*S2 Input*

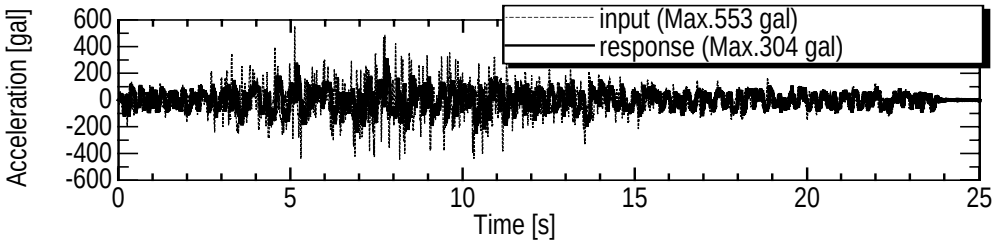

Fig. 12 Time History of Response Acceleration in Vertical Direction (0.3Hz HPF input)

Figure 13 shows the response spectrum of the input acceleration and of response acceleration of the building model in vertical direction. It is confirmed that the response spectrum is greatly decreased in a low area of the period than 0.5 seconds as shown in Fig.13.

We can see that the isolation performance also appears well in vertical direction.

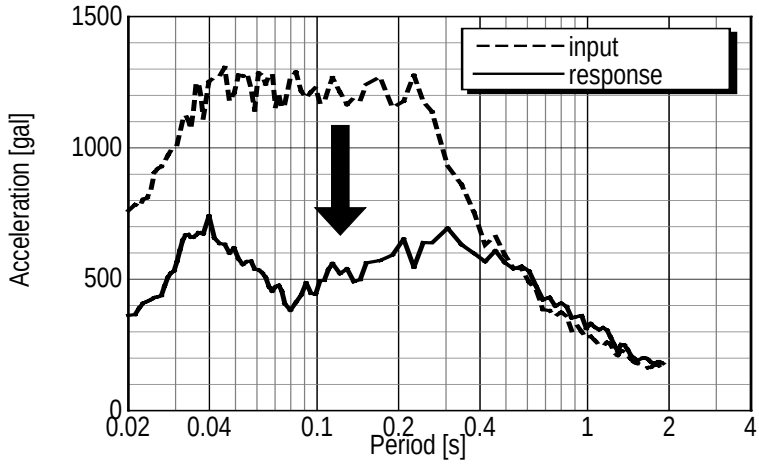

Fig. 13 Response Spectrum in Vertical Direction (0.3Hz HPF input)

4.3.4. Health to Excessive Level of Earthquake

Figure 14 shows the response spectrum of input acceleration and of response acceleration of the building model in case of

that 1.5*S2 wave in X (horizontal) direction and Z (vertical) direction input simultaneously. The shape of response spectrum in Fig.14 is almost similar to that in Fig.11 (which is that of 1.0*S2). Thus it is confirmed that the excessive level of earthquake input both in horizontal and in vertical direction does not affect the isolation performance.

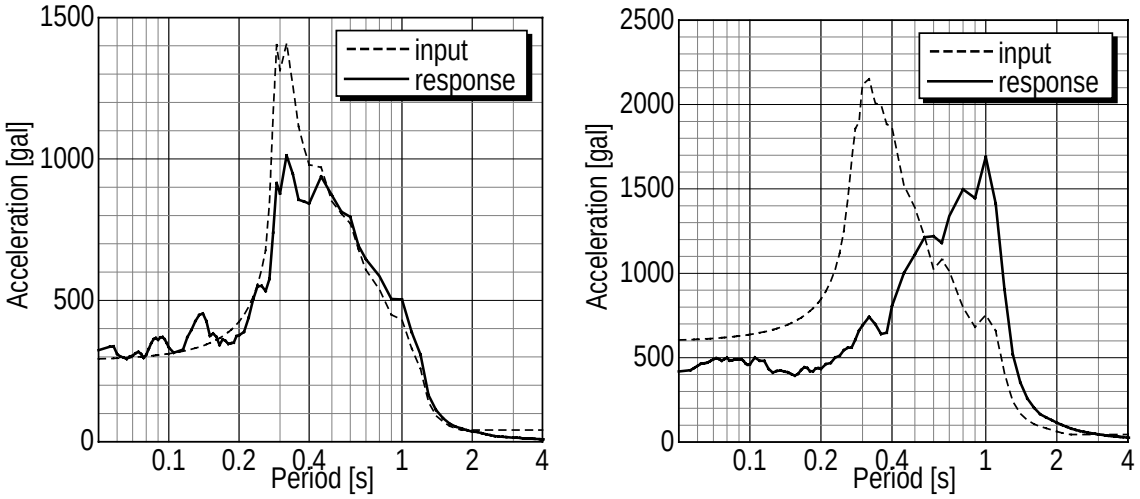

a. Vertical *b. Horizontal*

*Fig. 14 Response Spectrum in case of 1.5*S2 Input*

4.3.5. Independency of Performance in Horizontal and Vertical direction

Figure 15 shows the response spectrum in the case of the shaking table excited in X direction only, in X and Z direction and in X, Y and Z direction simultaneously. As shown in this figure, input condition does not affect the response spectrum both in horizontal direction and in vertical direction; in other words, isolation performance is almost independent from each other. This is a convenient characteristic to design the isolation performance.

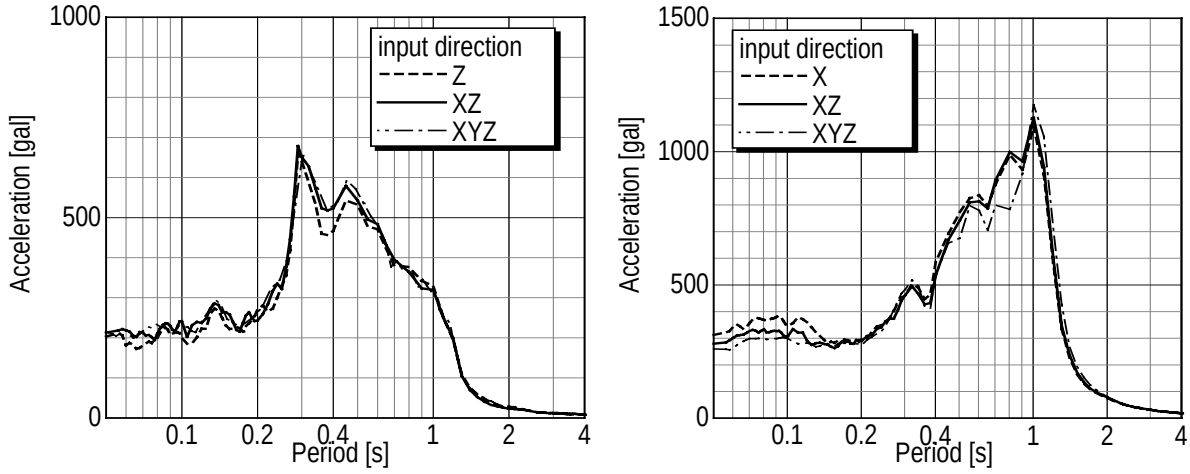

a. Vertical *b. Horizontal*

Fig. 15 Influence of Input Condition on Response

4.3.6. Performance of Rocking Suppression

Figure 16 shows the vertical response displacement due to the rocking motion at the load-carrying cylinder under the input condition of that excited in X, Y and Z direction simultaneously. The response displacement due to the rocking motion is only 1.35 mm. It indicates the effect of the rocking suppression is remarkable under three-dimensional seismic excitation.

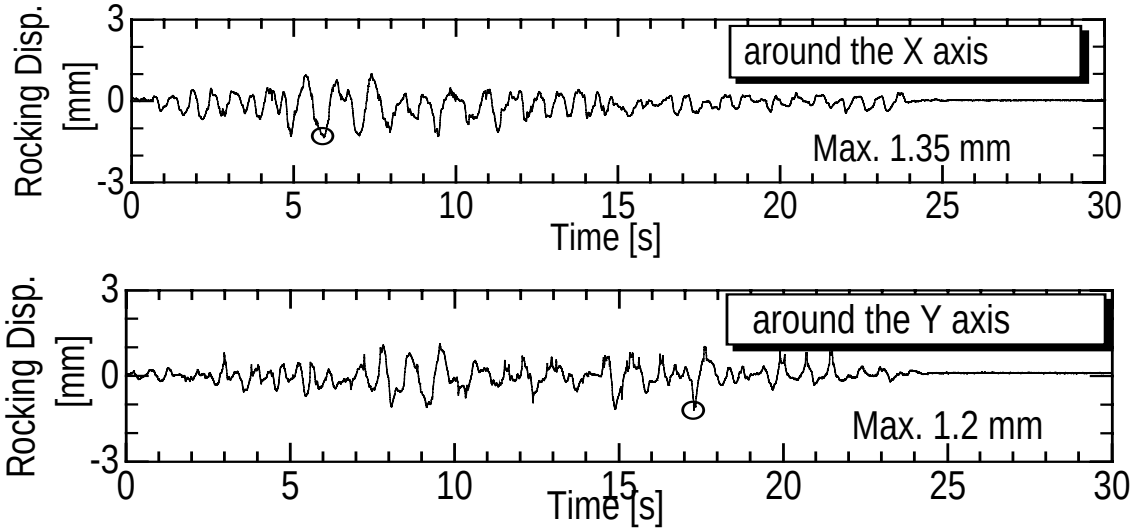

Fig.16 Vertical Displacement due to Rocking Motion

CONCLUSION

Shaking table tests of the 3D seismic isolation system that combined air springs and hydraulic rocking suppression devices were executed. Following points became clear as the results of the tests.

The device characteristics (natural frequency, damping factor, etc.) obtained from the test were almost equal to designed values.

The maximum response values in the test were almost equal to results of the prediction analysis.

The hydraulic rocking suppression devices proved to be effective to three-dimensional input excitations.

It is quite possible to actualize the air spring the burst pressure of which exceeds 20MPa.

In this isolation system, almost no interaction was observed between horizontal and vertical responses to 1.5 S2 input excitations.

Effectiveness of the seismic isolation system was confirmed through the test result that response vertical acceleration spectra greatly decreased in short period domain if high-pass filtered vertical S2 wave, which was close to original S2 wave, was input.

As the results shown above, it is confirmed that the 3D seismic isolation device is applicable to a nuclear power plant.

ACKNOWLEDGMENT

This study is a part of project sponsored by the Japanese government (METI) and was conducted by the Japan Atomic Power Company in collaboration with Japan Nuclear Cycle Institute. The authors wish to express their profound appreciation to the project committee members.

REFERENCE

[1] Fujita, T., “Technology for Earthquake-Resistant Structures in the Twenty-First Century”, “Journal of the Japan Society of Mechanical Engineers, Vol.99, No.935, pp.59-64

[2] Tetsuya Hagiwara, et al. Three-Dimensional Seismic Isolation Device with Rolling Seal Type Air Spring, 20004ASME PVP, Seismic Engineering

[3] Takahiro Shimada, et al. Study on Three-Dimensional Seismic Isolation System for Next-Generation Nuclear Power Plant: Hydraulic Three-Dimensional Base Isolation System, 2004ASME PVP, Seismic Engineering

[4] Kato, M., et al. Design study of the seismic-isolated reactor building of demonstration FBR plant in Japan, 13th SMiRT, Aug.1995, pp579-584

[5] Kato, A., Umeki, K., Morishita, M., Fujita, T. and Mi-dorikawa, S., “A Large Scale Ongoing R&D Project on Three-Dimensional Seismic Isolation for FBR in Japan”, Aug. 2002, ASME PVP

18th International Conference on Structural Mechanics in Reactor Technology (SMiRT 18)
Beijing, China, August 7-12, 2005
SMiRT18-K11-7

SEISMIC PROTECTION OF SECONDARY SYSTEMS IN NUCLEAR POWER PLANT FACILITIES

Yin-Nan Huang*
University at Buffalo
State University of New York
212 Ketter Hall, Buffalo, NY,14260, USA
Phone: 1-716-867-0983
Fax: 1-716-645-3733
E-mail: yh28@buffalo.edu

Andrew S. Whittaker
University at Buffalo
State University of New York, USA

Michael C. Constantinou
University at Buffalo
State University of New York, USA

Sanj Malushte
Bechtel Power Corporation, MD, USA

ABSTRACT

Numerical models of a sample nuclear power plant (NPP) reactor building, both conventionally constructed and equipped with seismic protective systems are analyzed for both Safe Shutdown and Beyond-Design-Basis earthquake shaking at two coastal sites in the United States. Seismic demands on secondary systems are established for the conventional and seismically isolated NPPs. The reductions in secondary-system acceleration and deformation demands afforded by the isolation systems are identified. The impact of isolation system choice on the response of the key secondary systems is presented.

Keywords: Nuclear power plant, secondary systems, seismic base isolation, viscous dampers.

1. INTRODUCTION

The United States Department of Energy (DOE) has identified a number of generic issues that could impact the viability of new nuclear power plant (NPP) construction in the United States, including economic competitiveness, nuclear safety, and management of spent nuclear fuel (SNF). Seismic protective systems, herein assumed to include seismic isolation and damping devices, can address each of these issues, enabling direct reductions in overnight capital cost and standardization of NPP and SNF facility designs and simplified design and regulatory review; facilitating design certification and the granting of early site permits and construction and operating licenses; and enhancing NPP and SNF safety at lower capital cost.

The primary focus of this paper is the characterization of seismic demands on secondary systems in NPP construction because the costs associated with analysis, design, construction, testing and regulatory approval of secondary systems can dominate the cost of NPPs. Substantial reductions in demands on secondary systems such as steam generators and piping systems will facilitate greater use of commercial-off-the-shelf equipment, simplify system and equipment qualification and design and regulatory review, and enhance NPP safety.

U.S. Nuclear Regulatory Commission (USNRC) Regulatory Guide RG 1.165 (USNRC, 1997) specifies that the Safe Shutdown Earthquake (SSE) for the seismic design of safety-related nuclear structures be based on a 5% damped median response spectrum with a return period of 100,000 years (or a median annual probability of exceedance of 1×10^{-5}). Chapter 1 of 10CFR (USNRC, 2005) writes that safety-related structures, secondary systems and components remain functional (undamaged) in the event of SSE shaking. For many NPP sites in the U.S., earthquake shaking associated with the SSE will result in high seismic acceleration and deformation demands in the stiff structural systems and extremely high demands on the safety-related secondary systems. Seismic isolation can substantially mitigate these high demands on primary structural components and secondary mechanical, electrical and piping systems by reducing the natural frequency of the NPP structure (by up to a factor of 20) and thus substantially separating the dominant frequencies of the secondary systems from the key natural frequency(s) of the primary system.

Seismic isolation and damping systems are widely used to protect mission-critical infrastructure. More than 3,000 buildings, bridges, and other types of structures have been isolated to date (Kelly, 2004). Seismic isolation has been incorporated into six reactor units, four in France and two in South Africa. In 1997, the Central Research Institute of Electric Power Industry in Japan issued isolation guidelines for applications to Fast Breeder reactors and Light Water reactors. In the United States, seismic isolation design procedures have also been included in the design code for safety-related nuclear structures (ASCE, 2000).

The potential benefits of applying seismic protective systems to the next generation of NPPs and SNF buildings prompted the study described in the remainder of this paper. Response-history analysis of numerical models of conventional and isolated reactor buildings was used to assess demands on structural and secondary systems. Herein, attention is focused on horizontal shaking only. Additional results will be available in Huang et al. (2006).

2. DYNAMIC MODELS OF THE FIXED-BASE AND BASE-ISOLATED REACTOR BUILDINGS

A lumped-mass stick model of a conventional next generation NPP reactor building was used to benchmark results from response-history analysis. (Information on the framing of the NPP reactor building was provided by a NPP supplier.) The model, shown in Figure 1, is composed of two *sticks*: one representing the containment structure and the other representing the internal structure. The two sticks are structurally independent and are connected only at the base. The mechanical properties of the frame elements that compose each stick were back-calculated from analysis of the 3-D reactor building. The reactor building was assumed to be founded on *west coast* rock. The mass of the structure and the secondary systems was lumped at discrete locations at key levels in the reactor building. The discrete masses were connected to the frame elements through rigid links to account for torsional effects. The total height of the containment structure is 59.5 meters and its first mode period is approximately 0.2 second. The height of the internal structure is 39 meters; the first mode period of the internal structure in both horizontal directions is approximately 0.14 second. The total weight of the NPP reactor building is approximately 75,000 tons.

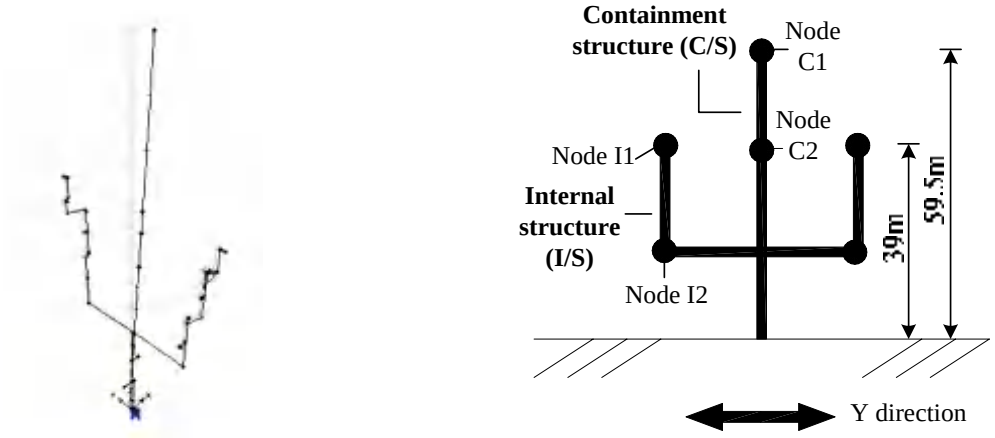

a. Model 1 and first mode shape b. Stick model sketch

Fig. 1. Model of the NPP building for response-history analysis

Nineteen numerical models were developed in the computer code SAP2000 Nonlinear (CSI, 2002) to study the impact of seismic protective systems on the response of the NPP reactor building and its secondary systems. The numerical models include representations of high damping rubber (HDR) bearings, lead-rubber (LR) bearings and Friction Pendulum™ (FP) bearings. Table 1 lists the properties of the isolation systems used in the models. Model 1 is the model of the conventionally framed NPP reactor building. Bilinear elements were used for the LRB and FP bearings; the key properties are shown in Figure 2. To study a wide range of isolator properties, the values of Q_d and F_y were set equal to either 3 or 6 percent of the supported weight and the second-slope period (related to K_d through the supported weight) was assigned values of 2, 3 and 4 seconds. The HDR bearings were modeled as linear viscoelastic elements and the problematic issues associated with scragging and modeling were not addressed. The linear viscoelastic models could equally well, and perhaps better, model an isolation system incorporating low damping rubber bearings and linear viscous dampers. Again, to study a wide range of isolator properties, consistent with isolators used in design practice, the dynamic properties of the HDR isolators included isolated periods of 2, 3 and 4 seconds and viscous damping ratios of 10% and 20% of critical. (Note that a period of 4 seconds is problematic for HDR and LR bearings due to isolator instability and that a damping ratio of 20% can only be realized in HDR isolators with supplemental damping devices.)

3. EARTHQUAKE HISTORIES USED FOR THE RESPONSE-HISTORY ANALYSIS

To judge the utility of seismic isolation for NPP and SNF applications, response-history analysis was performed using earthquake histories generated for east and west coast sites. The two bins of 10 pairs of earthquake histories were generated by Somerville et al. (1997) for firm soil sites in Boston and Los Angeles and a 2% probability of exceedance in 50 years. The Somerville seed motions were re-scaled for the response-history analysis reported herein. Each pair of earthquake histories was scaled to minimize the sum of the squared error between the target spectral values (developed from the USGS hazard maps for a 2% probability of exceedance in 50 years) and the geometric mean of the spectral ordinates for the pair at periods of 0.3, 2 and 4 seconds, where 0.3 second is representative of the natural period of a conventionally framed NPP and 2 and 4 seconds represent two of the isolated periods considered in the study. Acceleration spectra for the resulting 20 histories in each bin are shown in Figures 3a and 3c for the east and west coast sites, respectively. The variability in the spectral ordinates by bin and period is indicative of the scatter in recorded ground motions for a given combination of earthquake magnitude and distance. Figures 3b and 3d present the target spectrum, and median, 84th percentile and 16th percentile spectral ordinates for the 20 histories for the east and west coast sites, respectively. It should be noted that the spectral ordinates of the west coast (Los Angeles) histories are substantially larger in the long-period range than those of the east coast (Boston) histories.

The 2% probability of exceedance in 50 years corresponds to the return period of 2475 years: a return period much less than that required by RG 1.165 for SSE shaking. Although this could be considered a shortcoming of the analysis reported herein, the authors felt that it was more important to utilize a robust set of earthquake histories that accounted directly for randomness in the ground motion than to use motions matched to a site-specific spectrum. Importantly, the target spectra of Figures 3b and 3d could represent SSE shaking at sites on the east and west coast, although not in Boston or Los Angeles, respectively.

Safety assessment of NPP often requires a margins assessment, or an estimate of response for Beyond-Design-Basis (BDB) earthquake shaking, to ensure that shaking in excess of that associated with the SSE spectrum will not substantially compromise the safety and integrity of the NPP structure and secondary systems. No specific margin or multiplier is mandated by the USNRC for beyond-design-basis assessment. (The multiplier used in the United Kingdom is 1.4.) Per RG 1.165, SSE shaking is characterized by a 5% damped *median* spectrum. For this study, earthquake histories for the beyond-design-basis assessment were generated by amplifying the acceleration time series for each history from the *median* level to an *84th* percentile level. The acceleration time-series magnification factor was determined using ground-motion-attenuation relationships for east and west coast sites, recognizing that the ratio of the 84th and 50th (median) spectral ordinates (Y) is equal to the standard deviation of $\mathrm{Ln}Y$. The attenuation relationships of Campbell (2001) and Abrahamson and Silva (1997) were used to compute the multipliers for the east coast and west coast sites, respectively. Values for the multiplier were calculated for periods of 0.01 second, 0.15 second, 2.0 seconds and 4.0 seconds were computed. Results are shown in Fig. 4. For the beyond-design-basis assessment presented here, a magnification factor of 1.7 was used to scale up the earthquake acceleration histories.

Table 1. Description of response-history-analysis models

Model no.	Type of bearings	Description[1]
1	None	First mode periods of the containment and internal structures, in each horizontal direction, are (0.22 sec, 0.21 sec) and (0.14 sec, 0.13 sec), respectively
2	FP-isolated	$Q_d = 0.03W$; $T_d = 2$ seconds; $u_y = 1$ mm
3	FP-isolated	$Q_d = 0.03W$; $T_d = 3$ seconds; $u_y = 1$ mm
4	FP-isolated	$Q_d = 0.03W$; $T_d = 4$ seconds; $u_y = 1$ mm
5	FP-isolated	$Q_d = 0.06W$; $T_d = 2$ seconds; $u_y = 1$ mm
6	FP-isolated	$Q_d = 0.06W$; $T_d = 3$ seconds; $u_y = 1$ mm
7	FP-isolated	$Q_d = 0.06W$; $T_d = 4$ seconds; $u_y = 1$ mm
8	LR-isolated	$F_y = 0.03W$; $T_d = 2$ seconds; $K_u = 10K_d$
9	LR-isolated	$F_y = 0.03W$; $T_d = 3$ seconds; $K_u = 10K_d$
10	LR-isolated	$F_y = 0.03W$; $T_d = 4$ seconds; $K_u = 10K_d$
11	LR-isolated	$F_y = 0.06W$; $T_d = 2$ seconds; $K_u = 10K_d$
12	LR-isolated	$F_y = 0.06W$; $T_d = 3$ seconds; $K_u = 10K_d$
13	LR-isolated	$F_y = 0.06W$; $T_d = 4$ seconds; $K_u = 10K_d$
14	HDR-isolated	$T_i = 2$ seconds; $\xi_i = 0.10$
15	HDR-isolated	$T_i = 3$ seconds; $\xi_i = 0.10$
16	HDR-isolated	$T_i = 4$ seconds; $\xi_i = 0.10$
17	HDR-isolated	$T_i = 2$ seconds; $\xi_i = 0.20$
18	HDR-isolated	$T_i = 3$ seconds; $\xi_i = 0.20$
19	HDR-isolated	$T_i = 4$ seconds; $\xi_i = 0.20$

1. See Figure 2 for definitions of Q_d, F_y, K_d, K_u; T_d is related to K_d through the supported weight; T_i is the isolated period based on a rigid superstructure; ξ_i is the damping in the HDR isolation systems.

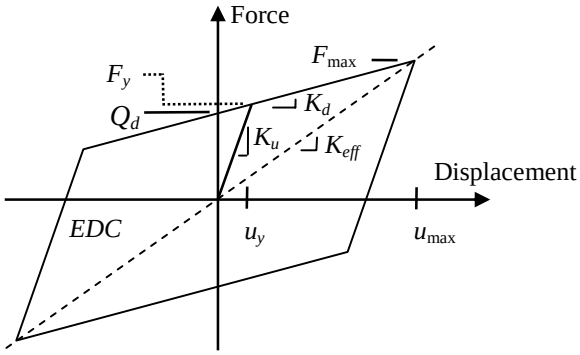

Fig. 2. Assumed properties of the LR and FP-bearings

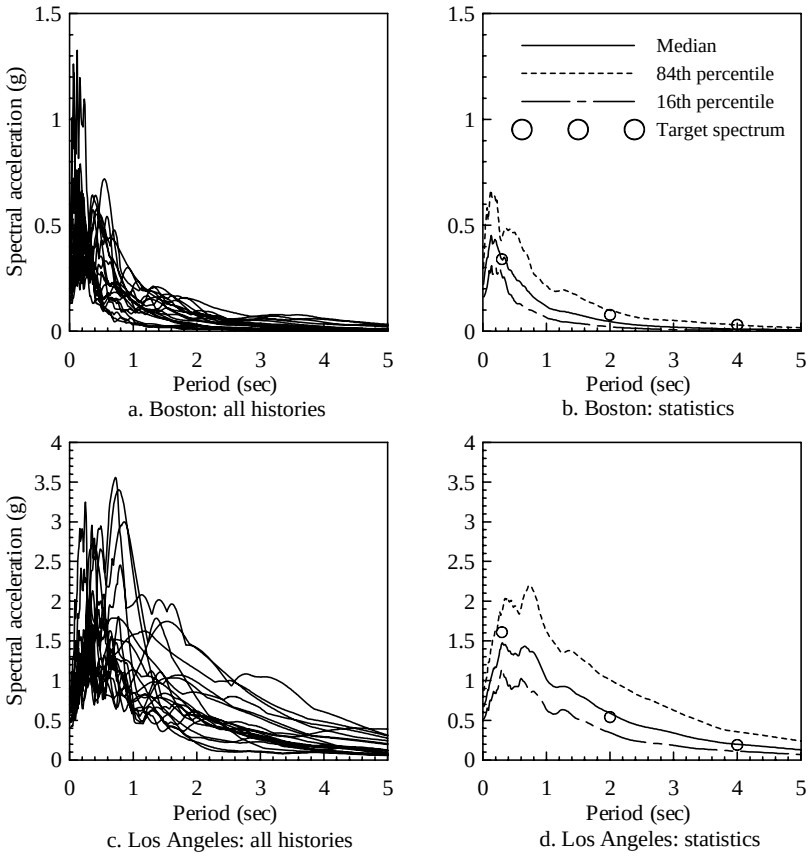

Fig. 3. Spectral accelerations of the ground motion bins for Boston and Los Angeles

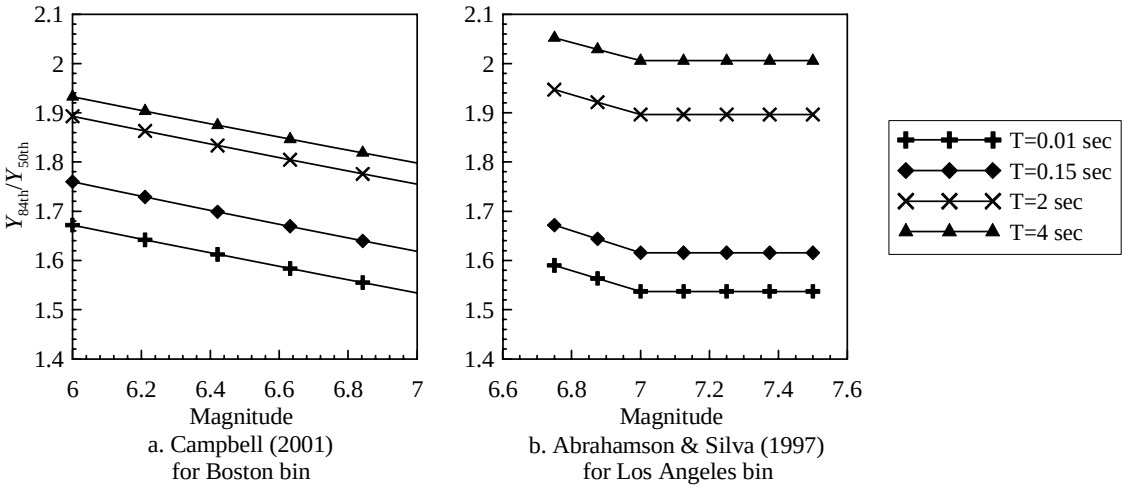

Fig. 4. Beyond-Design-Basis acceleration time-series magnification factors

4. SEISMIC DEMANDS ON SECONDARY SYSTEMS

4.1 Introduction

Response-history analysis was performed for each model and for three combinations of ground shaking and superstructure strength. Table 2 presents the combinations. Two levels of ground shaking were considered: SSE shaking and Beyond Design Basis (BDB) shaking, where BDB shaking is 170% of SSE shaking. Three levels of internal superstructure (exclusive of the isolators) strength were considered: infinite (elastic response), V_y and $1.20V_y$, where V_y in each frame element in each horizontal direction was taken as the median shear force demand of the 20 earthquake histories for SSE shaking on the conventionally framed NPP. Bilinear shear hinges with 10% post-yield stiffness were assigned to all frame elements in the internal-structure *stick*. The containment structure was assumed to remain elastic for SSE and BDB shaking. The strength of $1.20V_y$ represents a lower bound to the strength of the internal structural components. For each case, the same superstructure strength was employed for each model.

Table 2. Combinations of earthquake shaking and superstructure strength

Case	Ground motion	Yield strength of superstructure
I	SSE shaking	∞
II	BDB shaking	V_y
III	BDB shaking	$1.20V_y$

Results of the response-history analysis are presented below for the internal structure only because the secondary systems are supported primarily on this structure and not the containment structure. Unidirectional horizontal earthquake histories were applied to each model along each horizontal axis for a total of 40 simulations per model per bin. The statistical analysis of Section 4.2 below utilizes peak response data from each of the 40 simulations.

4.2 Response-History Analysis Results

Figures 5 and 6 present the maximum acceleration statistics at node I1, the top of the internal structure, as shown in Fig. 1b) and the drift ratio (relative displacement divided by height) statistics between node I1 and node I2 for all models, three cases and two bins of earthquake shaking. Accelerations at node I1 characterize peak demands at piping-system attachment points at the top of the internal structure. Node I1 and I2 drift ratios represent peak demands on deformation-sensitive components such as steam generators. Median, 16th percentile and 84th percentile

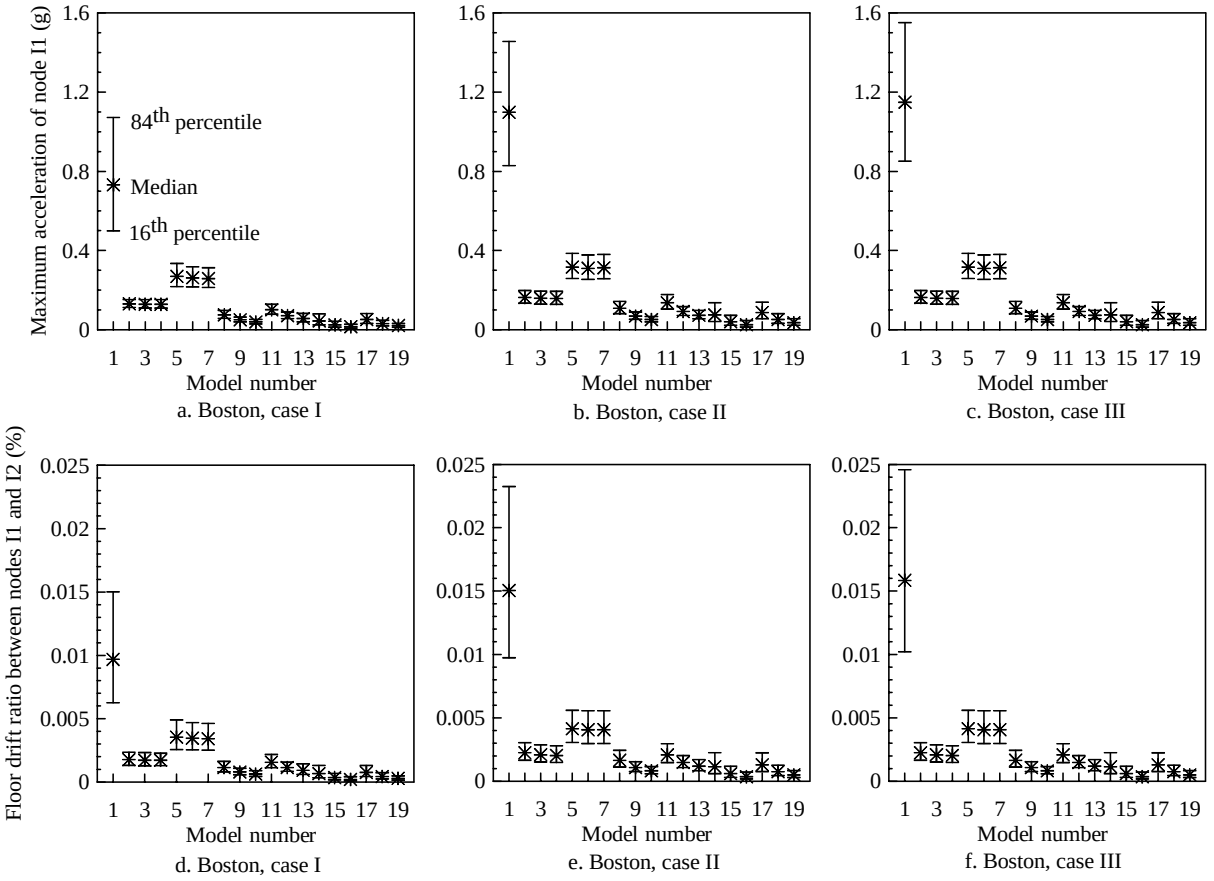

Fig. 5. Sample acceleration and drift ratio demands for the Boston earthquake histories

values are presented assuming that maximum values obtained from the response-history analysis are lognormally distributed. Table 3 lists the median response ratios of Figs. 5 and 6, calculated as the median response of the isolated NPP model divided by the median response of the conventional NPP model (Model 1).

Some general conclusions can be drawn on the basis of the data presented in Figs. 5 and 6 and Table 3. The use of seismic isolation leads to very significant reductions in acceleration and drift demands. The response reduction is greatest for the long-period isolated NPP (4 seconds), which is intuitive. Much greater percentage reductions are realized for the east coast (Boston) histories because the west coast (Los Angeles) histories have a much higher long-period content (see Figs. 3b and 3d). Importantly, the spectral accelerations of some of the Los Angeles histories are greater at a period of 2 seconds than at 0.14 second: the first mode period of internal structure.

For the Boston bin of earthquake histories, the demands on the secondary system are greater for the isolation systems with $Q_d = 0.06W$ (Models 5, 6 and 7) than for $Q_d = 0.03W$ (Models 2, 3 and 4). (The displacements across the isolation interface are smaller for Models 5, 6 and 7 than for Models 2, 3 and 4, respectively.) This result is due to larger forces developing in the $Q_d = 0.06W$ isolation systems at small displacements and the higher pre-yield stiffness of the $Q_d = 0.06W$ isolation systems (because the yield displacement was set at a constant value of 1 mm for all six FP isolation systems). Improved models of the FP bearings, accounting for the velocity dependence of the coefficient of sliding friction, will reduce the demands on the secondary systems. The trend observed for the FP bearings and the Boston ground motions does not hold for higher levels of earthquake shaking (i.e., the Los Angeles ground motions) for which comparable secondary-system demands are observed for the $Q_d = 0.06W$ and $Q_d = 0.03W$ isolation systems: see Table 3. For BDB shaking (Cases II and III), the increase in

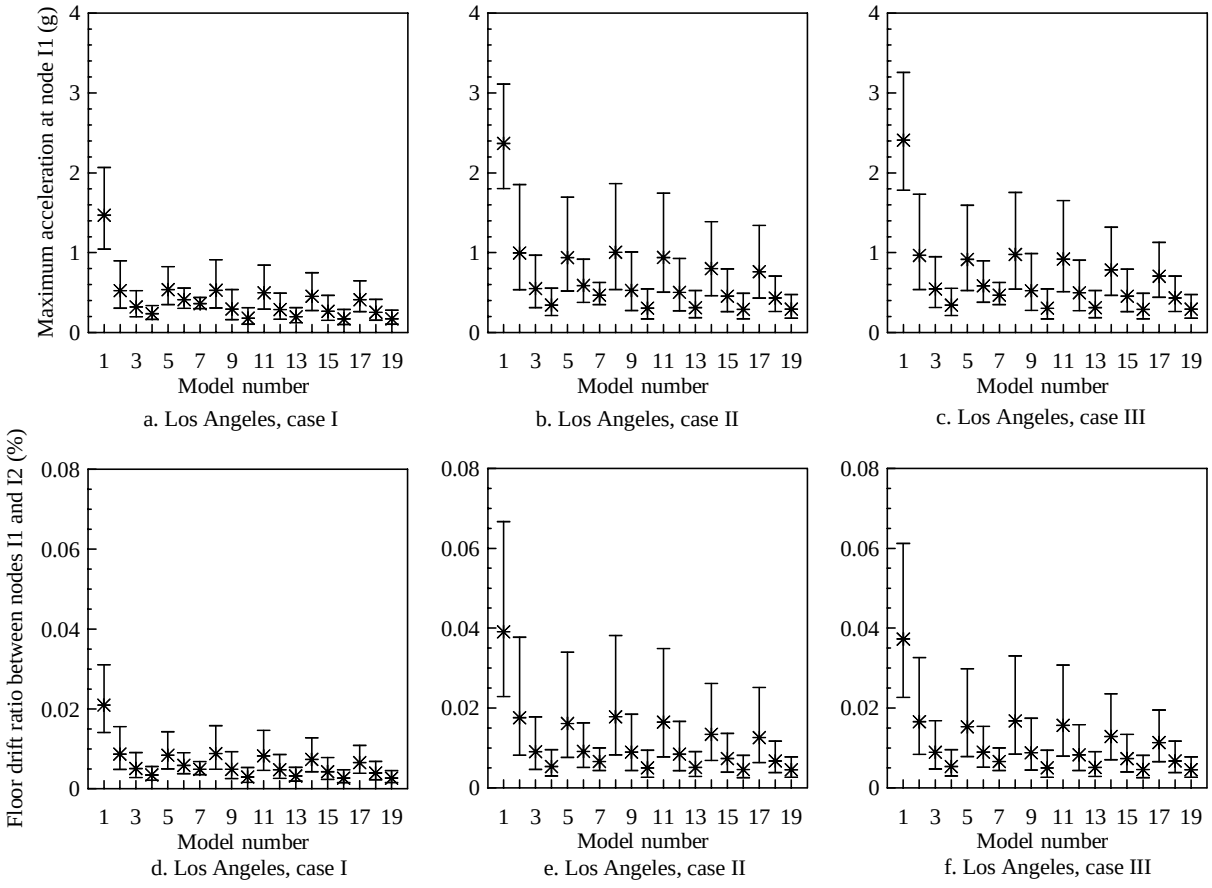

Fig. 6. Sample acceleration and drift ratio demands for the Los Angeles earthquake histories

median and 84th percentile accelerations and drift ratios is significant (of the order of 1.5) for the conventional NPP but small for the isolated NPPs, showing that an increase in the shaking intensity does not produce a similar increase in the demands on the secondary systems for the isolated NPPs. For the Boston earthquake histories, all of the isolated superstructures remained elastic for BDB earthquake shaking.

For the Los Angeles bin of BDB histories and case II yield strength (see Table 2), the superstructures of the isolated models with a period of 2 seconds yield (i.e., are damaged) for 10 of the 20 earthquake histories. (The number of instances of yielding decreases with an increase in isolation period.) Superstructure yielding for some earthquake histories produces the large differences in the 16th and 84th percentile responses of the 2-second isolated models in Fig. 6. Nonetheless, the introduction of an isolation system reduces substantially the median response of the NPP building and its secondary systems and the absolute dispersion of the responses are far smaller for the isolated NPPs than for the conventional NPP.

Floor Response Spectra (FRS) have been widely used in the nuclear industry (USNRC, 1978) to estimate demands on flexible secondary systems (Chen and Soong, 1998). In this study, absolute acceleration response histories were recorded at node I2 to develop representative FRS and to identify the difference in spectral responses for the conventional and isolated NPPs. (For the sample NPP under consideration, node I2 is located at the base of a tall steam generator.) Fig. 7 shows the median and 84th percentile floor acceleration response spectra for models 1, 3, 9 and 15 subjected to the Boston and Los Angeles SSE bins of ground motions, assuming that the peak responses are lognormally distributed. The frequency range of 5 to 33 Hz encompasses the frequencies of most NPP secondary systems. The reductions in floor spectra response resulting from the use of seismic isolators range between 3 and 15+ for the selected isolation systems and the frequency range of 5 to 33 Hz. The largest reductions in response are realized for the east coast (Boston) earthquake histories.

Table 3. Ratios of median responses in conventional and isolated NPPs

Bearing type	Model number	Boston motions						Los Angeles motions					
		Acceleration at node I1			Drift ratio between nodes I1 and I2			Acceleration at node I1			Drift ratio between nodes I1 and I2		
		Case I	Case II	Case III	Case I	Case II	Case III	Case I	Case II	Case III	Case I	Case II	Case III
FP	2	0.18	0.15	0.14	0.18	0.15	0.14	0.36	0.42	0.40	0.42	0.45	0.44
	3	0.18	0.14	0.14	0.18	0.14	0.13	0.22	0.23	0.23	0.24	0.23	0.24
	4	0.18	0.14	0.14	0.18	0.13	0.13	0.16	0.15	0.14	0.17	0.14	0.14
	5	0.37	0.29	0.28	0.37	0.27	0.26	0.37	0.40	0.38	0.40	0.41	0.41
	6	0.36	0.28	0.27	0.36	0.27	0.26	0.28	0.25	0.24	0.28	0.23	0.24
	7	0.35	0.28	0.27	0.35	0.27	0.26	0.25	0.20	0.19	0.23	0.17	0.18
LR	8	0.10	0.10	0.09	0.12	0.11	0.10	0.36	0.42	0.41	0.42	0.46	0.45
	9	0.07	0.06	0.06	0.08	0.07	0.07	0.20	0.22	0.22	0.23	0.23	0.24
	10	0.05	0.05	0.04	0.07	0.05	0.05	0.12	0.13	0.13	0.14	0.13	0.13
	11	0.14	0.12	0.12	0.16	0.14	0.13	0.34	0.40	0.38	0.39	0.42	0.42
	12	0.10	0.08	0.08	0.12	0.10	0.09	0.20	0.21	0.21	0.23	0.22	0.22
	13	0.08	0.07	0.06	0.10	0.08	0.07	0.13	0.13	0.13	0.15	0.13	0.14
HDR	14	0.06	0.07	0.07	0.07	0.08	0.07	0.31	0.34	0.33	0.35	0.34	0.35
	15	0.03	0.04	0.03	0.04	0.04	0.04	0.18	0.19	0.19	0.20	0.19	0.20
	16	0.02	0.02	0.02	0.02	0.02	0.02	0.12	0.12	0.12	0.13	0.12	0.12
	17	0.07	0.08	0.08	0.08	0.09	0.08	0.28	0.32	0.29	0.31	0.32	0.30
	18	0.04	0.05	0.04	0.04	0.05	0.05	0.17	0.18	0.18	0.19	0.17	0.18
	19	0.03	0.03	0.03	0.03	0.03	0.03	0.12	0.12	0.12	0.13	0.12	0.12

Figure 8 presents median, 16th and 84th percentile floor acceleration spectral values averaged over the frequency range from 5 to 33 Hz for each model, each case and each bin of histories. The trends of Fig. 8 are similar to those of Figs. 5 and 6. Table 4 lists the ratios of the median responses of the isolated and conventional NPPs shown in Fig 8.

4.3 Performance Spaces

The performance space is an alternate method for comparing demands on secondary systems and explicitly accounting for uncertainty and randomness in demand and response prediction (Astrella and Whittaker, 2004). Herein, the performance space is defined by two response quantities (e.g., acceleration and drift) and an 84% probability that the responses will lie within the performance space. For example, Fig. 9b presents the performance space associated with the drift ratio of node I1 and peak ground acceleration for the Boston SSE bin of earthquake histories. The choice of response quantities or indices used to define the performance space should be secondary-system dependent; typical quantities include maximum or spectral acceleration, velocity and displacement. The position of performance space indicates the overall level of structural response, the area of the space captures the randomness and uncertainty, and the shape of the space identifies the relationship (e.g., linear dependence) between the two chosen indices.

The relationship between the two chosen indices of interest must first be defined to characterize the performance space. Herein, the joint probability density function of the two indices is assumed to be a jointly lognormal. Consider Fig. 9b that is used to illustrate the calculation procedure. Figure 9b plots all 40 response points from the response-history analysis of the conventional NPP subjected to the case I Boston ground motions. The peak ground

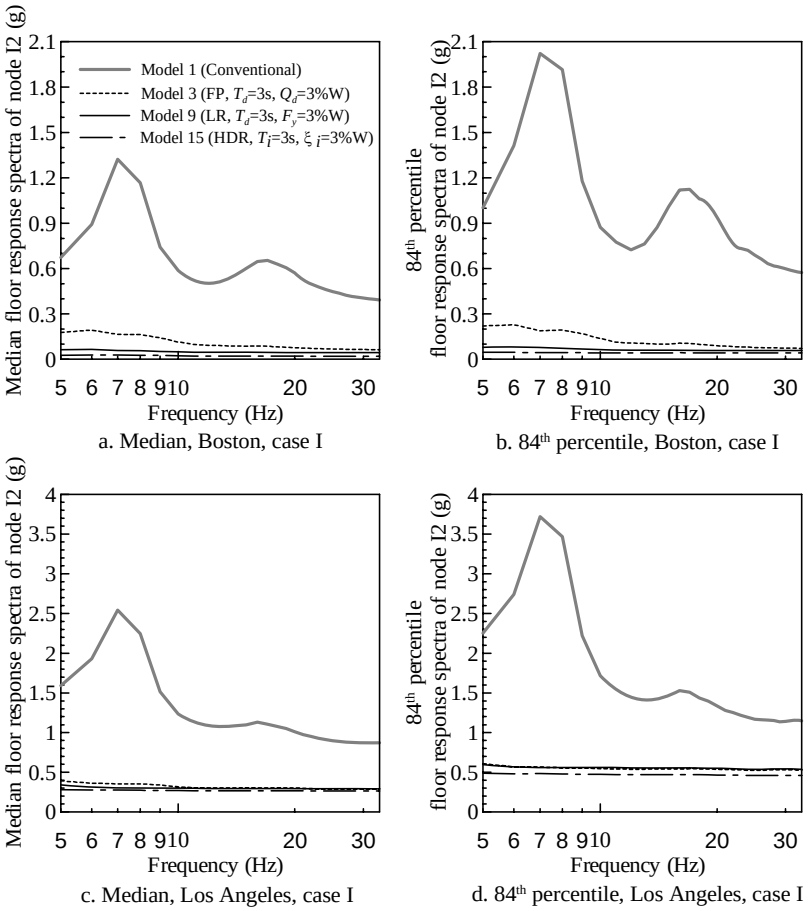

Fig. 7. Median and 84th percentile floor response spectra at node I2 for case 1

acceleration and peak drift ratio at node I1 are denoted as two random variables, *X* and *Y*, respectively. The joint probability density function of *X* and *Y* is calculated by the following equation

$$f_{XY} = \frac{1}{2\pi \cdot xy \cdot |\Lambda|^{0.5}} \exp\left[-0.5 \cdot (\tilde{z} - \tilde{m})^T \Lambda^{-1} (\tilde{z} - \tilde{m})\right] \quad (1)$$

where $\tilde{z} = [\ln x \ \ln y]^T$ and $\tilde{m}$ and Λ are the mean vector and covariance matrix of random variables ln*X* and ln*Y*; $\tilde{m}$ and Λ can be estimated from the sample points shown in the figure. Figure 9a shows the joint probability density function for this case. The total volume under the surface of the function is 1; the area in the XY plane corresponding to 84% of the total volume is the performance space of Fig. 9b.

Figure 10 performance spaces defined by the 5% damped average floor spectrum acceleration at node I2 over a frequency range of 5 and 33 Hz and the drift ratio between nodes I1 and I2. This performance space captures force demands on acceleration-sensitive components and systems attached at node I2 and the deformation demands on displacement-sensitive components and systems attached at nodes I1 and I2. The performance spaces associated with the isolated NPP models are much closer to the origin and smaller in area than those of the conventional NPP (Model 1), indicating much smaller seismic demands of reduced variability on the secondary systems in the isolated NPPs. The performance spaces of Fig. 11 permit a comparison of seismic demands on secondary systems for the conventional NPP and one isolated NPP (Model 13, lead-rubber isolators: see Table 1) at the Boston and Los Angeles sites for the three cases of Table 2. For the conventional NPP, the increase in demands (and absolute dispersion) on the secondary systems from SSE to BDB shaking is most significant compared with the changes in demand and dispersion for the isolated NPPs.

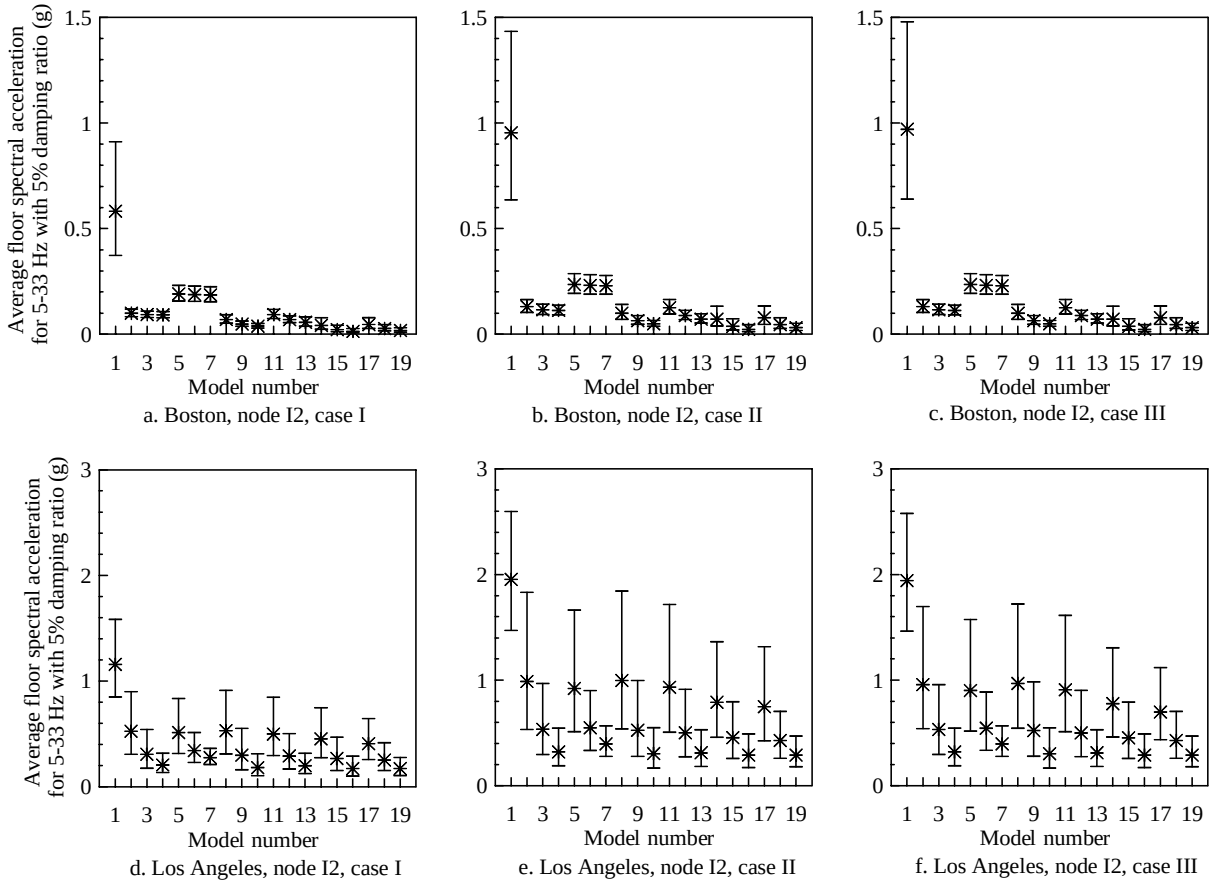

Fig. 8. Average floor spectral accelerations at node I2

5. CLOSING REMARKS

Nineteen numerical models of a conventional and seismically isolated NPP reactor building of modern construction were studied to judge the effectiveness of protective systems to mitigate earthquake-induced demands on secondary systems. Response-history analysis of linear elastic and simple bilinear models of the reactor building was performed using earthquake histories associated with SSE and BDB earthquake shaking for east and west coast sites in the United States. (Nonlinear action was permitted in the internal structure only; the containment structure was assumed to remain elastic for all levels of shaking.) Randomness in the seismic input at each site was considered by not spectrally matching the earthquake histories and only horizontal earthquake shaking was addressed. Approximate models of sliding, FP, and elastomeric, LR and HDR bearings (or more accurately, low damping rubber bearings and linear viscous dampers), were employed for the analysis. The mechanical properties of the isolators and the reactor building were not varied for the study reported herein.

Seismic demands on secondary systems were presented for sample locations (points of attachment of a steam generator and piping) in the reactor building for each site, SSE and BDB shaking, and for linear and nonlinear response in the internal structure. For each suite of analyses, the introduction of protective systems, regardless of type, led to substantial reductions in the seismic demands on the sample secondary systems. The greatest percent reductions in demand were realized for a) the east coast site (Boston ground motions), and b) the isolation systems with a period of 4 seconds (based on elastic stiffness for the HDR models and post-yield stiffness for the FP and LR models). Greater reductions in secondary-system demand were observed for the east coast ground motions because the ratios of the ground-motion spectral ordinates at the fundamental period of the internal structure and the isolated periods of 2, 3 and 4 seconds were substantially larger for the east coast motions. Although the use of the 4-second

Table 4. Ratios of median FRS responses in conventional and isolated NPPs

Bearing type	Model number	Boston			Los Angeles		
		Case I	**Case II**	**Case III**	**Case I**	**Case II**	**Case III**
FP	2	0.17	0.14	0.13	0.45	0.51	0.49
	3	0.16	0.12	0.12	0.27	0.27	0.27
	4	0.16	0.12	0.12	0.18	0.16	0.17
	5	0.33	0.25	0.24	0.44	0.47	0.46
	6	0.32	0.24	0.24	0.30	0.28	0.28
	7	0.32	0.24	0.24	0.24	0.20	0.20
LR	8	0.12	0.10	0.10	0.46	0.51	0.50
	9	0.08	0.07	0.07	0.26	0.27	0.27
	10	0.07	0.05	0.05	0.16	0.16	0.16
	11	0.16	0.13	0.13	0.43	0.48	0.47
	12	0.12	0.09	0.09	0.25	0.26	0.26
	13	0.10	0.08	0.07	0.17	0.16	0.16
HDR	14	0.07	0.08	0.07	0.39	0.40	0.40
	15	0.04	0.04	0.04	0.23	0.23	0.23
	16	0.02	0.02	0.02	0.15	0.15	0.15
	17	0.08	0.08	0.08	0.35	0.38	0.36
	18	0.05	0.05	0.05	0.22	0.22	0.22
	19	0.03	0.03	0.03	0.15	0.15	0.15

isolators minimized the seismic demands on the secondary systems, other factors must be considered in the selection of isolator period and isolator type for NPP and SNF structures, including a) the maximum permissible displacement across the isolation interface, b) the feasibility of fabricating *long-period* elastomeric bearings, c) Operating Basis Earthquake demands on the secondary systems, and d) the effects of vertical earthquake shaking.

Performance spaces were introduced as one means of judging the seismic demands on secondary systems in NPP reactor buildings. The sample performance spaces clearly demonstrated the benefits of seismically isolating NPP and SNF buildings for both SSE and BDB shaking: median demands and absolute dispersions are reduced by factors ranging between 2 and 20.

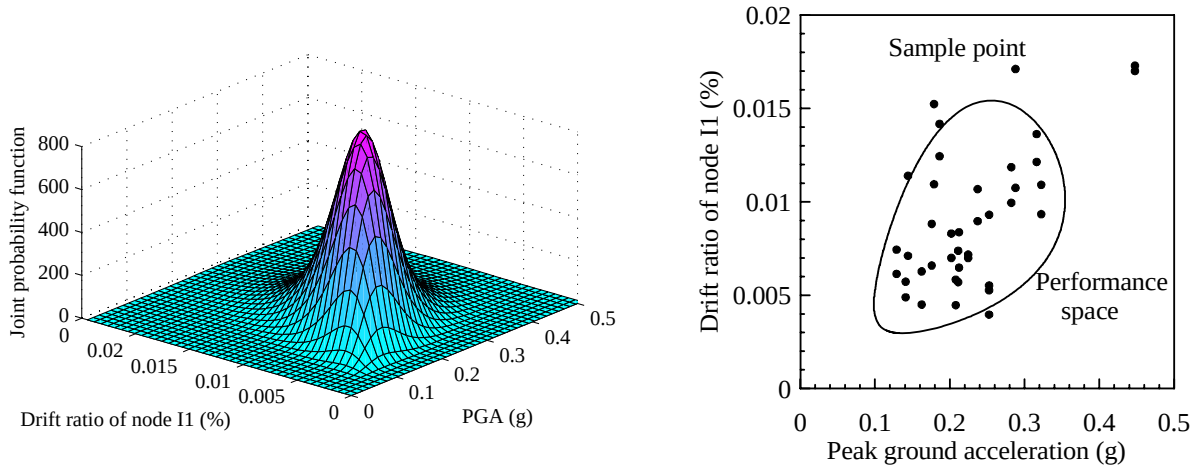

a. Joint probability density function

b. Performance space and all sample points

Fig. 9. Performance space data for the Boston SSE bin of earthquake histories

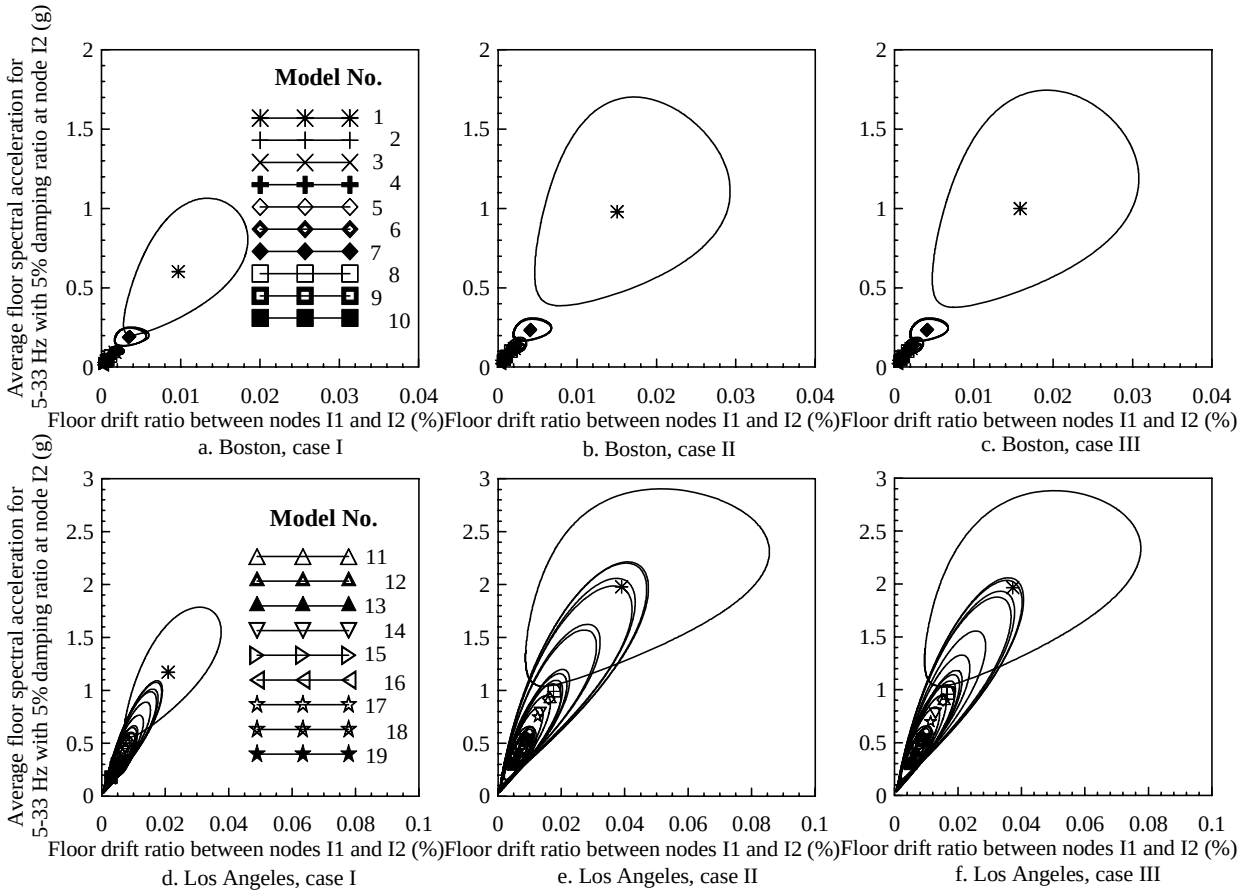

a. Boston, case I

b. Boston, case II

c. Boston, case III

d. Los Angeles, case I

e. Los Angeles, case II

f. Los Angeles, case III

Fig. 10. Performance spaces for all models and SSE motions for Boston and Los Angeles

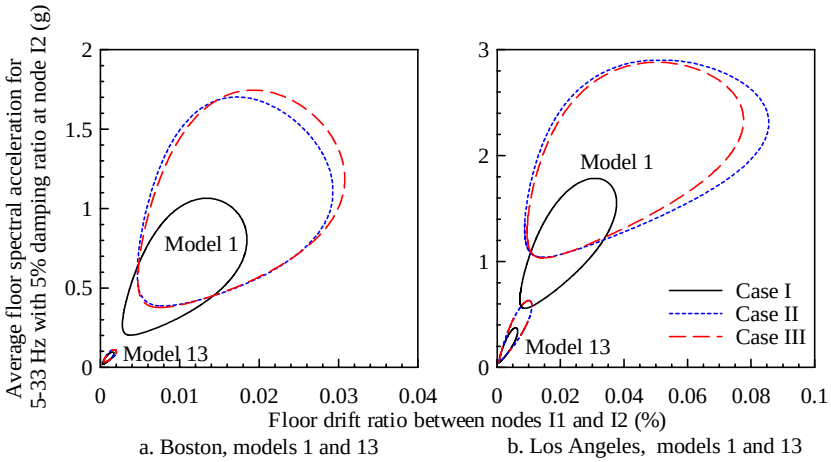

Fig. 11. Performance spaces of models 1 and 13 and cases I, II and III

ACKNOWLEDGEMENTS

Financial support for the studies described in this paper was provided in part by the Multidisciplinary Center for Earthquake Engineering Research (MCEER) through grants from the Earthquake Engineering Centers Program of the National Science Foundation (NSF), Award Number EEC-9701471, and the State of New York. The opinions, findings, conclusions expressed in this paper are those of the authors and do not necessarily reflect the views of the sponsors or the Research Foundation of the State University of New York. Dr. Ayman Saudy and Mr. Medhat Elgohary of Atomic Energy of Canada Limited (AECL) provided invaluable information on NPP reactor-building construction and provided review comments on the paper. The MCEER/NSF and AECL support is gratefully acknowledged.

REFERENCES

Abrahamson, N. A., and Silva, W. J. (1997). "Empirical response spectral attenuation relations for shallow crustal earthquakes." *Seismological Research Letters*, 68(1), 94-127.

American Society of Civil Engineers (ASCE). (2000). "Seismic analysis of safety-related nuclear structures and commentary." *ASCE 4-98*, Reston, VA.

Astrella, M. J., and Whittaker, A. S. (2004). "Changing the paradigm for performance-based seismic design." *International Workshop on Performance-Based Seismic Design - Concepts and Implementation*, Bled, Slovenia, 113-124.

Campbell, K. W. (2001). "Development of semi-empirical attenuation relationships for CEUS." *Report to the U.S. Geological Survey*, Reston, VA.

Chen, Y., and Soong, T. T. (1988). "State-of-the-art review: seismic response of secondary systems." *Engineering Structures*, 10(4), 218-228.

Huang, Y.-N., Whittaker, A. S., Constantinou, M. C., and Malushte, S. (2006). "Seismic demands on secondary systems in isolated safety-related nuclear facilities." Paper in preparation, *Earthquake Engineering and Structural Dynamics*, John Wiley.

Kelly, J. M. (2004). "*Seismic isolation*." Chapter 11 in Earthquake Engineering, Y. Bozorgnia and V. V. Bertero, eds., CRC Press, Boca Raton, FL.

CSI. (2002). *SAP2000 user's manual – version 8.0*. Computers and Structures, Inc., Berkeley, CA.

Somerville, P., Smith, N., Punyamurthula, S., and Sun, J. (1997). "Development of ground motion time histories for phase 2 of the FEMA/SAC steel project." *Report SAC/BD-97/04*, SAC Joint Venture, Sacramento, CA.

U.S. Nuclear Regulatory Commission (USNRC). (1978). "Development of floor design response spectra for seismic design of floor-supported equipment or components." *Regulatory Guide 1.122*, Washington, D.C.
U.S. Nuclear Regulatory Commission (USNRC). (1997). "Identification and characterization of seismic sources and determination of safe shutdown earthquake ground motion." *Regulatory Guide 1.165*, Washington, D.C.
U.S. Nuclear Regulatory Commission (USNRC). (2005). *NRC Regulations – Title 10,* Code of Federal Regulations, Washington, D.C.

18th International Conference on Structural Mechanics in Reactor Technology (SMiRT 18)
Beijing, China, August 7-12, 2005
SMiRT18-K11-6

ADAPTATION OF HIGH VISCOUS DAMPERS (HVD) FOR ESSENTIAL DECREASING OF IN-STRUCTURE FLOOR RESPONSE SPECTRA

Victor V. Kostarev
CKTI-Vibroseism Co. Ltd., St. Petersburg, Russian Federation
Phone: +7 812 327 8599,
Fax: +7 812 327 8599
E-mail: vvk@cvs.spb.su

Andrei V. Petrenko
CKTI-Vibroseism Co. Ltd., St. Petersburg, Russian Federation
Phone: +7 812 327 8599,
Fax: +7 812 327 8599
E-mail: andrey@cvs.spb.su

Peter S. Vasilyev
CKTI-Vibroseism Co. Ltd., St. Petersburg, Russian Federation
Phone: +7 812 327 8599,
Fax: +7 812 327 8599
E-mail: peter@cvs.spb.su

Karl-Heinz Reinsch
GERB Schwingungsisolierungen GmbH & Co KG, Berlin, Germany
Phone: +49 30 41 91 110,
Fax: +49 30 41 91 139
E-mail: karl-heinz.reinsch@gerb.de

ABSTRACT

This paper concerns a further development of High Viscous Damper (HVD) approach for essential decreasing of structure's floor response spectra. Usually restraining of components and pipelines by HVD is used for significant decreasing of operational vibration and seismic loads. A new approach consists of dampers installation for essential upgrading of a whole system's damping that is much more efficient in both technical and economical points of view than restraining of each component of the system. In that way using of HVD means high energy dissipation for whole dynamic system "Building-Components' subjected to the base seismic or other extreme load excitation.

The specific feature of each NPP site is an existing of a few closely spaced buildings: reactor building, turbine hall and so on. As the rule such buildings play sufficiently different roles in NPP operation and therefore have sufficiently different design, natural frequencies (periods) and distortion of floors and different rocking modes on a soil. The main idea explained in the paper is an interconnection of buildings by HVD. Then differences in their mechanical properties provide their out-of-phase relative motions during an earthquake and therefore effective dissipative work provided by HVD devices. At the same time implementation of HVD approach allows to eliminate possible interactions and collisions in the gaps between building structures that wears potential threat of building failure.

The detailed 3D finite element models of reactor building, turbine hall and special building were developed for NPP with VVER-1000 MWt reactor type. Performed analysis has shown high efficiency of suggested approach for protection of buildings, structures, systems and components against seismic and other impacts.

Keywords: Damper Structure Component Floor Response Spectra

1. INTRODUCTION

Nowadays VES and VD High Viscous Dampers (HVD), manufactured by GERB GmbH are well-known source for providing dynamic safety for piping, components and systems. Several thousands of HVD have demonstrated their effectiveness and reliability at nuclear and conventional power plants, heavy industry and chemical facilities in the last twenty years of the extensive worldwide usage (Berkovski, 1997), (Fomin, 2001), (Katona, 1994) and (Masopust, 1994).

Fig. 1 VD-Damper Installed on Pipeline of NPP (Turbine Hall)

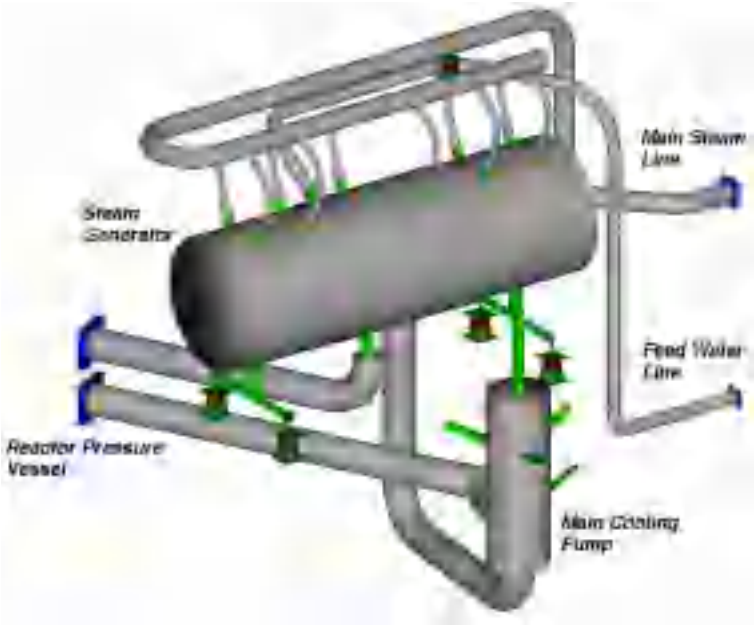

Fig.2 VD-Dampers Installed on Primary Coolant Loop of NPP (Reactor Building)

The wide spreading of HVD is determined by its unique capabilities and obvious advantages to other devices:

- To reduce vibration and dynamic response of systems in all degrees of freedom by tremendous increasing of system's damping with possibility to tune to optimal damping;
- To develop high damping forces under any dynamic impact whereas slow motions are free;
- To react on vibration immediately without any delay;
- Stability to high temperature, humid, toxic and radiation environment;
- Maintenance free design and handling. No parts for wear and tear. Cost-effective solution.

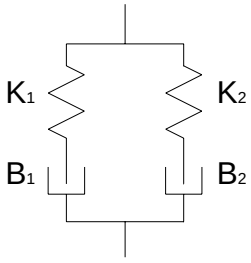

Fig.3 Model of HVD (K_1, K_2 – Stiffness, B_1, B_2 – Damping)

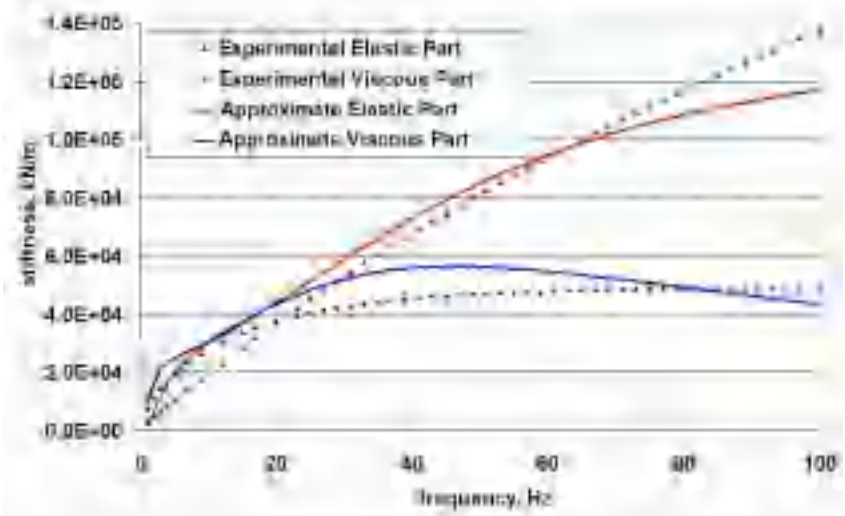

Fig.4 Dynamic Stiffness of HVD (Corresponding to the Model and Experimental)

Each HVD type has a mathematical model based on the parameters determined by numerous experiments (see in fig. 3). The comparison of the experimental characteristics with the characteristics corresponding to the mathematical model for "VD-630/325-15" damper is shown in fig. 4 (Kostarev, 1994). There can be significant both conservative and nonconservative errors in the case of simplified or ideal damper HVD models using for analysis purposes (Berkovski, 1995). The procedure of the selection of the HVD type and their number for any pipeline system is implemented in piping analysis software dPipe (CKTI-Vibroseism) and can also be fulfilled with the help of any general-purpose finite element software.

2. HVD-APPROACH: USING VD DAMPERS FOR THE SYSTEMS WITH DIFFERENT DYNAMIC PROPERTIES

Energy dissipation plays positive role providing reducing of response motion during dynamic extreme loads such as earthquake, explosion etc. At the same time structure's inertial loads and components also decrease. Usually the energy dissipation level of NPP buildings and structures is considered in the range of 2 – 10% modal damping and it corresponds to the response motion on the general mode shapes. Application of additional devices for further increasing of a structure's energy dissipation could bring significant positive effect in decreasing all-structure dynamic response. Historically a great number of the devices based on dry friction, viscous and internal hysteretic damping was used for resolving specific problems of seismic base isolation.

The proposed method of High Viscous Damper (HVD-approach) is also oriented on increasing of total energy dissipation of NPP buildings and structures. From this point of view the degree of dissipation increment determines the efficiency of reducing of inertial loads and response motions excited by the external dynamic loads. The main idea of HVD-approach is to use general systems or subsystems that can independently move about each other under external loads. Then such their property can be used for efficient energy dissipation by VD dampers connection of system to system or subsystems.

The linear system of two oscillators is considered to evaluate the efficiency of HVD-approach and the probable area of its application (see in fig. 5). Each oscillator is defined by its mass m_i, natural frequency f_i and modal damping ξ_i for $i = 1, 2$. These oscillators are assumed to be connected with the help of the some number of VD dampers. The number of dampers can be varied. The synthesis acceleration made with the help of standard response spectrum is used to define earthquake excitation with intensity of 0.2 g (see in fig.6).

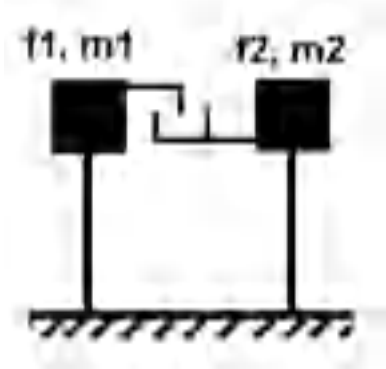

Fig.5 System of Two Oscillators

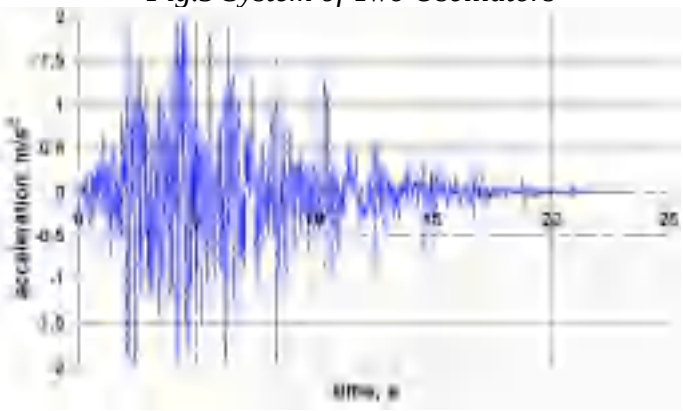

Fig.6 Free Surface Seismic Horizontal Acceleration

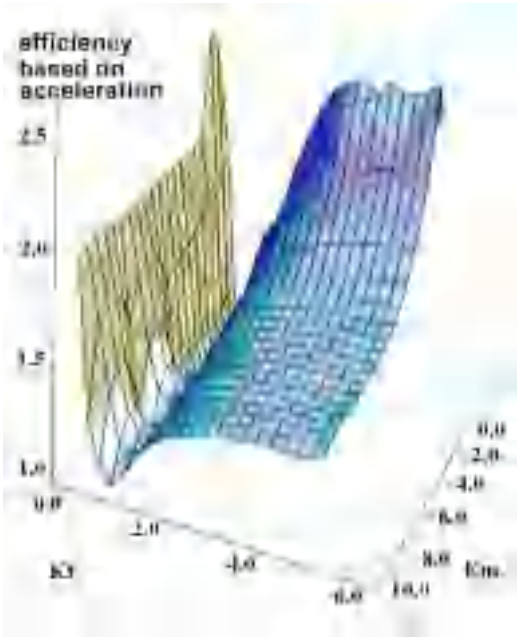

Fig.7 HVD-Approach Efficiency (Modal Damping 4%)

It is assumed for instance that the properties of the first oscillator are $m_1 = 3.3 \cdot 10^7$ kg, $f_1 = 5.2$ Hz, $\xi_1 = 4\%$. At the same time the modal damping of the second oscillator is defined constant as $\xi_2 = 4\%$ but its mass and natural frequency are varied. The time history dynamic analysis for the system of oscillators is carried out for the various pairs of (m_2, f_2) to determine the efficiency of damping connection using various numbers of dampers. Under term 'efficiency' we define the ratio of maximum response acceleration of the first oscillator in the system without dampers to the same value in system with dampers. The possible range of number of dampers is considered from 10 up to 500. The further increasing of the number of dampers has no sense from technical and financial points of view and since the corresponding viscous-elastic connection becomes totally elastic and rigid (see in fig.4). The additional parameters $K_m = m_1 / m_2$ and $K_f = f_1 / f_2$ are used to vary the properties (m_2, f_2) of the second oscillator. They are changed in the following ranges: $K_m = 0.1 \div 10.0$, $K_f = 0.2 \div 5.0$.

The surface of efficiency was determined as the result of multi-step seismic analysis with numerous different values of parameters K_m and K_f from the ranges mentioned above (see in fig. 7). Each point of the surface corresponds to some values K_m and K_f and also to the optimal number of dampers to get the highest value of possible efficiency of HVD-approach.

The surface's valley shows that dampers do not work in the case of the equivalence of the oscillators frequencies ($K_f = 1.0$) at any value of K_m. In this situation oscillators move in-phase and have no motion about each other. On the left side of the valley there is the region with $K_f < 1.0$ corresponded to the second oscillator stiffer than the first one. This case is desirable since the efficiency of the dampers connection rises very fast and reaches the highest values. On the right side of the valley there is the part of surface with $K_f > 1.0$ for the second oscillator more ductile than the first one. In that case efficiency rises more slowly but it shows the possibility to damp a ductile system about the stiff one with the proposed approach.

Further the system of oscillators with the following parameters is analyzed: $m_1 = 3.3 \cdot 10^7$ kg, $f_1 = 5.2$ Hz, $\xi_1 = 4\%$, $f_2 = 3.07$ Hz, $m_2 = 3.6 \cdot 10^7$ kg, $\xi_2 = 4\%$. In that way the reactor building substructures, namely outer envelope and internal support structures for the reactor vessel (see the next item), are simplify modeled. The dependence of efficiency on the number of VD dampers is shown in fig.8. Additionally the efficiency based on the ratio of the energy of response motions in the system without dampers to the same value in the system with dampers is demonstrated. The energy of response motion can be evaluated with the help of integral of PSD of response acceleration through the motion duration.

As indicated in fig. 8 the 165 VD dampers provide the highest decreasing of response acceleration (efficiency based on acceleration ≈ 1.9). The number of 190-240 VD dampers allows getting efficiency based on energy about ≈ 1.8. Such a great number of dampers is not a cost effective. However, the connection with 90-100 dampers provides rather high efficiency about ≈ 1.6 - 1.7.

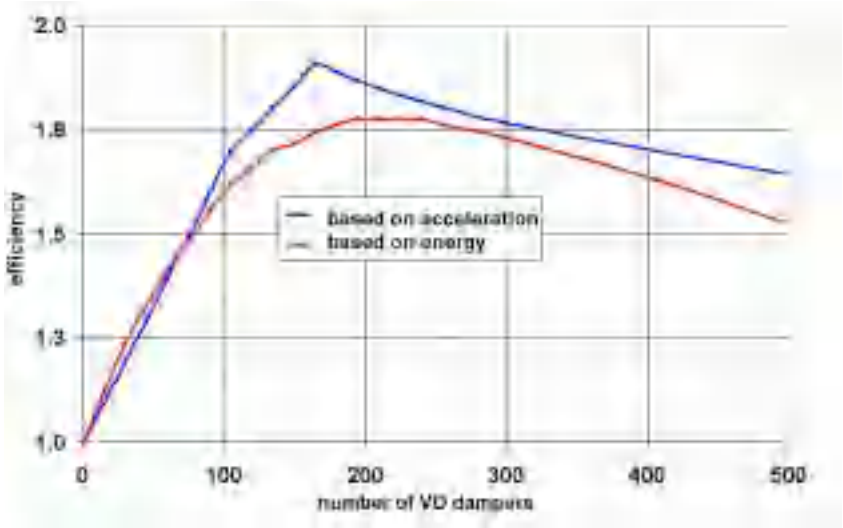

Fig.8 Efficiency of HVD-approach for "Envelope – Internal Structures" System (Two Oscillators)

It is usually important to reduce the response seismic energy on the natural frequencies of equipment as well as the total level of energy and acceleration. The response spectra and PSD of response acceleration of the first

oscillator are shown in fig. 9, 10 to demonstrate frequency distribution of seismic energy. It can be observed that the peak value of response spectrum drops twice and the peak value of PSD becomes 2.8 times less with dampers.

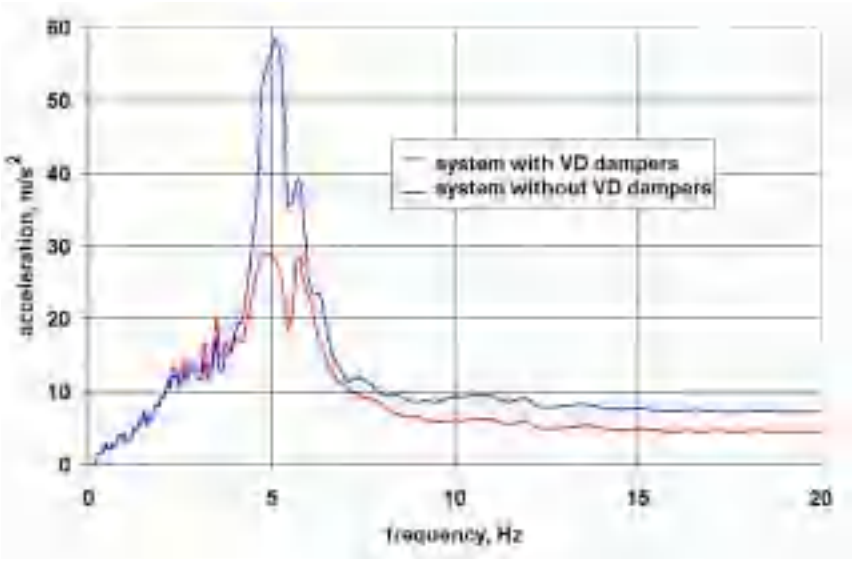

Fig.9 Acceleration Response Spectra for "Envelope – Internal Structures" System with 90 VD Dampers and without Them (Two Oscillators)

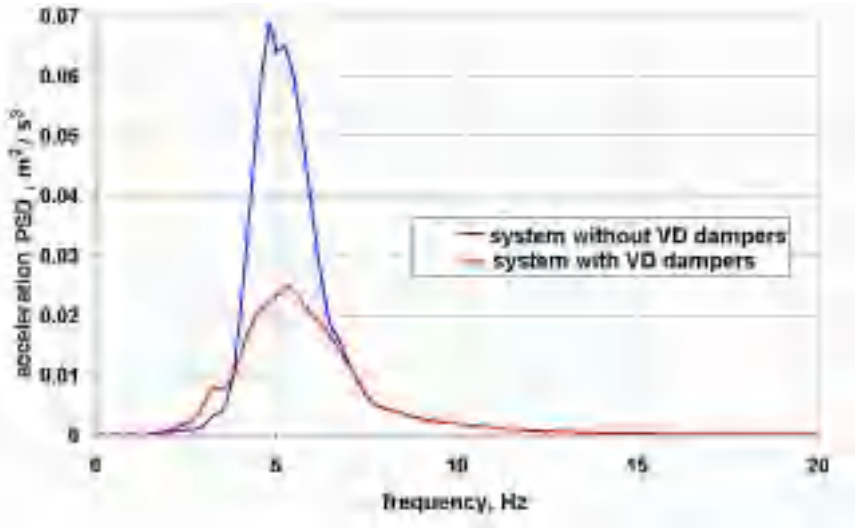

Fig.10 Power Spectral Density for "Envelope – Internal Structures" System with 90 VD Dampers and without Them (Two Oscillators)

3 USING VD DAMPERS FOR THE SUBSYSTEMS WITH DIFFERENT DYNAMIC PROPERTIES IN THE NPP REACTOR BUILDING

The efficiency of HVD-approach is analyzed on the base of the NPP reactor building of VVER-1000 type. That building is a reinforced concrete structure with pre-stressed concrete containment. The reactor building has a conventional design and consists of the following parts: fundamental part, outer envelope and internal support structures for reactor vessel. In that case the containment itself and internal structures are independent subsystems based on the common fundamental part. The independence of the containment allows avoiding additional stresses due to the possible temperature displacement during an accident. In that building scheme the upper slab of internal structures can be connected to the containment with the help of VD dampers (see in fig. 11-13). Then the accidental temperature displacements do not produce additional significant loads to the containment since they have quasistatic nature.

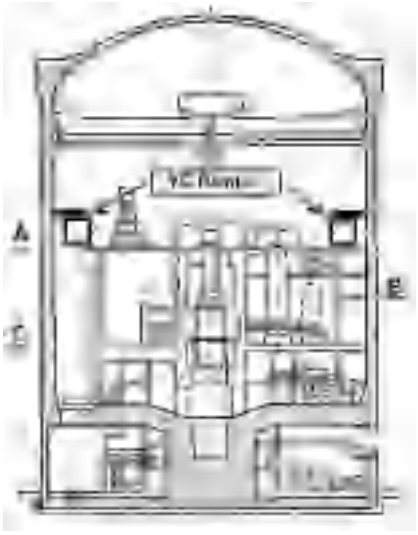

Fig.12 Vertical Section of NPP Reactor Building. The Installation of Dampers

Fig.13 Spatial Model. Mode Shape with Frequency 5.2 Hz and Modal Mass 20%

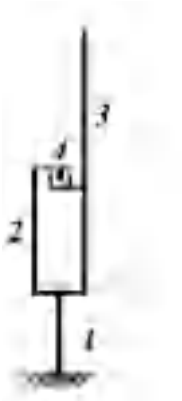

Fig.11 Stick Model

1 – Fundamental Part,
2 – Internal Structures,
3 – Outer Envelope,
4 – VD Dampers Connection

Two finite element models are developed for the reactor building based on the rock site. The first one is a simplified stick model that is widely used for the seismic design (see in fig. 11)). The second one is the detailed spatial model with the accurate modeling of the geometry and the material properties of the subsystems (see in fig. 13). The main natural frequencies of the both models are in a good accordance with each other. Their differences are less than 5%.

The reactor building has two significant natural shapes with the largest modal mass for the horizontal direction (50% и 23% of total mass) and frequencies 3.1 Hz и 5.2 Hz. One of them is demonstrated in fig.13.

On the one hand, the basic part of the earthquake energy is transmitted on the frequency range of 3 - 7 Hz. Therefore the mode shapes mentioned above are greatly excited during a possible earthquake. It means that the general response motion corresponds to the oscillations at these shapes. On the other hand, the motion at these shapes is followed by the significant relative movement of the internal structures about the outer envelope (see in fig. 13). In that case the dampers installed between such subsystems provide effective dissipation of seismic energy and decreasing the intensity of motion and inertial loads.

The seismic analysis is carried out to determine the optimal number of VD dampers in proposed connection with the help of both stick and spatial models. The horizontal ground acceleration is used with the spectrum shown in fig. 16. As the result of the analysis the efficiency of decreasing of response acceleration and energy for level A of internal structures is investigated (see in fig. 14, 15).

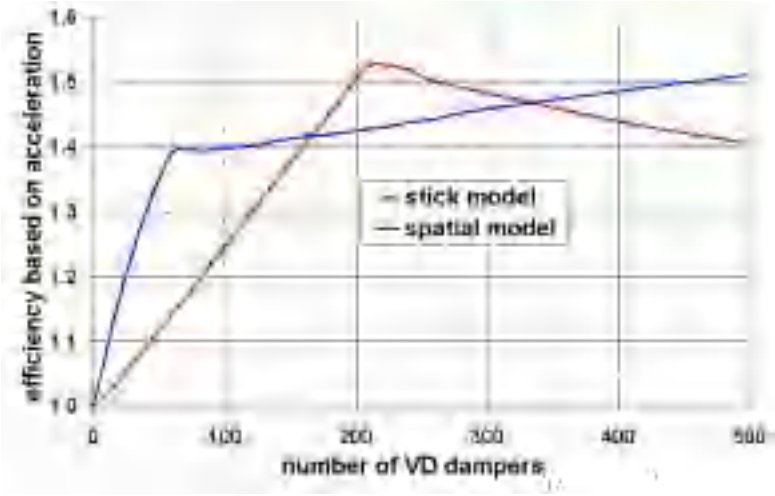

Fig.14 HVD-approach Efficiency Based on Acceleration

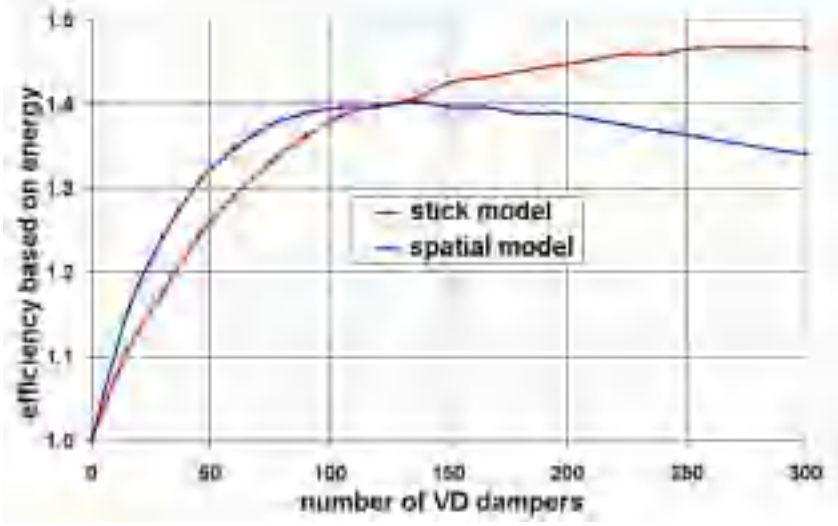

Fig.15 HVD-approach Efficiency Based on Energy

It can be observed that the obtained efficiency of HVD-approach is significantly different for spatial model, for stick model and for the system of the oscillators (fig. 8). This result proves that the dampers efficiency depends on the local features of the connected structures as well as on their global dynamic properties: masses, damping levels and frequencies. Therefore, the final solution on an optimal number of dampers should be done on the base of the detailed spatial model of the building. In current case the number of 90 VD dampers is the optimal to be installed in the reactor building and actually is a cost effective decision considering number of devices needed for restraining of numerous safety related components in the building (see in fig. 14, 15).

For currently investigated building it was shown that the most efficiency of HVD approach could be achieved in case of the rock base or hard soil conditions representing majority of the reactor building installations (Kostarev, 2003). So that case is assumed further.

The additional analysis of the building with 90 dampers and without them is performed under loads of plane crash and explosion. The time history dependency of explosion pressure is represented in fig.17. The two points of the top of the reactor building are chosen as the possible places of the plane crash impact (see in fig. 18). The military Phantom plane is considered with the time history impact force shown in fig.19.

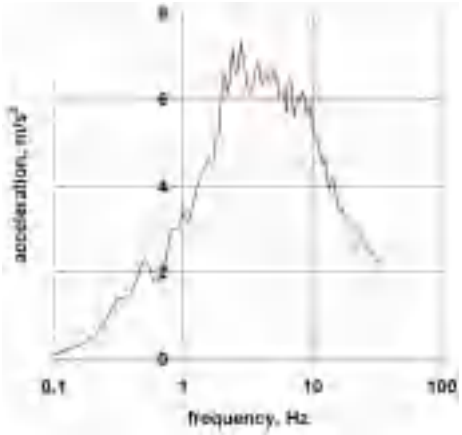

Fig.16 Seismic Response Spectrum (Damping 4%)

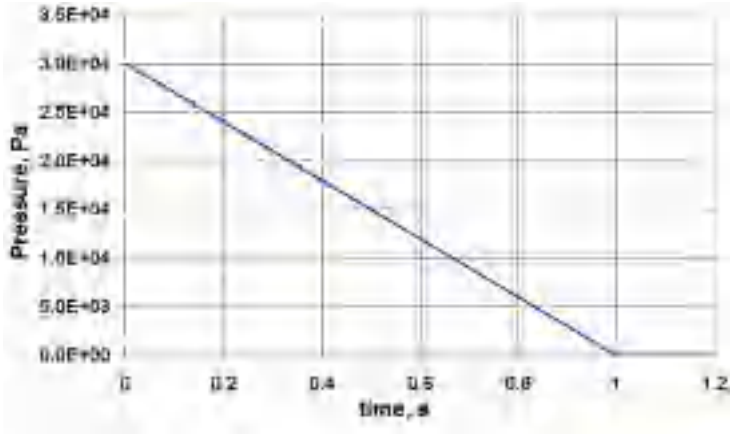

Fig.17 Explosion Wave Pressure

Fig.18 Plane Crash Points

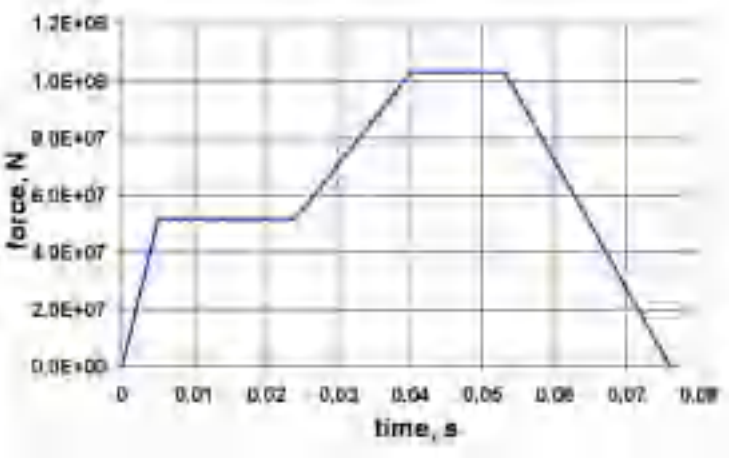

Fig.19 Phantom's Crash Load

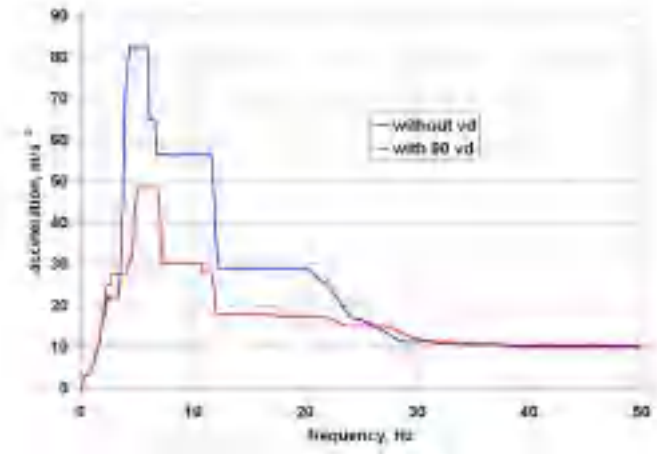

Fig.20 Broaden Envelope Response Spectra for Internal Structures at Level A (Explosion, Plane Crash u Earthquake)

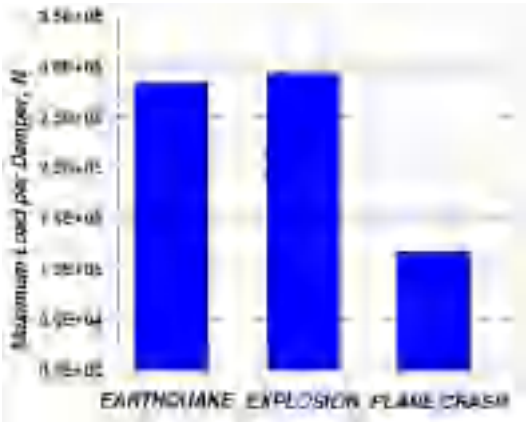

Fig.21 Maximum Time History Load on the VD Damper

As the result the broaden envelope spectra are obtained for all considered external loads: earthquake, plane and explosion. Such spectra for level A (see in fig. 20) and the values of accelerations in Table 1 show high efficiency of dampers for reducing inertial loads on the equipment supported by building structures under general kinds of external events. At the same time the maximal Time History acceleration decreases by up to 50% and the maximal spectra acceleration reduces by up to 70%.

The performed dynamic analysis allows evaluating maximal time history dynamic loads acting in each VD dampers during external events. The corresponding values are shown in fig.21. For the currently used dampers the safe load is $3.5 \cdot 10^5$ N per device. It means that the condition of load capacity is met.

Moreover the maximal total seismic forces and moments are determined in the horizontal section of building (see in fig 22, 23). Generally they are also reducing by 15-20% that proves also the efficiency of HVD-approach.

Table 1 Maximal Time History and Spectral Acceleration for Reactor Building under Earthquake, Plane Crash Impact and Explosion with and without HVD (rock base)

Reactor Building Part	Maximal Time History Acceleration, m/s^2	Maximal Spectral Acceleration, m/s^2 (damping 2%)

		Without HVD	With 90 HVD	Without HVD	With 90 HVD
level	A	10.2	6.8	82.5	48.5
	B	8.2	5.6	67.2	39.0
	C	6.8	5.0	58.9	35.0
Top of the Containment		9.7	9.4	81.7	79.1

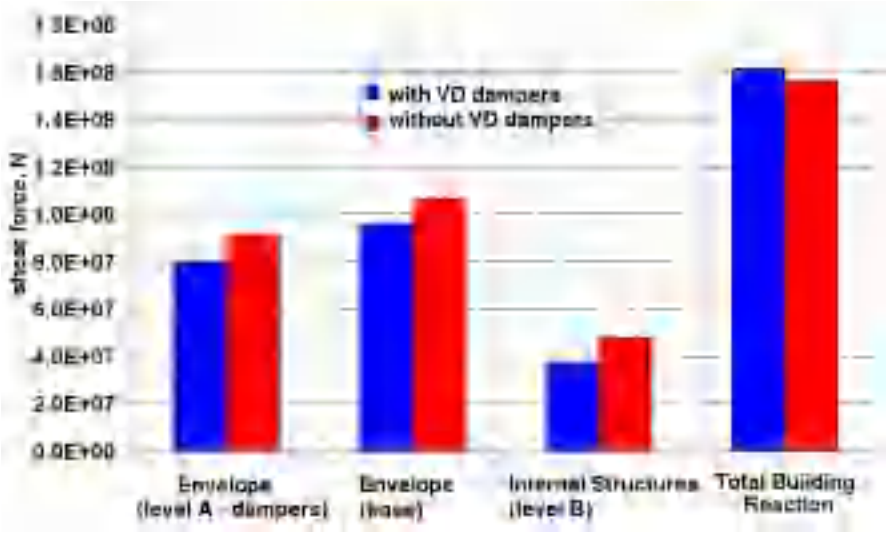

Fig.22 Maximal Total Shear Forces in Horizontal Sections of the Reactor Building under Earthquake

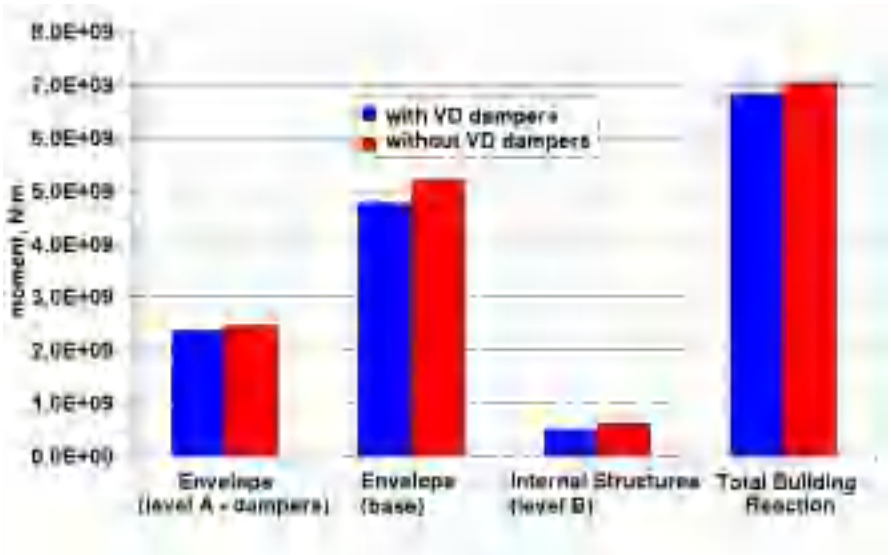

Fig.23 Maximal Total Bending Moment in Horizontal Sections of the Reactor Building under Earthquake

4 USING VD DAMPERS FOR THE SYSTEMS WITH DIFFERENT DYNAMIC PROPERTIES - NPP ADJACENT BUILDINGS

The proposed HVD-approach may be used successfully for the adjacent buildings with the different dynamic properties. The NPP buildings are most suitable for this. On the one hand, the NPP buildings should stay near each other to provide all necessary functional interconnections. Usually such buildings are connected with a great number of pipelines, electric cable trays and so on. On the other hand, the main NPP buildings are used for absolutely different purposes. Thereby they have dissimilar structure and accordingly the different dynamic

properties. The consideration of the most important building of NPP with VVER-1000 MWt reactor type follows below.

The reactor building has a massive structure made of reinforced concrete. There are usually one or two independent protective containment or/and structures with eigenvalues about 3-5 Hz of main bending mode shapes. At the same time there are the fundamental part and sometimes the auxiliaries with the stiff reinforced concrete structure. Usually the eigenvalues of general mode shapes of the whole reactor building are in the range of 1.5 – 4.0 Hz taking into account soil conditions.

The turbine hall building may consist functionally of several parts. Some of them are stiff and made of reinforced concrete. The others are flexible skeleton structures with columns and girders. The eigenvalues of the main mode shapes can be about 1 Hz for the turbine hall with the described structure. The reactor building and the turbine hall should be neighbor because they are connected by means of the system of the pipelines of steam and feed water.

The special building adjoins to the reactor building and it is responsible for the processing of liquid radioactive wastes. It has stiff structure made of reinforced concrete. The corresponding eigenvalues of the main mode shapes of the rocking of the building on soil can be in the range of 5.0 – 10.0 Hz.

The argumentations represented above are followed by the conclusion about principal possibility of usage of HVD-approach for the main NPP buildings. For example, the efficiency of HVD-approach is analyzed on the base of the reactor building and the special building (see in fig. 24). The possible case of VD dampers installation to connect the buildings is shown in fig. 25. The higher care should be paid to the points where dampers are attached to the buildings. The slabs are most suitable for the dampers attachment. In this case whole horizontal section of the building is involved and simultaneously it can be assumed to be undeformed in horizontal plane. Otherwise there is the possible negative influence of the local flexibility in the case of the dampers attachment to the walls of the building. Indeed the dampers connection has to constraint the relative motion of the buildings with total masses about $2 \cdot 10^8$ kg.

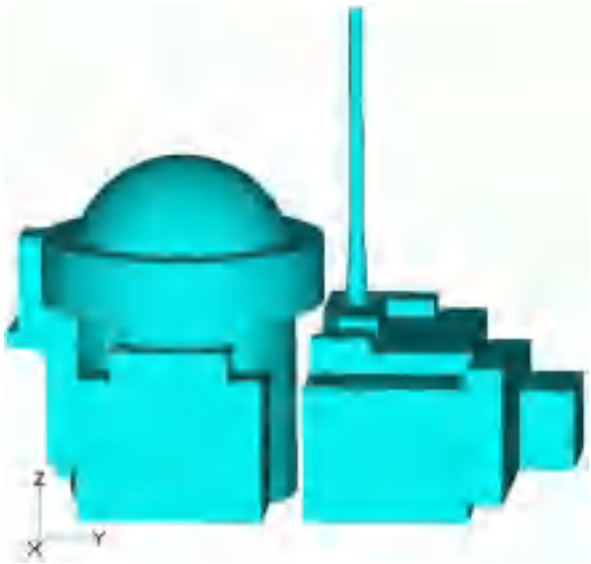

Fig. 24 The Reactor Building and the Special Building

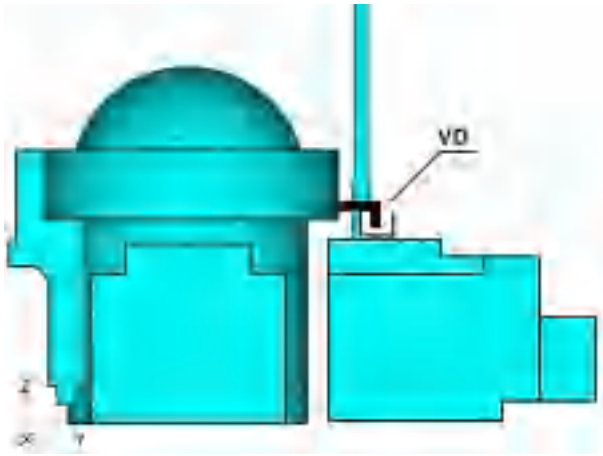

Fig. 25 Possible Installation of VD Dampers

The main mode shapes of the system “Reactor Building – Special Building” are shown in fig.26-29. The typical significant displacements of the buildings about each other are clearly observed. First, the corresponding eigenvalues are essentially different for the different buildings. Thus, the main mode shapes correspond to the rocking of the envelope with frequencies of 3.54 and 3.75 Hz for the reactor building. The special building has the main mode shapes with lateral shear of the slabs with frequencies 7.66 and 8.66 Hz. Second, the frequencies of such mode shapes are in the ordinary frequency range of the earthquake. So these shapes become strong excited during the earthquake. Therefore the general motion of the system “Reactor Building – Special Building” is carried out on these shapes with strong relative displacements. So the dampers connection is supposed to be effective.

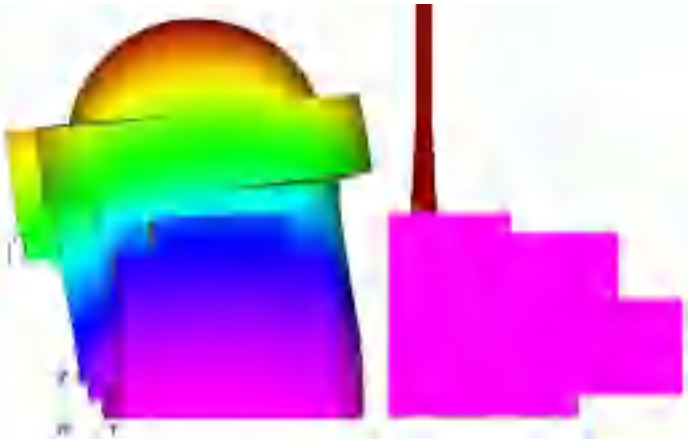

Fig. 26 General Mode Shape of the Reactor Building (3.54 Hz)

Fig. 27 General Mode Shape of the Reactor Building (3.75 Hz)

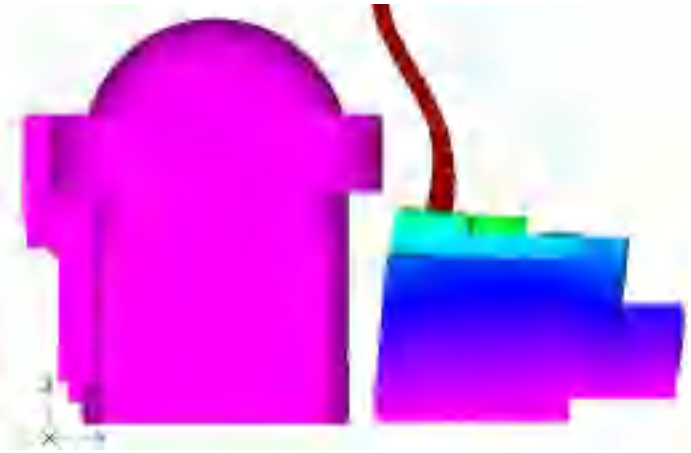

Fig. 28 General Mode Shape of the Special Building (7.66 Hz)

Fig. 29 General Mode Shape of the Special Building (8.66 Hz)

The seismic analysis of the "Reactor Building – Special Building" system is performed to evaluate actual efficiency of the HVD-approach. The connections of 50 and 100 VD dampers are considered. The response spectra are determined for the reactor building and the special building (see in fig. 30-31). The connection of 100 VD dampers can provide the decreasing of maximal Time History acceleration by 20% and maximal spectral acceleration by 40% for the reactor building.

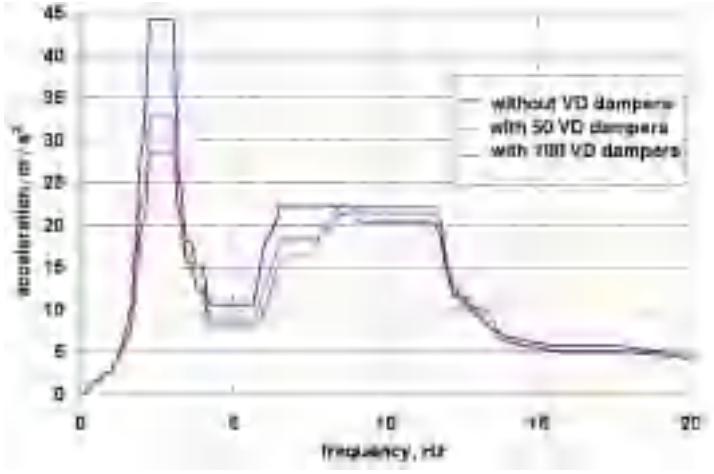

Fig.30 The Seismic Broaden Response Spectra for the Containment Gallery of the Reactor Building (Damping 2%)

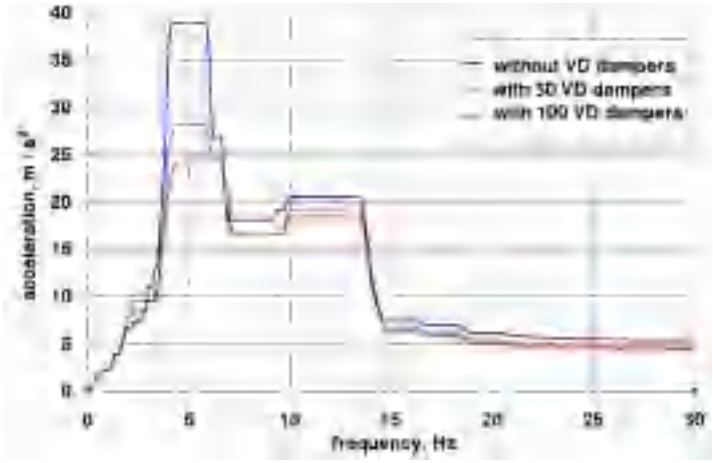

Fig.31 The Seismic Broaden Response Spectra for the Roof of the Special Building (Damping 2%)

5 CONCLUSIONS

An approach for essential reduction of structures' dynamic responses under all kinds of extreme external events was comprehensively investigated and has shown its effectiveness and reliability. It could be recommended for practical application for a new design as well as operating plants.

REFERENCES

Berkovski A., Kostarev V., Schukin A., Kostov M., Boiadjiev A., Boiadjiev Z., (1997), Seismic analysis of the safety related piping and PCLS of the WWER-440 NPP. Transactions of the 14th SMiRT, Lyon.

Fomin V., Kostarev V., Reinsch K., (2001), Elimination of Chernobyl NPP Unit 3 Power Output Limitation Associated with High Main. Transactions of the 16th SMiRT, Washington DC.

Katona T., Ratkai S., Delinic K., Zeitner W., (1994) Reduction of operational vibration of feed-water piping system of VVER-440/213 at PAKS. Proceedings of the 10th ECEE, Vienna.

Masopust R., (1994), Viscous dampers in applications for pipelines and other components in Czechoslovak nuclear power plants. ASME PVP, Prague.

Kostarev V., Berkovski A., Kireev O., Vasilyev P., (1994), Application of mathematical model for high viscous damper to dynamic analysis of NPP. Proceedings of 10th ECEE, Vienna.

Berkovski A., Kostarev V., Schukin A., Vasilyev P., (1995), Seismic Analysis of VVER NPP primary coolant loop with different aseismic devices. Transactions of the 13th SMiRT, Porto Alegre.

Kostarev V., Petrenko A., Vasilyev P., (2003), A New Method for Essential Reduction of Seismic and External Loads on NPP's Structures, Systems and Components, Transactions of the 17th SMiRT, Prague.

